A functional analysis of *RYR1* mutations causing malignant hyperthermia

A thesis presented to Massey University in partial fulfillment of the requirements for the degree of Doctor of Philosophy in Biochemistry

Keisaku Sato

2009

ACKNOWLEDGEMENTS

I would especially like to thank my supervisors, Associate Professor Kathryn Stowell and Associate Professor John Tweedie for their help, advice and patience in my study.

I came to New Zealand in 2000, not expecting to complete a PhD, but it was always an option that I had considered. The nine years I have spent at Massey University have not always been easy and I found the last few years, trying to complete my PhD very difficult. It has been a stressful time in very many ways and I do not think I would have completed the PhD if it had not been for the support of my supervisors and my lab mates.

I would particularly like to thank Natisha who has always been my friend as well as someone to discuss my work with. Special thanks also go to Robyn for technical support and as a travelling companion in Spain after attending a conference in Lund. Hilbert and his wife Liat made travelling in Europe an interesting experience, and William, Lili and her husband Cameron have also been my friends. It was fun to work in the lab next to Miranda and I will always remember the good times we had as a group.

I would especially like to thank my friends Dr Aiko Tanaka and Dr Daigo Takemoto working in Japan. They understand me and are always there for me over the internet or at the other end of an email.

I am grateful for the scholarship provided by Mid Central Health, without which my PhD study would not have been possible.

Finally I would like to thank my mother living in Japan. I have been away from home for a long time and it has not been easy either for me or for her as I am her only son. I am looking forward to going back to Japan and renewing those ties that are most important to me.

ABSTRACT

Malignant hyperthermia (MH) is a rare pharmacogenetic disorder in humans induced by volatile anaesthetics and depolarising muscle relaxants. An MH reaction shows abnormal calcium homeostasis in skeletal muscle leading to a hypermetabolic state and increased muscle contracture. A mutation within the skeletal muscle calcium release channel ryanodine receptor gene (*RYR1*) is associated with MH and is thought to cause functional defects in the RYR1 channel leading to abnormal calcium release to the sarcoplasm and consequent MH reactions. Mutations within *RYR1* are also associated with a rare congenital myopathy, central core disease (CCD). CCD is characterised by muscle weakness and is thought to be caused by insufficient calcium release from the RYR1 channel during excitation-contraction (EC) coupling.

To investigate functional effects of *RYR1* mutations, the entire coding region of human *RYR1* was assembled and cloned into an expression vector. Mutant clones containing *RYR1* mutations linked to MH or CCD were also constructed. Wild-type (WT) and mutant *RYR1* clones were used for transient transfection of HEK-293 cells. Western blotting was performed after harvesting and expressed WT and mutant RYR1 proteins were successfully detected. Immunofluorescence showed co-localisation of RYR1 proteins and the endoplasmic reticulum in HEK-293 cells. [^{3}H]ryanodine binding assays showed that RYR1 mutants linked to MH were more sensitive to the agonist 4-chloro-*m*-cresol (4-C*m*C) and less sensitive to the antagonist Mg^{2+} compared with WT. Two C-terminal RYR1 mutants T4826I and H4833Y were very significantly hypersensitive to 4-C*m*C and they may also result in a leaky channel. This hypersensitivity of mutants linked to MH may result in abnormal calcium release through the RYR1 channel induced by triggering agents leading to MH reactions. RYR1 mutants linked to CCD showed no response to 4-C*m*C showing their hyposensitive characteristics to agonists.

This study showed that the human RYR1 proteins could be expressed in HEK-293 cells. Moreover, using the recombinant human RYR1 clone, a single mutation within *RYR1* resulted in a functional defect in expressed RYR1 proteins and functions of mutant RYR1 proteins varied from hypersensitive to hyposensitive depending on the mutation and whether it was linked to MH or CCD.

ABBREVIATIONS

A	absorbance
APS	ammonium peroxodisulfate
ATP	adenosine triphosphate
bp	base pair
BSA	bovine serum albumin
CCD	central core disease
cDNA	complementary DNA
CHAPS	3-[(3-cholamidopropyl)dimethylammonio]-1-propanesulfonate
CHCT	caffeine-halothane contracture test
4-C*m*C	4-chloro-*m*-cresol
cpm	counts per minute
C-terminal	carboxy terminal
DAPI	4’,6-diamino-2-phenylindole dihydrochloride
DMEM	Dulbecco’s modified eagle’s medium
DNA	deoxyribonucleic acid
DEPC	diethylpyrocarbonate
DHPR	dihydropyridine receptor
DNase	deoxyribonuclease
DMSO	dimethyl sulphoxide
dNTPs	deoxynucleoside triphosphates
DTT	dithiothreitol
EC	excitation-contraction
EC_{50}	half maximal effective concentration
ECCE	excitation-coupled calcium entry
EDTA	ethylenediaminetetraacetic acid

EGTA	ethyleneglycol-bis(2-amino-ethylether)-N,N,N’,N’-tetraacetic acid
ER	endoplasmic reticulum
FITC	fluorescein isothiocyanate
IC_{50}	half maximal inhibitory concentration
IgG	immunoglobulin G
IVCT	*in vitro* contracture test
kb	kilobase
kDa	kilo Dalton
MEGAWHOP	megaprimer PCR using whole plasmids
MH	malignant hyperthermia
MHE	malignant hyperthermia equivocal
MHN	malignant hyperthermia negative
MHS	malignant hyperthermia susceptible
MmD	multi-minicore disease
mRNA	messenger RNA
N-terminal	amino terminal
PAGE	polyacrylamide gel electrophoresis
PIPES	piperazine-1,4-bis(2-ethanesulfonic acid)
POPOP	1,4-bis(5-phenyl-2-oxazolyl)benzene
PPO	2,5-diphenyloxazole
pBS	pBlueScript
PBS	phosphate buffered saline
pc	pcDNA
PCR	polymerase chain reaction
PDI	protein disulfide isomerase

RNase	ribonuclease
RT	reverse transcriptase
RT-PCR	reverse transcription-polymerase chain reaction
RYR1	ryanodine receptor 1
SDS	sodium dodecyl sulphate
SEM	standard error of the mean
SERCA	sarco/endoplasmic reticulum Ca^{2+}-ATPase
SLB	super LB
SOCE	store-operated calcium entry
SR	sarcoplasmic reticulum
TAE	Tris-acetate-EDTA buffer
TEMED	N,N,N’,N’-tetramethylethylenediamine
TBS	tris buffered saline
TBST	tris buffered saline Tween 20
TE	Tris-EDTA buffer
Tris	tris(hydroxymethyl)aminomethane
TRITC	tetramethylrhodamine isothiocyanate
TRPC	transient receptor potential channel
T-tubule	transverse tubule
UV	ultraviolet light
WT	wild-type

LIST OF FIGURES

LIST OF TABLES

Page

TABLE OF CONTENTS

CHAPTER TWO : MATERIALS AND METHODS

CHAPTER THREE : RESULTS

CHAPTER FOUR : DISCUSSION

CHAPTER ONE : INTRODUCTION

1.1 Malignant hyperthermia

Malignant hyperthermia (MH), first reported in 1960, is a pharmacogenetic disorder of skeletal muscle that can lead to a hypermetabolic crisis. It has also been reported that anaesthetics can cause hyperthermia and even death in several families [Denborough and Lovell, 1960; Denborough, et al., 1962]. MH reactions occur when a susceptible individual is exposed to a triggering agent. Reactions have variable intensity and time course, and hence none of the clinical symptoms can be regarded as specific signs of MH [Hackl, et al., 1990]. Typical clinical symptoms of MH, however, include muscle rigidity, tachycardia, acidosis, rhabdomyolysis and rapid temperature elevation [Rosenberg, et al., 2007]. The incidence of MH on a worldwide scale has been estimated to be 1:15,000 and 1:50,000 anaesthesias for children and adults, respectively [Kalow, et al., 1979] although the occurrence of MH susceptibility is considerably higher with estimates of 1:2000 suggested [Stowell, 2008]. About 50 MH families have been identified in New Zealand, and the incidence of MH is higher in the lower North Island than other regions because of several very large MH families resident in this region. It has been estimated that one patient will be diagnosed and treated as MH susceptible for every 120 patients in general surgery at Palmerston North Hospital (personal communication with Dr Neil Pollock). Seventy % of affected patients died, during or as a result of anaesthesia, in the 1970s usually from cardiac arrest. Dantrolene sodium was introduced as an antidote for MH in 1979 and consequently mortality has dropped to under 5% today [Denborough, 1998; Friesen, et al., 1979].

MH reactions can be caused by volatile anaesthetics used in general anaesthesia. These include halogenated anaesthetics such as halothane and sevoflurane. Depolarising muscle relaxants such as succinylcholine are also triggering agents [Kalow and Britt, 1973]. Some rare cases have been reported where MH reactions can also be triggered by excess exercise, heat or stress [Denborough, 1982; Hopkins, et al., 1991; Wappler, et al., 2000]. After observations that halothane can trigger MH reactions and patients who recovered from an MH crisis often showed higher muscle contracture against

halothane and caffeine [Ellis, et al., 1971; Kalow, et al., 1970], a protocol for a diagnostic test was established [European Malignant Hyperpyrexia Group, 1984; Larach, 1989]. This *in vitro* contracture test (IVCT) is the "gold standard" diagnostic method widely used today. The caffeine-halothane contracture test (CHCT) is also used in North America with minor changes from the IVCT [Larach, 1989]. A piece of quadriceps muscle excised by surgery is exposed to these triggering agents and the tension of the muscle is measured as the response. The IVCT diagnosis is MH-susceptible (MHS) if the muscle specimen shows abnormal contracture against the drugs halothane and caffeine, otherwise the patient is diagnosed as MH-normal (MHN). The IVCT, however, cannot always diagnose clearly and often establishes an equivocal status (MHE) if a muscle specimen shows an abnormal response to either of the drugs, halothane or caffeine, but not against both. It is also known that the IVCT can produce a false diagnosis. The IVCT has a reported 97-99% sensitivity and 78-93.6% specificity depending on the protocol [Allen, et al., 1998]. As the IVCT requires invasive surgery and is expensive, as well as having a degree of uncertainty in diagnosis, refinements in testing protocols or other methods have been suggested and reported [Girard, et al., 2004; Islander, et al., 2002]. 4-Chloro-*m*-cresol (4-C*m*C) is a strong and specific agonist of RYR1 proteins and hence it may be a useful triggering agent for the IVCT [Herrmann-Frank, et al., 1996].

Although the exact mechanism of variable MH reactions is not understood, it is believed that calcium homeostasis in skeletal muscle cells plays an important role in expression of phenotype [Carrier, et al., 1991]. MHS patients have shown higher concentrations of cytosolic calcium ions (Ca^{2+}) during MH reactions and also in normal conditions without exposure to triggering drugs [Lopez, et al., 1985]. In addition, the type 1 ryanodine receptor (RYR1) of sarcoplasmic reticulum (SR) in skeletal muscle cells has been reported to be responsible for the abnormal calcium release in ~70% of affected families [Mickelson, et al., 1988].

1.2 Excitation-contraction coupling

Intracellular Ca^{2+} regulates a wide range of cellular processes including cell growth, mitochondrial function, gene expression and muscle contraction. Cells have an

intracellular Ca^{2+} concentration of ~100 nM in the resting state, and when activated this level rises rapidly to about ten times higher and then Ca^{2+} regulates cellular events through Ca^{2+}-binding proteins [Berridge, et al., 2000]. Ca^{2+} plays a fundamental role in excitation-contraction (EC) coupling of skeletal muscle cells [Melzer and Dietze, 2001]. The wave of depolarisation from nerves is detected by a voltage sensor protein called the dihydropyridine receptor (DHPR). The DHPR is an L-type voltage-dependent Ca^{2+} channel located in the wall of the transverse tubule (T-tubule). The DHPR transmits the signal to the functionally coupled calcium release channel RYR1. Although the DHPR consists of many subunits, the α_{1S} subunit is believed to play an important role in this process [Grabner, et al., 1999]. A depolarising signal is received by the α_{1S} subunit leading to a conformational change in this subunit. The RYR1 is located on the SR membrane in skeletal muscle and detects the conformational change of the α_{1S} subunit of the DHPR which in turn opens the channel, releasing Ca^{2+} from the SR to the sarcoplasm (Figure 1-1). The released Ca^{2+} activates a muscle fibre, actin and myosin filaments, and then muscle contraction occurs. The intracellular free Ca^{2+} is pumped back to the SR readily by a Ca^{2+}-ATPase pump called sarco/endoplasmic reticulum Ca^{2+}-ATPase (SERCA). The concentration of free Ca^{2+} in the sarcoplasm is returned to normal and muscle relaxation occurs. This series of Ca^{2+} elevation occurs in milliseconds and hence muscle contraction does not last long [Nelson and Sweo, 1988].

The RYR1 consists of four monomers, 565 kDa each, forming a huge Ca^{2+} channel complex [Coronado, et al., 1994; Wagenknecht, et al., 1989]. Approximately 80% of the RYR1 including the amino terminal (N-terminal) region is exposed in the cytoplasm forming the foot structure and the remaining carboxyl terminal (C-terminal) region is embedded in the SR membrane [Takeshima, et al., 1989]. The RYR1 is thought to interact with the DHPR in a 1:2 ratio [Melzer, et al., 1995], and hence, a channel complex consists of four RYR1 monomers and eight DHPRs forming a macro molecular complex. Many other proteins are associated with this channel machinery including calmodulin, triadin and calsequestrin. These proteins regulate RYR1 activity or contribute to the active Ca^{2+} release process during EC coupling although the detailed roles and functions of individual proteins are still unknown [Feng, et al., 2002;

Lee, et al., 2004; Yamaguchi, et al., 2001]. Thus the overall channel complex has a molecular mass of more than 2×10^6 Da [Treves, et al., 2005].

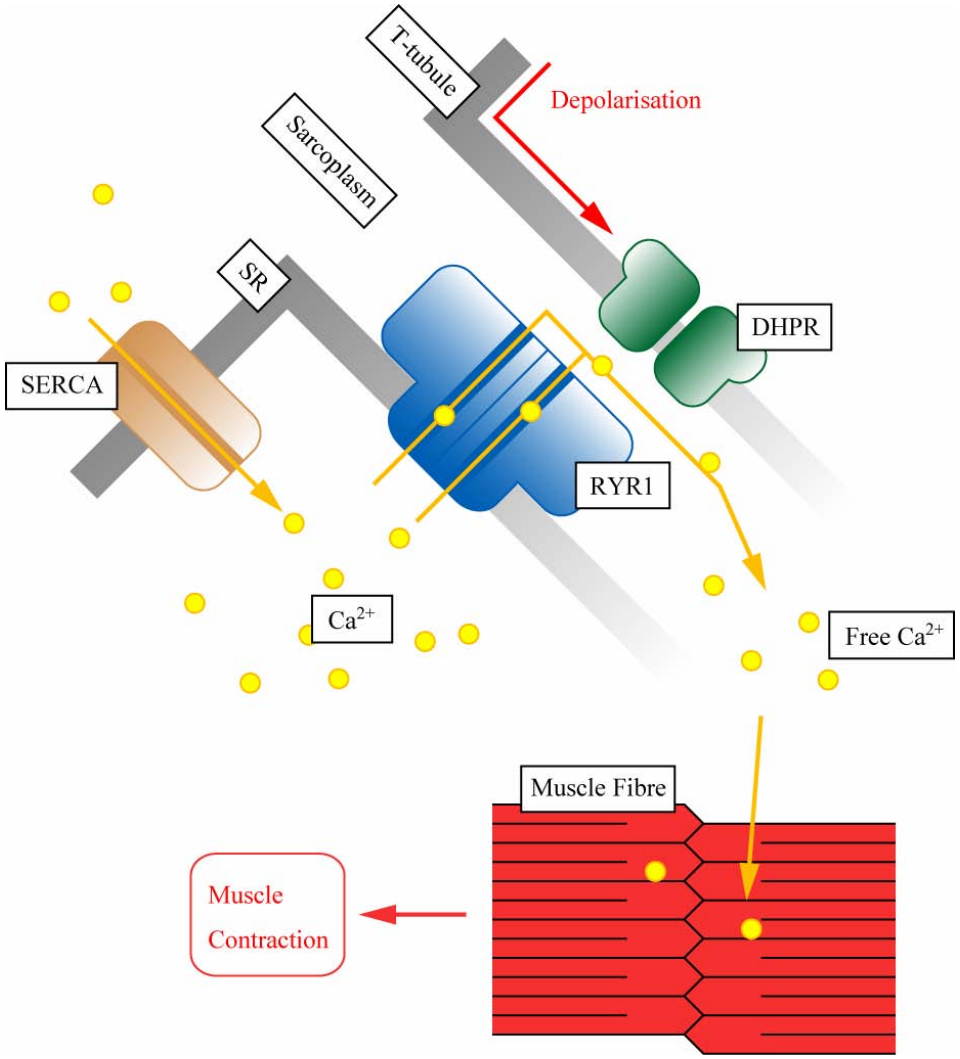

Figure 1-1 Excitation-contraction coupling

Membrane depolarisation is detected by a voltage sensor, dihydropyridine receptor (DHPR). The DHPR activates the calcium channel, ryanodine receptor (RYR1) to the open state through a conformational change. The RYR1 releases Ca^{2+} from the sarcoplasmic reticulum (SR) to the sarcoplasm. Intracellular Ca^{2+} induces muscle contraction and other cellular events, and is then pumped back to the SR through the sarco/endoplasmic reticulum Ca^{2+}-ATPase (SERCA). Only two of four RYR1 monomers and two DHPRs are shown and other associated proteins are omitted for simplification. Diagram adapted from the reference Litman and Rosenberg (2005).

1.3 Animal models

The pig is the most common animal model of MH and these animals have been widely investigated, since first reported, to understand the mechanism of MH reactions and to identify a causative gene [Hall, et al., 1966]. The SR isolated from skeletal muscle of MHS swine has shown an abnormal release of Ca^{2+} caused by halothane and caffeine indicating the cause of MH reactions [Kim, et al., 1984; Nelson, 1983]. Linkage analysis has shown that chromosome 6q is linked to porcine MH and the susceptible locus encodes *RYR1*, the gene encoding the RYR1 protein [Harbitz, et al., 1990]. Another report has shown that the RYR1 shows a prolonged duration of the open state and has a defect in a low-affinity Ca^{2+} binding site in muscle specimens from MHS swine [Fill, et al., 1990]. Hence, it is thought that MHS swine have a dysfunctional RYR1 protein which can be triggered to be opened by anaesthetics and does not close readily allowing large amounts of Ca^{2+} to pass through to the sarcoplasm in muscle cells. This abnormal release of Ca^{2+} to the sarcoplasm causes various symptoms during MH reactions. Ca^{2+} binds to troponin C activating actin and myosin filaments leading to muscle contraction. Excess activation of troponin C induces abnormal muscle contraction and masseter spasm, and excessive muscle contracture causes membrane damage of muscle cells leading to rhabdomyolysis. Excess Ca^{2+} also results in increased metabolic flux causing increased ATP, CO_2 and heat production as well as increased O_2 consumption leading to acidosis, tachycardia and hyperthermia. These events may cause death because of cardiac arrhythmia or cardiac arrest.

Sequencing porcine *RYR1* identified the first mutation, R615C (accession #M91452) which is associated with porcine MHS and co-segregates with the affected phenotype in porcine MH in a homozygous recessive manner [Fletcher, et al., 1993; Mickelson, et al., 1992]. The porcine R615C mutation corresponds to the R614C mutation (#J05200) in human *RYR1*, and this finding has led to the identification of additional MH mutations in humans. In addition, molecular genetic testing was developed to predict porcine MH susceptibility by detecting the R615C mutation within *RYR1* [Rempel, et al., 1993]. This technique suggested that diagnostic testing of MH could be simplified to a blood test instead of an invasive muscle biopsy test for some human MH families.

MH has also been found in dogs, cats and horses and is linked to the *RYR1* gene in these animals as well [Bellah, et al., 1989; Roberts, et al., 2001; Waldron-Mease, et al., 1981].

1.4 *RYR1* mutations in human

As with porcine MH, linkage analysis has shown that *RYR1* located on human chromosome 19q is a candidate gene associated with MH in humans [MacLennan, et al., 1990; McCarthy, et al., 1990]. The R614C mutation which is homologous to the porcine R615C mutation (the only *RYR1* mutation in swine MH), has been identified in some human MH families [Rueffert, et al., 2001]. The mutation has been shown to co-segregate with the MH phenotype in MHS families and heterozygous mutations lead to MH susceptibility showing an autosomal dominant trait for this disorder. To date, a large number of *RYR1* mutations has been identified from MHS families worldwide. Although more than 60 mutations have been reported in the literature, it has also been suggested that there are over 200 MH mutations identified throughout the world [Robinson, et al., 2006]. Some selected *RYR1* mutations are listed in Table 1-1.

RYR1 is organised into 106 exons and the RYR1 protein consists of 5,038 amino acids. Most *RYR1* mutations identified are clustered in specific “hotspot” regions (Figure 1-2) – region 1 (N-terminal, Cys^{35}-Arg^{614}), region 2 (central, Asp^{2129}-Arg^{2458}), region 3 (C-terminal, Ile^{3910}-Ala^{4942}) [McCarthy, et al., 2000; Robinson, et al., 2006]. Two hotspot regions, 1 and 2, are located within a cytosolic “foot” segment, and a transmembrane segment including hotspot region 3 is located in the SR membrane (Figure 1-2).

It is thought that hotspot regions 1 and 2 interact with each other in the N-terminal foot segment and region 3 is located within the pore region of the channel in the C-terminal transmembrane segment [Kobayashi, et al., 2004]. The interaction between regions 1 and 2 may be responsible for stabilising the closed state of the RYR1 (zipping) and interaction may be lost when the channel is activated to an open state (unzipping) (Figure 1-3). It is thought that a mutation within these hot spots may affect the function of the RYR1 and lead to MH susceptibility.

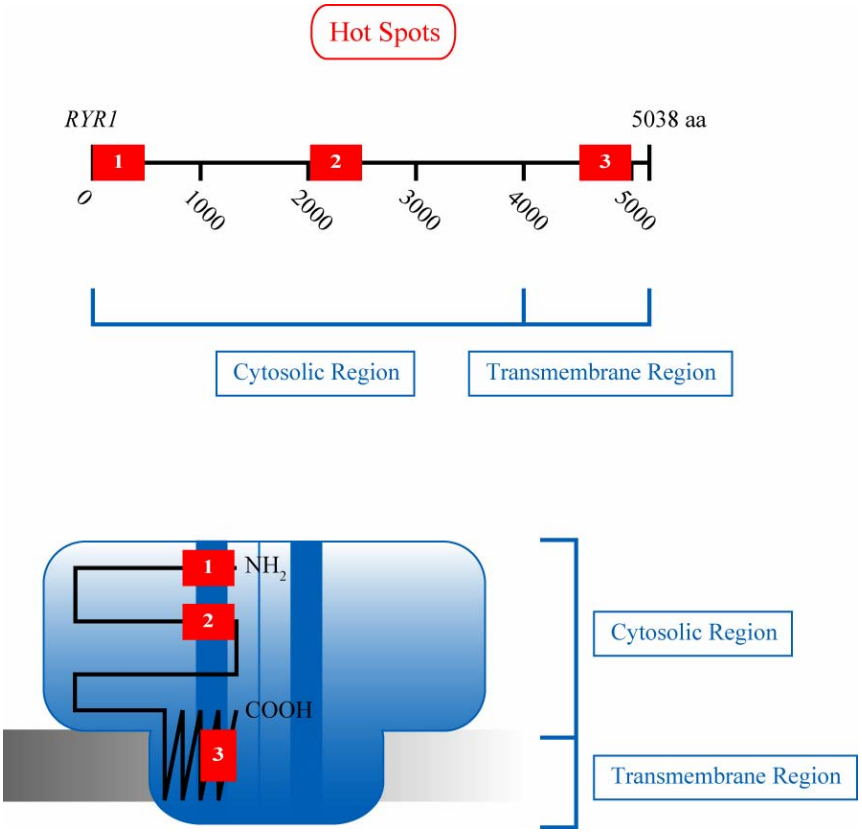

Figure 1-2 Hotspots for MH mutations in *RYR1*

Most *RYR1* mutations are clustered in three specific regions (top). Regions 1 and 2 are within the "foot" segment located in the sarcoplasm and region 3 is within the transmembrane segment located on the SR membrane (bottom). Diagram adapted from the reference Treves, et al. (2005).

Recent studies have reported the structure of the RYR1 protein showing the binding sites for other proteins or modulators such as calmodulin and FKBP12 as well as the location of some *RYR1* mutations linked to MH [Hamilton and Serysheva, 2009]. Some N-terminal *RYR1* mutations located within hotspot region 1 are localised to the clamp-shaped region of the channel structure. Another study using the crystalised N-terminal region (1-210 amino acids) of rabbit RYR1 has shown that the N-terminal *RYR1* mutations linked to MH, C36R, R164C and R178C (C35R, R163C and R177C in humans) are located in an outside loop of the RYR1 exposed to the cytosol, and these mutations did not affect stability or folding of the structure of this region [Amador, et al., 2009]. This result indicates that these mutations may not lead to

conformational changes in the RYR1 but may affect the interaction with other proteins such as the DHPR which contributes to MH susceptibility.

Hot spot	Exon	Nucleotide change	Amino acid change	Disorder	Reference
1	2	T103C	C35R	MH	[Lynch, et al., 1997]
1	6	C487T	R163C	MH, CCD	[Quane, et al., 1993]
1	9	G742A	G248R	MH	[Gillard, et al., 1992]
1	12	C1209G	I403M	CCD	[Quane, et al., 1993]
1	14	A1565C	Y522S	MH, CCD	[Quane, et al., 1994]
1	17	C1840T	R614C	MH	[Gillard, et al., 1991]
2	39	C6487T	R2163C	MH	[Manning, et al., 1998b]
2	45	G7300A	G2434R	MH	[Keating, et al., 1994]
2	45	G7304A	R2435H	MH, CCD	[Zhang, et al., 1993]
2	46	C7372T	R2458C	MH	[Manning, et al., 1998a]
3	100	C14477T	T4826I	MH	[Brown, et al., 2000]
3	100	C14497T	H4833Y	MH	[Anderson, et al., 2008]
3	101	G14582A	R4861H	CCD	[Tilgen, et al., 2001]
3	102	G14671C	G4891R	CCD	[Tilgen, et al., 2001]
3	102	T14693C	I4898T	CCD	[Lynch, et al., 1999]
3	102	G14695A	G4899R	CCD	[Tilgen, et al., 2001]
3	102	C14717T	A4906V	CCD	[Tilgen, et al., 2001]

Table 1-1 Common *RYR1* mutations associated with MH and/or CCD

Selected *RYR1* mutations most commonly identified to date are shown. Some mutations are thought to be associated with both MH and CCD while others have been identified from patients affected with only either of the two disorders.

Three separate genes identified as *RYR1*, *RYR2*, and *RYR3* have been found to encode the RYR, and each is predominantly expressed in skeletal muscle, cardiac muscle or brain and smooth muscle, respectively [Hakamata, et al., 1992; Marks, et al., 1989; McPherson and Campbell, 1993; Otsu, et al., 1990]. Mutations have also been identified within *RYR2* and they are thought to be linked to ventricular tachycardia and cardiac sudden death [Jiang, et al., 2004]. Some *RYR2* mutations have also been identified from families affected with arrhythmogenic right ventricular cardiomyopathy type 2 [Tiso, et al., 2001]. These *RYR2* mutations are not identical to *RYR1* mutations linked to MH or CCD although some mutations localise the homologous regions of *RYR1* hotspots.

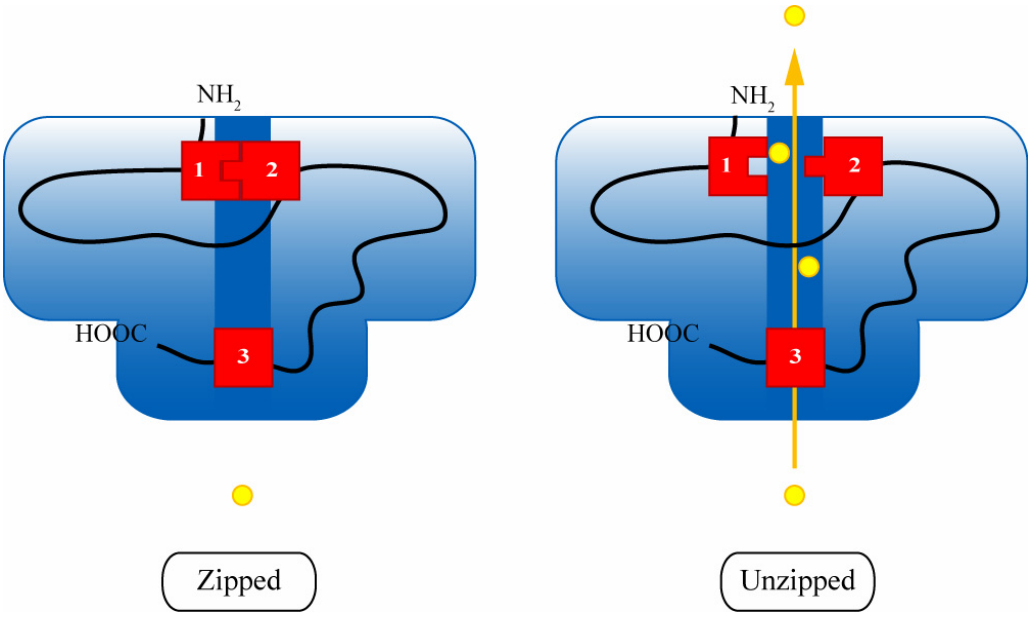

Figure 1-3 A proposed role of region 1 and 2 in Ca^{2+} release

Many MH mutations have been identified within region 1 and 2, and these regions are thought to interact with each other. This suggests that these domains may play an important role as a "gate" of the RYR1. Mutations within these domains may cause the functional loss of the gate and de-stabilise the closed state leading to abnormal Ca^{2+} homeostasis. A role for region 3 is unclear although it is thought to be located in the pore region of the channel. Diagram adapted from the reference McCarthy and Mackrill (2004).

1.5 *CACNA1S* mutations

As *RYR1* mutations clearly co-segregate with MH susceptibility in some families, molecular genetic testing may be useful to predict susceptibility instead of the IVCT for those families [Fletcher, et al., 1995]. It is possible to establish an MHS diagnosis by detecting a causative mutation if all MHN individuals do not contain the mutation and all individuals carrying the mutation are MHS in certain families [Healy, et al., 1996; Rueffert, et al., 2001]. This technique, however, can only be used for some families because discordance between genotype and IVCT phenotype has been observed in other families [Fagerlund, et al., 1997; Serfas, et al., 1996].

It has been reported that between 50 and 80% of MHS families show linkage to *RYR1*. This means that MH is genetically heterogeneous and defects at other loci can result in MH susceptibility [Deufel, et al., 1992]. A genome-wide scan has shown strong linkage on chromosome 1q encoding the α_{1S} subunit of the DHPR (*CACNA1S*) in an MH family with no linkage to chromosome 19q encoding *RYR1* [Robinson, et al., 1997]. Subsequent screening of the *CACNA1S* gene identified an R1086H mutation that co-segregated with the MHS phenotype in this family [Monnier, et al., 1997]. Functional analyses for the R1086H mutation have also shown an abnormal effect on EC coupling [Weiss, et al., 2004]. Some other putative mutations in this gene have been identified from MH families and hence *CACNA1S* may be a second candidate gene although the functional effects of these mutations are still unknown [Carpenter, et al., 2008].

The DHPR is a voltage sensor protein which transmits a signal from nerves to the RYR1 through a conformational change. It has been reported that a loop between domains II and III of the α_{1S} subunit is important for signal transmission suggesting that a mutation within this II-III loop may cause a critical impact on signal transmission and RYR1 activation leading to abnormal calcium homeostasis [Kugler, et al., 2004]. Although the causative MH mutation in *CACNA1S*, R1086H is located outside the II-III loop, it is located in a neighbouring loop between domains III and IV (Figure 1-4). It has been reported that compared with the wild-type (WT), an α_{1S} subunit with the R1086H mutation induces increased Ca^{2+} release from the RYR1

triggered by caffeine [Weiss, et al., 2004]. A further study has also shown that the III-IV loop does not directly affect EC coupling but does affect DHPR gating transitions that are involved in EC coupling [Bannister, et al., 2008]. These observations indicate that a single mutation which is not located in *RYR1*, but within another gene, can cause abnormal EC coupling and lead to MH susceptibility.

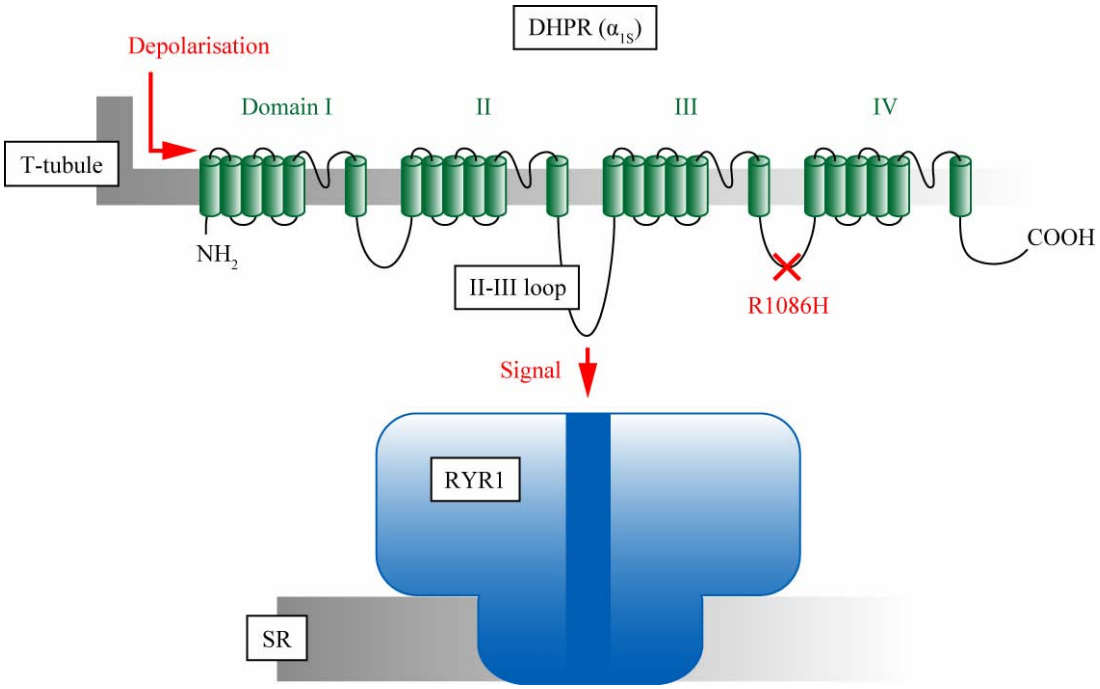

Figure 1-4 A role of the α_{1S} subunit of the DHPR

Only the α_{1S} subunit of the DHPR and one RYR1 monomer are shown. The II-III loop transmits a signal from nerves to the RYR1 by conformational change. It also negatively regulates Ca^{2+} release from the RYR1. The R1086H mutation within the III-IV loop disrupts this allosteric regulation leading to unregulated Ca^{2+} release from the RYR1 and MH reactions. Diagram adapted from the reference Avila (2005).

1.6 Other candidate loci to MH

Because of genetic heterogeneity of MH, linkage analyses and genome-wide studies have been performed for some MH families which do not show linkage on

chromosome 19q. The *CACNA1S* gene is the sole gene apart from *RYR1* which is clearly associated with MH and from which a causative mutation has been identified in an MH family. Although genome-wide studies have demonstrated linkage on chromosomes 3q, 5p, 7q and 17q, causative mutations or even candidate genes have not been identified at any of these alternative loci [Iles, et al., 1994; Iles, et al., 1993; Robinson, et al., 1997; Sudbrak, et al., 1995]. Although most studies have been performed on the RYR1 protein in MH studies to date, DNA sequencing of *RYR1* does not always identify a mutation. Some MHS patients show a strong positive reaction in the IVCT with no associated mutation in *RYR1* even though sequence analysis covers the entire *RYR1* coding region. This discordance makes genotype/phenotype correlations in MH difficult to understand, and hence linkage analyses may still be useful in identifying other candidate loci or genes associated with this disorder.

As MH reactions are caused by abnormal calcium homeostasis in skeletal muscle, candidate genes may be involved directly or indirectly in pathways associated with calcium signaling. A recent study has shown that transgenic knockout mice that lack skeletal muscle calsequestrin (*CASQ1*) show MH-like reactions showing sensitivity to halothane and overheating [Protasi, et al., 2009]. Calsequestrin-1 is a skeletal muscle calcium binding protein of the SR and this result suggests that *CASQ1* could be another candidate gene for MH. The RYR1 protein interacts with other proteins including triadin and junctin in the lumen of the SR [Beard, et al., 2009]. These proteins may also influence calcium homeostasis directly or indirectly through interactions with the RYR1. Another study has shown that triadin and junctin can activate the RYR1 channel and hence they may also play an important role in EC coupling [Wei, et al., 2009].

Muscle contracture is caused by increased Ca^{2+} concentrations in the sarcoplasm in skeletal muscle cells. Calcium entry is accounted for not only by Ca^{2+} release from intracellular Ca^{2+} stores but also by extracellular Ca^{2+} entry: store-operated calcium entry (SOCE) and excitation-coupled calcium entry (ECCE). EC coupling and muscle contracture have often been discussed without consideration of extracellular Ca^{2+}, and SOCE and ECCE in skeletal muscle have been identified only recently [Dirksen, 2009]. There are several proteins, however, involved in these calcium entries including STIM1, Ca^{2+} sensor protein, Orai1, Ca^{2+} permeable channel and transient receptor

potential channel (TRPC), and hence functional defects of these proteins may influence calcium homeostasis and may cause MH-like reactions [Dirksen, 2009]. Mouse myotubes cultured from transgenic knock-in mice that contain an *RYR1* mutation linked to MH, R163C, have shown enhanced ECCE compared with WT [Cherednichenko, et al., 2008]. Although current data are too limited to discuss the correlation between MH and SOCE and/or ECCE, these mechanisms for Ca^{2+} entry suggest that several other proteins may be involved in MH reactions. Therefore, the cellular mechanisms resulting in MH reactions may include those governing both intracellular and extracellular Ca^{2+} influxes.

1.7 Central core disease

Mutations in *RYR1* can also result in other myopathies including central core disease (CCD). CCD is an inherited non-progressive congenital myopathy characterised by a structural defect in muscle fibres and muscle weakness [Jungbluth, 2007a]. CCD was originally reported in a family as congenital muscle weakness [Magee and Shy, 1956]. Later observations revealed the characteristic absence of oxidative enzyme activity due to mitochondrial depletion [Dubowitz and Pearse, 1960]. Typical clinical symptoms of CCD are hypotonia, muscle weakness and skeletal abnormalities, and are generally presented in infancy or in early childhood with muscle weakness or delayed development. Clinical variability is often observed even within the same family and hence some affected individuals can have severe symptoms while other siblings have only minor ones [Bethlem, et al., 1971]. Therefore, diagnoses are established based on histopathological characteristics using muscle biopsy instead of clinical symptoms. Histochemical staining of muscle biopsy shows the absence of oxidative enzymatic activity from central core regions which are typically observed in type 1 muscle fibres. Although central cores may be single or multiple and the location of cores may be variable, they are an important factor for establishment of diagnoses [Sewry, et al., 2002]. Electron microscopy can be used to observe reduction or absence of mitochondria and variable degrees of myofibrillar disorganisation which are also typical findings for this disorder.

CCD shows both autosomal dominant and sometimes recessive traits [Romero, et al.,

2003], and association between MH and CCD has been observed in some families [Denborough, et al., 1973; Frank, et al., 1980]. Many CCD patients have an abnormal response in the IVCT obtaining MHS diagnoses or show MH reactions during anaesthesia suggesting the co-existence of these disorders. CCD mutations identified to date are clustered in the three *RYR1* hotspots together with MH mutations, and interestingly, most CCD mutations have been identified in the C-terminal region 3, particularly in exons 100 to 102 [Robinson, et al., 2006; Romero, et al., 2003].

Mutations identified from MH families are recognised as MH mutations that are associated only with MH because MHS patients generally do not show CCD. Mutations identified from CCD families, however, cannot be recognised only as CCD mutations because CCD patients often show MH susceptibility. Some mutations have been identified from CCD patients only, so that they do not show MH susceptibility and thus these mutations are recognised as CCD mutations. On the other hand, some patients exhibit both MH and CCD characteristics and carry an *RYR1* mutation. In this case, the mutation is thought to be responsible for both disorders and hence one mutation may be able to cause both MH and CCD at the same time. Table 1-1 includes examples of mutations which are associated with only CCD or both MH and CCD.

1.8 Hypersensitive RYR1

MH reactions are believed to be caused by abnormal release of Ca^{2+} to the sarcoplasm through the RYR1 and *RYR1* mutations may cause a functional defect in this channel. Since a number of *RYR1* mutations have been identified from MHS families, scientists have tried to understand the functional effect of *RYR1* mutations and the underlying mechanisms causing MH reactions. Cultured skeletal muscle cells excised from MHS patients who carry the *RYR1* mutation R163C have shown higher intracellular Ca^{2+} release triggered by anaesthetics compared to cells from MH negative individuals [Censier, et al., 1998]. A cloned rabbit *RYR1* cDNA has also been used for functional studies and expressed mutant rabbit RYR1 proteins which carry an MH mutation including R164C (corresponding to the human R163C mutation) have shown a more sensitive response compared to wild-type (WT) against triggering drugs [Tong, et al., 1997; Yang, et al., 2003]. Mutant RYR1 proteins have shown channel opening and

intracellular Ca^{2+} release at lower concentrations of agonists compared to WT. This means that the mutant RYR1 may be sensitive to agonists like halothane, and open the channel at a lower threshold leading to abnormal Ca^{2+} release resulting in an MH episode while the WT RYR1 is still closed and does not release Ca^{2+} to the sarcoplasm (Figure 1-5). These studies have shown hypersensitivity of mutant RYR1 proteins associated with MH and this "hypersensitive hypothesis" is widely believed to explain the mechanism of MH.

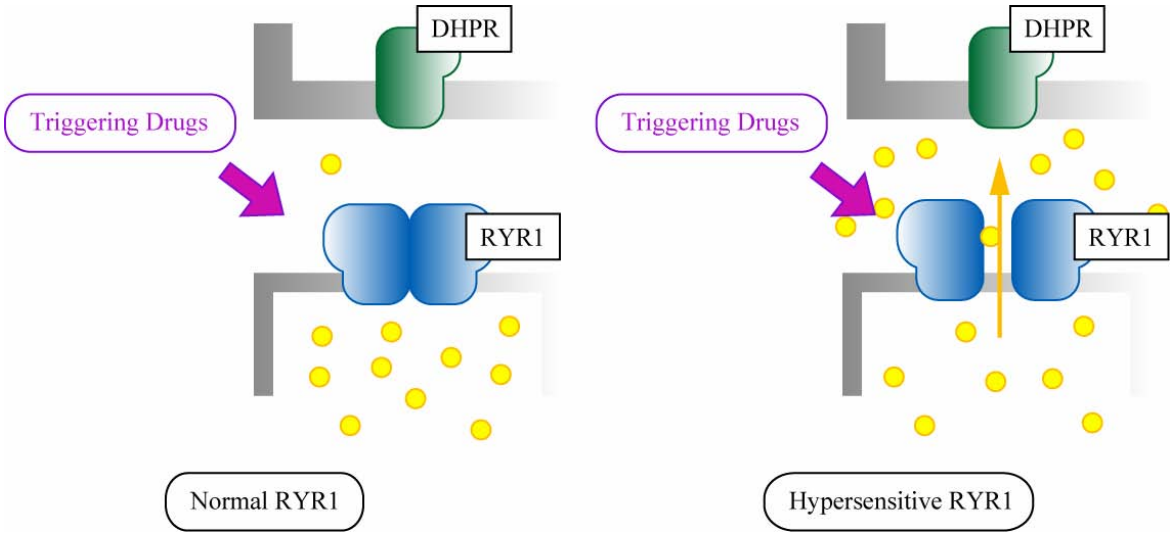

Figure 1-5 Hypersensitive RYR1

The mutant RYR1 (right) reacts to triggering agents at lower concentrations releasing excess Ca^{2+} into the sarcoplasm leading to MH reactions while the WT (left) RYR1 still stays stably in the closed state at the same concentrations of triggering agents without releasing Ca^{2+}. Diagram adapted from the reference Treves, et al. (2005).

The mechanisms responsible for the functional defects in the protein are still unclear. Many MH mutations are located on the hotspot regions 1 and 2 that are thought to be interacting with each other (Figure 1-3). A mutation within one of these domains may cause the loss of domain-domain interactions under the influence of triggering agents and de-stabilise the closed state of the channel. Therefore, the RYR1 with a mutation

transforms to the open state at a lower threshold of triggering drug concentration showing hypersensitivity to volatile anaesthetics. A C-terminal mutation within region 3, however, can also cause hypersensitivity [Yang, et al., 2003]. Many mutations have been reported as hypersensitive and responsible for MH, using a range of methods in functional studies. There is only one hypothesis to date for understanding MH reactions.

1.9 Leaky RYR1

The exact mechanism underlying CCD is also unclear. As many *RYR1* mutations have been identified from CCD patients, functional studies have been performed for some of these as well as for MH mutations. These studies, however, have shown different results depending on the position of the CCD mutation and the experimental conditions used. This has led to three hypotheses for understanding CCD.

Cells with expressed mutant RYR1 proteins carrying CCD mutations have sometimes shown higher intracellular resting Ca^{2+} concentrations than cells with the WT RYR1 or with MH mutants [Tong, et al., 1999]. The Y522S (Y523S in rabbit *RYR1*) mutation has been well studied for this observation. This mutant has shown higher resting Ca^{2+} concentrations and lower Ca^{2+} release triggered by channel agonists [Brini, et al., 2005]. It is thought that the Y523S mutant may be a leaky channel which releases Ca^{2+} continuously without any triggering drugs, thus depleting Ca^{2+} from the stores, and hence the mutant channel can release only a reduced amount of Ca^{2+} when it is activated by drugs due to the depleted store of Ca^{2+} (Figure 1-6). This means cells with the mutant RYR1 may not have sufficient Ca^{2+} to respond to a signal from the DHPR during EC coupling. Low free Ca^{2+} concentrations in the sarcoplasm cannot induce proper muscle contracture and this insufficient Ca^{2+} release through the RYR1 may be the cause of muscle weakness, one of the common symptoms of CCD. This “leaky channel hypothesis” was the first proposed mechanism for CCD and several CCD mutations have been reported to cause a leaky channel [Avila and Dirksen, 2001]. High resting Ca^{2+} concentrations and low Ca^{2+} release triggered by drugs are the main characteristics contributing to the development of this hypothesis.

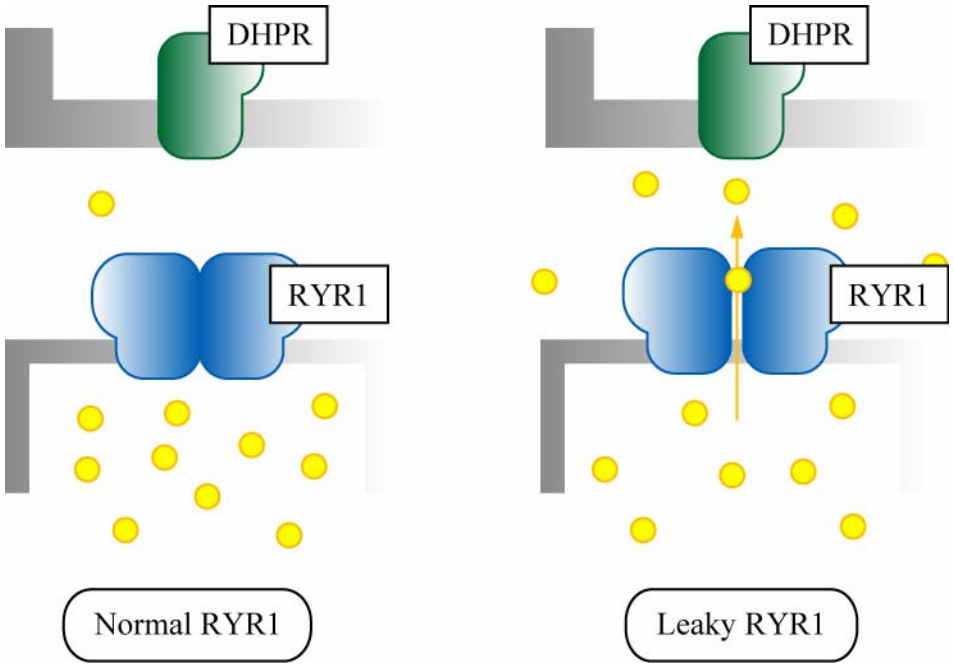

Figure 1-6 Leaky RYR1

Some RYR1 mutants (right) which have CCD mutations show higher intracellular resting Ca^{2+} concentrations than the WT protein (left) suggesting that the mutant channels are leaky. This hypothesis suggests that low Ca^{2+} storage in the SR due to the leaky RYR1 causes insufficient Ca^{2+} release as a response to a signal during EC coupling. Low Ca^{2+} release is believed to cause muscle weakness. Diagram adapted from the reference Treves, et al. (2005).

1.10 Hyposensitive RYR1

Functional studies using *RYR1* cDNA have not always shown high resting Ca^{2+} for CCD mutations. CCD mutants, for example I4897T in rabbits (I4898T in humans), have shown similar resting Ca^{2+} concentrations compared to cells with the WT RYR1 [Brini, et al., 2005]. The I4897T mutant, however, has also shown less response than WT against caffeine. This mutant has released almost no Ca^{2+} to the cytosol during drug activation indicating a lower sensitivity of this mutant to agonists [Lynch, et al., 1999]. Other studies have also reported similar observations for I4897T and other CCD mutations [Avila, et al., 2001; Du, et al., 2001]. It has also been reported that some CCD mutations can cause hyposensitivity against voltage activation [Avila, et al.,

2003]. These observations have led to the hyposensitive (EC uncoupling) hypothesis (Figure 1-7). This hypothesis suggests that CCD mutations make the RYR1 insensitive to triggering drugs and electrical stimulation and the mutant RYR1 cannot release sufficient concentrations of Ca^{2+} during EC coupling leading to muscle weakness. This hypothesis is characterised by normal resting Ca^{2+} concentrations and lower or no Ca^{2+} release triggered by drugs.

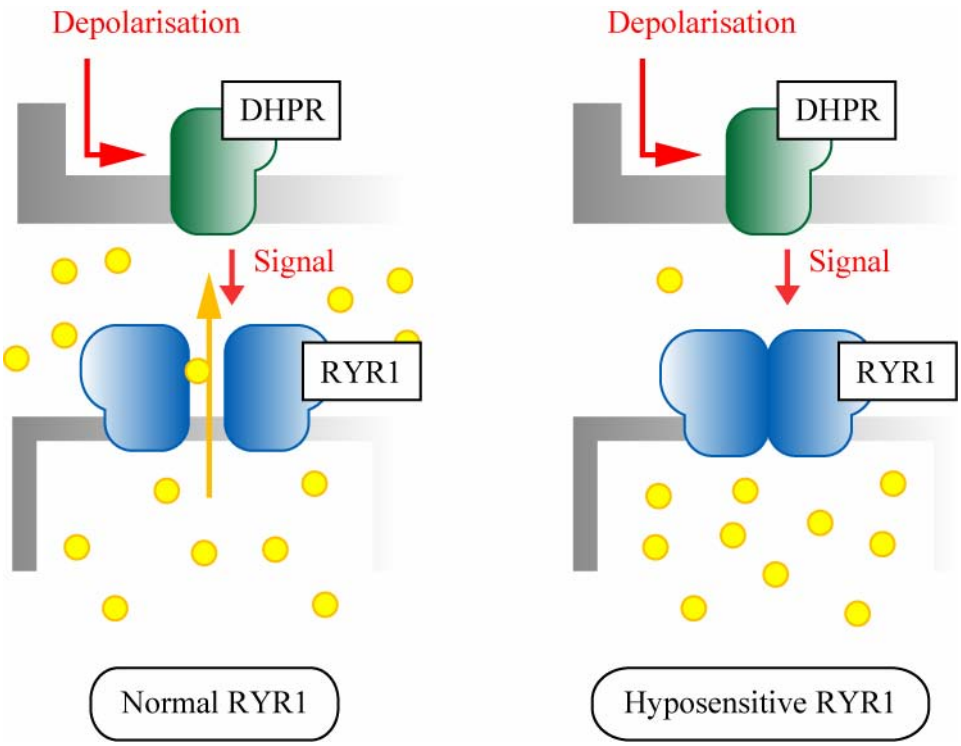

Figure 1-7 Hyposensitive RYR1

Some RYR1 mutants which have CCD mutations show a lower Ca^{2+} release to triggering drugs or voltage activation. The WT RYR1 releases sufficient amounts of Ca^{2+} during EC coupling (left), while the mutant RYR1 cannot react against the signal leading to low Ca^{2+} release and muscle weakness (right). Diagram adapted from the reference Treves, et al. (2005).

1.11 Reduced expression of the RYR1

The latest hypothesis to explain CCD has been suggested from western blotting analyses of CCD patients' skeletal muscle biopsies. Some CCD patients who carry novel CCD mutations have shown reduced RYR1 protein expression, in skeletal muscle, compared to WT and CCD patients with other known mutations [Zhou, et al., 2007]. This reduced RYR1 expression has been identified in patients with recessive mutations [Zhou, et al., 2006]. Reduced expression levels of RYR1 in skeletal muscle may lead to insufficient Ca^{2+} release in the SR during EC coupling and this may be the cause of CCD for some patients (Figure 1-8).

Although the mechanism of decreased RYR1 expression is unclear and there are only a limited number of reports, a mutation could affect protein assembly, protein stability or allele silencing causing a quantitative lack of functional RYR1 protein in skeletal muscle cells. This "reduced RYR1 expression hypothesis" is characterised only by western blotting for RYR1 and further functional studies will need to be performed to test this theory.

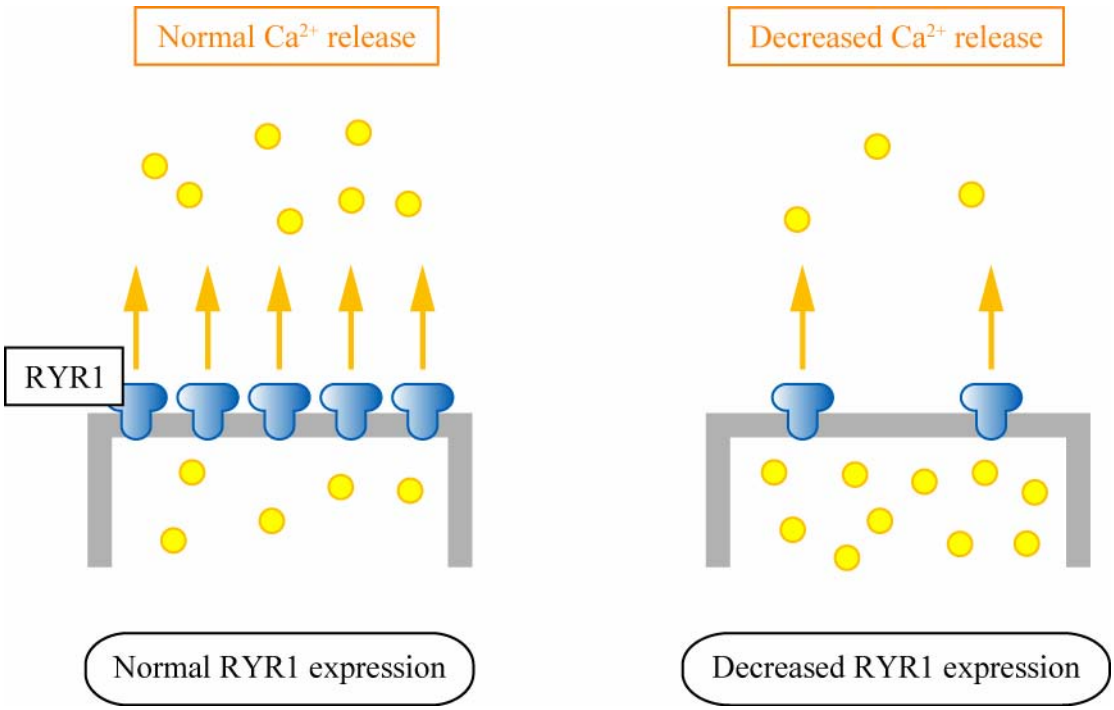

Figure 1-8 Reduced RYR1 expression

CCD mutations could affect the RYR1 expression level in skeletal muscle cells. Western blotting has revealed the decreased RYR1 expression for some CCD patients carrying recently identified *RYR1* mutations. This hypothesis suggests that insufficient Ca^{2+} is released from the SR leading to subsequent muscle weakness of CCD. Diagram adapted from the reference Dirksen and Avila (2002) and Zhou, et al. (2007).

1.12 Controversy

There is one hypothesis to explain MH and three to explain CCD. The MH hypothesis suggests excess Ca^{2+} release through the RYR1 triggered by channel agonists due to a hypersensitive channel, and CCD hypotheses suggest insufficient Ca^{2+} release during EC coupling (Figure 1-9). There are still many questions and controversies remaining for *RYR1* mutations and these two disorders because MH and CCD appear to co-exist in some patients. It is well known that CCD patients are often diagnosed as MHS by the IVCT and they sometimes show severe MH susceptibility [Robinson, et al., 2002]. Therefore, the question remaining is: if one hypothesis can explain two distinct

disorders at the same time, or two different MH and CCD hypotheses can co-exist phenotypically then how can two phenotypes due to one mutation co-exist in some patients? There is still no acceptable explanation for this dilemma.

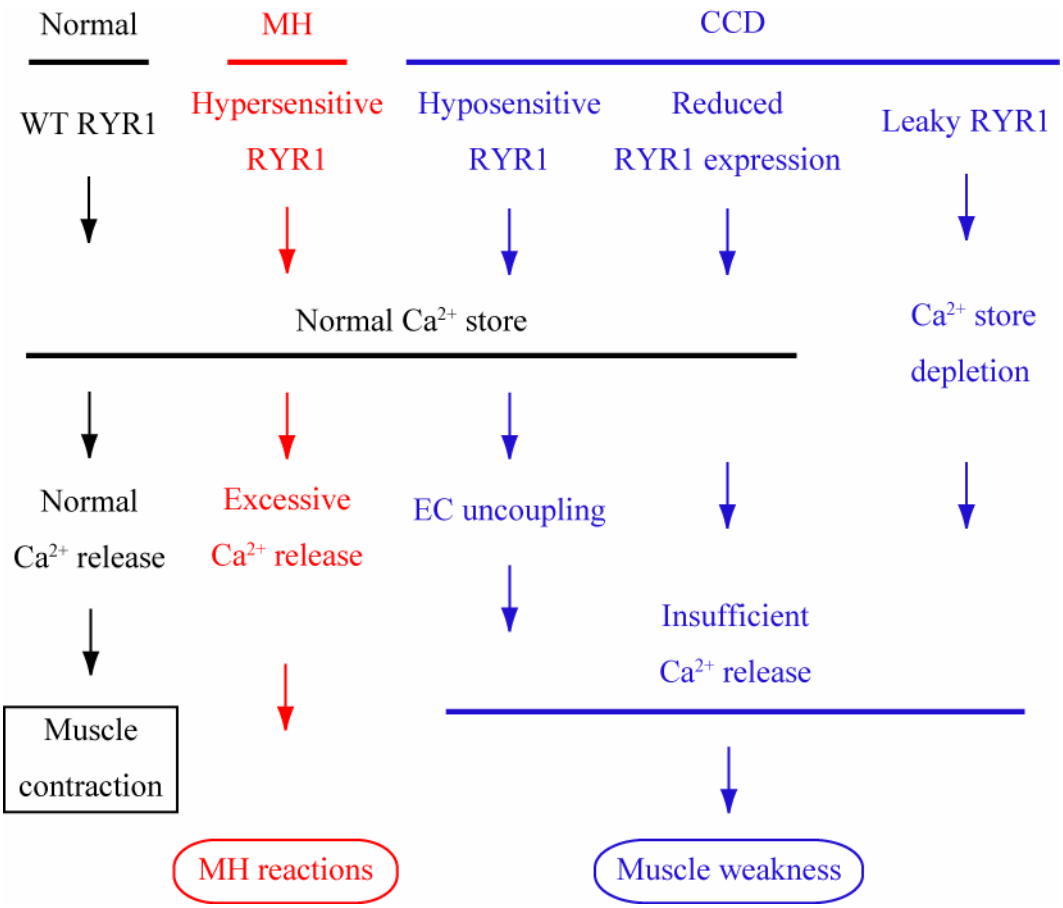

Figure 1-9 Schematic description of mechanisms of MH and CCD

Both MH and CCD are skeletal muscle disorders and are believed to be caused by malfunction of the RYR1 and abnormal Ca^{2+} homeostasis during EC coupling. In normal conditions, the RYR1 receives a signal from the DHPR and opens the channel releasing the appropriate amount of Ca^{2+} to the SR. An MH mutation leads the RYR1 to be hypersensitive and mutant channels are easily triggered by anaesthetics causing excess Ca^{2+} release and muscle rigidity. CCD mutations lead to insufficient Ca^{2+} release during EC coupling regardless of the mechanism and this may cause the muscle weakness of CCD.

Patients affected with MH generally do not show CCD symptoms because CCD is a congenital myopathy and is normally recognised in childhood. Mutations identified from MH patients are hence recognised as MH mutations. Some mutations such as R163C, however, have been identified in both MH and CCD patients with different phenotypes. Functional studies for the corresponding R164C mutation in rabbit cDNA have shown hypersensitivity of the mutant RYR1 [Tong, et al., 1997; Yang, et al., 2003]. It has also been reported that resting Ca^{2+} concentrations ($[Ca^{2+}]_i$) for R164C mutants are not significantly different from the WT RYR1 and hence this mutation is usually regarded as an MH mutation in functional studies [Tong, et al., 1999; Yang, et al., 2003]. Another report, however, has shown that R164C causes high resting Ca^{2+} and less sensitivity against drugs because the channel may be leaky [Avila and Dirksen, 2001]. Although detection of $[Ca^{2+}]_i$ depends on the experimental system and can differ significantly in different environments, these data are completely inconsistent and both cannot explain the co-existence of MH and CCD in relation to the R163C *RYR1* mutation.

CCD patients, on the other hand, often show MH susceptibility diagnosed by the IVCT and hence mutations identified from these patients may be responsible for both disorders. The Y522S mutation (Y523S in rabbits) is well studied as a leaky channel in functional studies. This mutant has shown high resting Ca^{2+} and low response against agonists [Brini, et al., 2005; Tong, et al., 1999]. Another report, however, has shown high sensitivity against agonists which is inconsistent [Tong, et al., 1997]. Furthermore, Y522S is a mutation that can be associated with both MH and CCD. These data again cannot explain the co-existence of the two disorders.

The I4898T mutation is a common CCD mutation and has been used for functional studies showing EC uncoupling using rabbit *RYR1* cDNA (I4897T in rabbits) [Avila, et al., 2001; Lynch, et al., 1999]. This mutation has never been identified in MHS families and it is recognised as a CCD mutation. Two members of a CCD family, however, have been diagnosed as MHS by IVCT indicating that MH and CCD may co-exist in this family although the diagnosis of MH by the IVCT is not always specific [Lynch, et al., 1999]. As all family members have not been diagnosed by the IVCT and the I4898T mutation may be responsible for only CCD and MH

susceptibility may be caused by another trait, it is still unknown whether the I4898T is associated not only with CCD but also with MH. It is possible, however, that CCD patients who carry an EC uncoupling mutation show MH susceptibility in the IVCT and then a single *RYR1* mutation may be responsible for both disorders diagnostically. The hypersensitive hypothesis and EC uncoupling hypothesis are mechanistically inconsistent and it is unlikely that both disorders can be explained by the two hypotheses. If hyposensitive I4898T can also cause hypersensitive MH reactions, no reasonable hypothesis could be put forward to explain the condition. Further case studies and diagnoses will be required to confirm that EC uncoupling mutations are responsible for only CCD and not for MH.

1.13 Methodology of functional studies

Functional studies have been performed using various techniques and experimental systems. Organisms include humans, swine and mice, and cell lines include COS-1, HEK-293, RYR1-knockout (dyspedic) myotubes and immortalised B lymphocytes. Knock-in mice are the latest system for functional studies.

Skeletal muscle cells excised from affected individuals are widely used for functional studies. Cultured myotubes established from skeletal muscle can be used for calcium assays to analyse resting Ca^{2+} concentrations or Ca^{2+} release triggered by agonists [Brinkmeier, et al., 1999; Duke, et al., 2004]. This technique has been used for humans and swine [Lopez, et al., 2000]. The advantage of this method is that experimental conditions almost mimic those of patients *in vivo*, it does not require cloning of RYR1 cDNA and it is also easier and faster than other methods. The disadvantage is that it requires patients' skeletal muscle from biopsy tissue. Results of experiments using patient skeletal muscle can also be inconclusive or non-specific if another trait is associated with the disorder. Skeletal muscle myotubes contain all proteins associated with EC coupling and hence even if functional studies show abnormalities of muscle cells from an MHS patient whom carries an *RYR1* mutation, it is still possible that another protein such as the DHPR is also involved in the abnormal response. As a single individual can have more than one mutation in *RYR1*, it is also necessary to sequence all regions of *RYR1* to ensure that the patient of interest has no other

mutation although this would not exclude the involvement of other genes.

Since it has been reported that the RYR1 protein is also expressed in B lymphocytes, immortalised B lymphocytes isolated from patients' blood samples have also been used for functional studies [Sei, et al., 1999]. B lymphocytes isolated from MHS patients have shown higher drug sensitivity and calcium release than those from MHN individuals [Girard, et al., 2001; Sei, et al., 2002]. This technique requires blood samples instead of a skeletal muscle biopsy and thus patients do not need surgery. It improves availability of samples and hence it helps in screening *RYR1* in large numbers of MHS patients to identify a mutation [Levano, et al., 2009]. Depending on blood samples means that investigation of a specific *RYR1* mutation requires patients who carry the mutation. As B lymphocytes do not have endogenous DHPR and other skeletal muscle triad associated proteins, functional studies can focus on RYR1 function. It means, however, the experimental conditions may not mimic patients' conditions *in vivo*.

If blood samples are not available or if a specific mutant RYR1 is needed to be created and investigated, cloning of *RYR1* cDNA is the alternative method. Cloned WT and mutant *RYR1* cDNAs have been used for transient and stable expression of the RYR1 protein. Site-directed mutagenesis allows introduction of any mutation within *RYR1* and it does not require affected patients' samples. Various cell lines have been used for expression of the WT and mutant RYR1 including COS-1, HEK-293 and dyspedic mouse myotubes [Chen, et al., 1993; Tong, et al., 1997; Yang, et al., 2003]. Myotubes seem to be the most physiologically relevant system and HEK-293 cells are most commonly used depending on the type of functional analyses, as the latter cannot be used in electrophysiological experiments. The most difficult part of this technique is cloning of the *RYR1* cDNA. The *RYR1* cDNA is over 15 kb long coding 5,038 amino acids and this size affects the efficiency of RT-PCR amplification, cell growth during cloning and transient transfection. Construction of the entire *RYR1* coding region in a vector requires successive ligations of contiguous fragments prepared using restriction endonucleases. Enzyme selection and combination are critical in *RYR1* cloning. Current studies with this method reported to date use rabbit *RYR1* cDNA with unique enzyme sites for the construction of mutants.

A new approach in functional studies has been established recently. Knocking in an *RYR1* mutation into mice to create transgenic mice can allow the study of functional effects of the mutation *in vivo*. This technique has shown that the R163C mutation in mice leads to a hypersensitive RYR1 and Y522S causes Ca^{2+} leakage and abnormalities in mitochondria [Durham, et al., 2008; Yang, et al., 2006]. The Y522S knock-in mouse has also shown muscle contracture triggered by overheating (41°C) [Chelu, et al., 2006]. It has also been reported that the CCD I4898T mutation (I4895T in mice) causes skeletal muscle abnormalities and developmental defects in fetuses probably leading to CCD [Zvaritch, et al., 2007]. These studies have shown strong evidence for functional defects of *RYR1* mutations *in vivo*. The disadvantage of this method is the difficulty of creating knock-in mice. This technique is expensive and special equipment is required and moreover, it may take at least two years to create and propagate transgenic mice and hence it may not be feasible to analyse many *RYR1* mutations. The conditions in mice may not mimic those in humans and hence the results may differ from those using human sources for functional studies. While the transgenic knock-in mice are an extremely valuable experimental tool, their use is limited to well-funded and well-resourced laboratories.

1.14 Project outline

The sole laboratory studying MH in New Zealand is located in IMBS, Massey University. In the past decade, the main focus was screening *RYR1* using blood or muscle RNA and DNA samples obtained from regional patients, determining familial relationships and molecular genetic testing for selected MH families. Novel *RYR1* mutations have been identified in New Zealand families including R401C, T4826I and H4833Y [Anderson, et al., 2008; Brown, et al., 2000; Davis, et al., 2002]. Since a large number of mutations have been identified, functional studies of *RYR1* mutations have become the major interest to date. Identification of novel *RYR1* mutations is now very common, and they are often not reported in the literature without accompanying functional data.

Previous functional studies have adapted various methods and materials for experimental procedures and hence it is sometimes not easy to compare one result to

another. To compare several mutations, MH and CCD mutations for instance, at the same time using the same experimental conditions, it seems to be more reasonable to construct the *RYR1* cDNA and introduce mutations of interest rather than collect blood or muscle samples of patients who carry mutations. Previous work has used the rabbit *RYR1* cDNA instead of the human cDNA probably because of problems with ethical approval or the availability of unique restriction endonuclease sites. There is a previous work which has reported human *RYR1* cDNA cloning although details of cloning has not been shown and human *RYR1* cDNA has never been used for expression and functional studies [Zorzato, et al., 1990]. While the amino acid sequence identity between rabbit and human is 97%, the use of human *RYR1* cDNA may be more appropriate for comparison of mutations as there may be some structural and functional differences between RYR1 proteins from the two species. The human RYR1 mutants, for example, may provide more relevant data especially for CCD mutations because there has been no previous report of an *in vivo* animal model for CCD indicating that CCD may occur only in humans. Cloning and transfection of the human *RYR1* cDNA may contribute to further understanding of mutant RYR1 functions. Functional analyses using human cDNA may discriminate between the phenotypes resulting from MH and/or CCD mutations. In this study, the human *RYR1* cDNA was cloned into a mammalian expression vector. Site-directed mutagenesis was performed to introduce selected *RYR1* mutations associated with MH and/or CCD. The WT and mutant cDNA was then used for transient transfection.

Cell lines used for transient transfection differ depending on previous reports. Mouse dyspedic myotubes which lack the RYR1 protein represent the most physiologically relevant system to skeletal muscle compared to MHS patients. HEK-293 cells have often been used previously for expression of RYR1 proteins. As dyspedic myotubes are currently not available in New Zealand, HEK-293 cells were used for transient transfection. Transiently expressed WT and mutant RYR1 proteins were detected by western blotting and immunofluorescence.

Functional analyses in previous studies have been performed mainly by two techniques, calcium release assays and [^{3}H]ryanodine binding assays. Calcium assays detect intracellular Ca^{2+} concentrations directly. These allow the study of resting Ca^{2+}

concentrations and Ca^{2+} release as a response to triggering agents. [^{3}H]ryanodine binding assays can be used in the open state or the closed state of RYR1. Ryanodine is a plant alkaloid which specifically binds to the RYR1 only in the open state. Therefore higher ryanodine binding means a more open state of RYR1 proteins. The open state RYR1 should release Ca^{2+} to the SR in skeletal muscle cells, and hence ryanodine binding is an indirect measure of Ca^{2+} release. This analysis requires liquid scintillation counting while calcium assays require a microscope for Ca^{2+} imaging or a spectrofluorometer. In this study, the [^{3}H]ryanodine binding assay was performed as the only available equipment was a scintillation counter.

1.15 Project aims

- To clone the human *RYR1* cDNA into a mammalian expression vector
- To introduce MH and/or CCD mutations into the cloned *RYR1* cDNA using site-directed mutagenesis
- To express the WT and mutant *RYR1* cDNA in HEK-293 cells and detect expressed proteins by western blotting and immunofluorescence
- To characterise the functional effects of these mutations on the RYR1 by [^{3}H]ryanodine binding assays

CHAPTER TWO : MATERIALS AND METHODS

2.1 Materials

TRIZOL™ reagent was purchased from Invitrogen, Auckland, New Zealand.

Diethylpyrocarbonate (DEPC), chloroform and formamide were from BDH Laboratory Supplies, Poole, England. Ammonium chloride, magnesium sulfate and potassium hydrogencarbonate were from Riedel-de Haen Fine Chemicals, Seelze, Germany. Ethylenediaminetetraacetic acid (EDTA) and formaldehyde were from Ajax Chemicals, Auburn, Australia. Agarose LE was from F. Hoffmann-La Roche, Basel, Switzerland. Ethyleneglycol-bis(2-amino-ethylether)-N,N,N',N'-tetraacetic acid (EGTA), piperazine-1,4-bis(2-ethanesulfonic acid) (PIPES), bromophenol blue, xylene cyanol FF and Ficoll were purchased from Sigma-Aldrich, Auckland, New Zealand.

Platinum® *Pfx* DNA Polymerase, SuperScript™ First-Strand Synthesis System, DNase I and 1 kb plus DNA ladder were from Invitrogen.

Wizard® SV Gel and PCR Clean-Up System was from Promega, Sydney, Australia, Quantum Prep® Plasmid Miniprep Kit was from Bio-Rad, Sydney, Australia and PureLink™ HiPure Plasmid Midiprep Kit was from Invitrogen.

pBlueScript II KS or SK (+) was from Stratagene, CA, USA and pcDNA3.1(+) was from Invitrogen.

Restriction endonucleases and buffers including BSA were purchased from Roche or New England Biolabs, MA, USA.

T4 DNA ligase and RNase A were from Invitrogen.

T75 flasks, cryo tubes, 6-well plates and 96-well microtiter plates were from Nunc, Roskilde, Denmark.

Dulbecco's modified eagle's medium (DMEM) and dimethyl sulphoxide (DMSO), penicillin/streptomycin, fetal bovine serum and trypsin were from Invitrogen.

FuGENE 6 and HD, and Complete mini, EDTA-free protease inhibitor cocktail tablets were from Roche.

Bradford reagent and the mini gel system were from Bio-Rad. BM Chemiluminescence Blotting Substrate (POD) was from Roche. X-ray film, developer and fixer were from Eastman Kodak, NY, USA.

Primary antibodies including 34C, anti-PDI and anti-α-tubulin, and secondary antibody horseradish peroxidase-conjugated anti-mouse IgG were purchased from Sigma-Aldrich. Secondary antibodies used for immunofluorescence including fluorescein isothiocyanate (FITC)-conjugated anti-mouse and tetramethyl rhodamine isothiocyanate (TRITC)-conjugated anti-rabbit IgG were purchased from Jackson ImmunoResearch, PA, USA. 4',6-diamidino-2-phenylindole dihydrochloride (DAPI) was from Sigma-Aldrich.

3-[(3-cholamidopropyl)dimethylammonio]-1-propanesulfonate (CHAPS), dimethyl sulphoxide (DMSO), L-α-phosphatidylcholine, poly-D-lysine, 2-mercaptoethanol, ammonium peroxodisulfate (APS), N,N,N',N'-tetramethylethylenediamine (TEMED) and Tween 20 were from Sigma-Aldrich.

[^{3}H]ryanodine was purchased from PerkinElmer, MA, USA. GB-140 glass fibre filters were from ADVANTEC MFS, CA, USA.

All other chemicals and reagents used were of analytical grade or better.

2.2 RNA handling

Cloning of human *RYR1* started with extraction of total RNA. Complementary DNA (cDNA) was synthesised by reverse transcriptase (RT) using extracted mRNA. Synthesised cDNA was used as a template for polymerase chain reaction (PCR). Total RNA was extracted from blood or skeletal muscle samples that were obtained from MHN individuals with informed consent. Blood and muscle samples were stored at -20°C or -80°C, respectively.

2.2.1 RNA extraction from muscle

TRIZOL™ reagent is a mono-phasic solution for the isolation of total RNA from fluids, tissues or cells of a wide range of species including humans. It consists of phenol and guanidine isothiocyanate and is an improved method of the previous one developed in 1987 [Chomczynski and Sacchi, 1987]. During sample homogenisation or lysis, TRIZOL reagent maintains the integrity of RNA and prevents RNase degradation. Added chloroform separates the solution into an aqueous phase and an organic phase. The aqueous phase retains RNA exclusively, but DNA and proteins transfer to the organic phase. RNA in the aqueous phase is recovered by precipitation with isopropyl alcohol. This technique allows the use of small quantities of tissue (50 mg) and cells (5×10^6), or large quantities of tissue (>1 g) and cells ($>10^7$). Total RNA isolated by this reagent is free of protein and DNA contamination, and can be used for several types of experiments including RT-PCR (reverse transcription-polymerase chain reaction). Expected yields of RNA from human skeletal muscle are 1-1.5 μg per 1 mg tissue (manufacturer's instructions).

As RNA is easily degraded by RNase, which is quite stable, it is important to guard against contamination by RNase and subsequent RNA degradation. All equipment coming in contact with RNA including tips, tubes and glassware, was treated with DEPC-treated water. Sterile water was treated with 0.01% (v/v) diethylpyrocarbonate (DEPC), and plastic and glass items were soaked in DEPC-treated water overnight, and then autoclaved.

Frozen skeletal muscle (50-100 mg) was placed on a cold steel plate and crushed to a

fine powder using a mortar designed for rock crushing. Muscle tissues and steel tools were kept cold using liquid nitrogen. The powdered tissue was transferred to a 15 mL round-bottom centrifuge tube containing 0.75 mL of TRIZOL reagent. The solution was homogenised using an ultra-Turax T25 and allowed to stand 5 minutes at room temperature. Addition of 0.2 mL of chloroform followed by centrifugation separated the solution into an aqueous phase and an organic phase. After removal of the aqueous phase, the RNA pellet was collected by precipitation with 0.5 mL of isopropanol. The pellet was washed with 1 mL of 75% ethanol and completely dried using a speedvac for 5 minutes. The RNA pellet was redissolved in 30 µL of DEPC-treated water and was stored at 4°C although RNA samples were normally all used within a few days. Concentrations of RNA samples were calculated by absorption at 260 and 280 nm using an Ultraspec 3000 UV/Visible Spectrophotometer (Pharmacia Biotech) with 100 µL cuvettes. An absorbance of 1.0 at 260 nm is equivalent to an [RNA] of 40 µg/mL while, an $A_{260/280}$ ratio of 2.0 is considered to be pure RNA [Sambrook, et al., 1989].

2.2.2 RNA extraction from blood

The RYR1 proteins are expressed in white blood cells as well as in skeletal muscle cells and hence blood samples can also be a source of *RYR1* mRNA. The total RNA including *RYR1* was isolated from human leukocytes using TRIZOL reagent as reported previously [Kraev, et al., 2003]. One half to 1 mL of a blood sample was mixed with three volumes of ice-cold red blood cell lysis buffer containing 150 mM NH_4Cl, 10 mM KH_2CO_3 and 0.1 mM EDTA for 10 minutes on ice. Reaction mixtures were centrifuged 10 minutes at 1,500 g and the supernatant was removed. The pellet was suspended in 0.75 mL of TRIZOL reagent and homogenised by vigorous pipetting. RNA was extracted using the same procedures as for muscle samples as described in section 2.2.1.

2.2.3 First-strand cDNA synthesis

Total RNA including *RYR1* mRNA extracted from blood or muscle samples of MHN individuals was used as a template for synthesis of first-strand of cDNA using SuperScript™ First-Strand Synthesis System. The first-strand cDNA synthesis was catalysed by SuperScript™ III Reverse Transcriptase. Random hexamers were used to

prime the first-strand synthesis for all reactions. One half to 1.0 µg of total RNA was mixed with 1 µL of random hexamers (50 ng/µL), 1 µL of 10 mM dNTP mix and DEPC-treated water to achieve a 13 µL total volume. The mixture was incubated at 65°C for 5 minutes for initial denaturation, and then placed on ice for 1 minute. Seven µL of reaction mixture prepared as a cocktail was then added to the solution. The reaction mixture contained 4 µL of 5× First-strand buffer (250 mM Tris-HCl, pH 8.3, 375 mM KCl, 15 mM $MgCl_2$), 1 µL of 0.1 M DTT, 1 µL of RNaseOUT™ Recombinant RNase Inhibitor (40 units/µL) and 1 µL of SuperScript™ III RT (200 units/µL). The solution was then incubated at 25°C for 5 minutes for annealing of random hexamers followed by incubation at 50°C for 1 hour for elongation. The reaction was terminated by incubation at 70°C for 15 minutes. The mixture was placed on ice and 1 µL of RNase H (2 units/µL) was added and incubated at 37°C for 20 minutes for degradation of template total RNA. Solutions were stored -20°C until use, and 1-2 µL of 10-fold dilutions were used as a template for subsequent PCR.

2.3 DNA handling

2.3.1 PCR

The Polymerase Chain Reaction (PCR) was used to amplify *RYR1* cDNA fragments using first strand cDNA as a template. Reaction cycles were performed using an FTS-320 thermal sequencer (Corbett Research) or GeneAmp® PCR System 2700 (Applied Biosystems). Platinum® *Pfx* DNA Polymerase (Invitrogen) was used in this project for cloning and site-directed mutagenesis. This enzyme has 3’ to 5’ exonuclease proofreading activity and thus provides higher fidelity than *Taq* polymerase. Reaction composition and cycles were designed as general procedures according to the manufacturer’s instructions.

2.3.2 Site-directed mutagenesis

Site-directed mutagenesis for mutant *RYR1* cDNA construction was performed with megaprimer PCR using whole plasmids (MEGAWHOP) [Miyazaki and Takenouchi, 2002]. This is a modified technique of the QuikChange® method amplifying initial megaprimers. PCR was performed using Platinum® *Pfx* DNA Polymerase and either

forward or reverse primers containing a mutation. PCR reactions for mutagenesis consisted of 1 cycle of 94°C for 5 minutes for denaturation followed by 20 cycles of 94°C for 30 seconds, 60°C for 30 seconds and 68°C for 30 seconds followed by 25 cycles of 94°C for 1 minute, 60°C for 1 minute and 68°C for 10 minutes followed by 1 cycle of 68°C for 5 minutes. Reaction mixtures were then diluted two fold with water and incubated with 1 µL of *Dpn*I at 37°C for 1 hour.

2.3.3 DNA electrophoresis

DNA fragments were analysed by gel electrophoresis using 1% agarose LE, 0.4 µg/mL ethidium bromide and 1× TAE (40 mM Tris-acetate, 1 mM EDTA, pH 8.0) as the electrophoresis buffer. DNA samples were loaded onto gels with 5× DNA loading buffer (0.4% bromophenol blue, 0.1% xylene cyanol FF, 15% Ficoll in water). The gels were electrophoresed for 60 minutes at 80-100 V and DNA fragments were visualised under UV light.

2.3.4 DNA purification

DNA fragments needed to be purified for direct sequencing, endonuclease digestion or ligation. PCR fragments and DNA fragments after endonuclease digestion were purified using Wizard® SV Gel and PCR Clean-Up System (Promega) and plasmids constructed for *RYR1* cloning were purified using Quantum Prep® Plasmid Miniprep Kit (Bio-Rad) or PureLink™ HiPure Plasmid Midiprep Kit (Invitrogen). DNA quantification was performed by measuring absorbance at 260 and 280 nm using an Ultraspec 3000 UV/Visible Spectrophotometer (Pharmacia Biotech) with 100 µL cuvettes. An absorbance at 260 nM of 1.0 is equivalent to a [DNA] of 50 µg/mL, while an $A_{260/280}$ ratio of 1.8 is considered to be pure DNA [Sambrook, et al., 1989].

2.3.5 Direct sequencing

After subcloning followed by purification, 300-500 ng/µL of plasmid DNA was directly sequenced using an ABI 3730 Genetic Analyser with Big Dye terminator chemistry. Sequencing primers were diluted to 3.2 pmol/µL for use. This procedure was performed at the Allan Wilson Centre Genome Service by Ms Lorraine Berry (Massey University). The sequencing data were analysed using CLUSTAL W

[Thompson, et al., 1994].

2.4 Cloning

The human *RYR1* cDNA is 15,117 bp long and therefore it was not feasible to amplify the full length of this coding region from mRNA in one step. Approximately 1 kb fragments were amplified by PCR using the first strand cDNA as a template, and then these PCR products were subcloned in pBlueScript II KS or SK (+) (Stratagene) and were sequenced directly. Plasmids were then digested by restriction endonucleases for subsequent ligation and subcloning. The entire *RYR1* cDNA was cloned in the mammalian expression vector, pcDNA3.1(+) (Invitrogen) for RYR1 protein expression in HEK-293 cells.

2.4.1 Restriction endonuclease digestion

Plasmids were digested with one or two restriction endonucleases to obtain *RYR1* cDNA fragments. Conditions including buffer and temperature are dependent on the combination of restriction endonucleases although most reactions were performed overnight at 37-50°C in a total volume of 20 µL with 1 µg DNA, 100 µg/mL of bovine serum albumin (BSA) and 1 µL (~20 units) of restriction endonuclease. Reaction mixtures were electrophoresed and DNA fragments of interest were excised from the gel and purified using Wizard® SV Gel and PCR Clean-Up System (Promega) if the fragments were required for subsequent cloning.

2.4.2 Ligation

Ligation was performed using T4 DNA ligase (Invitrogen) according to the manufacturer's instructions. Most reactions were performed in a total volume of 10 µL including 1 µL (1 unit/µL) of ligase, 2 µL of 5× ligase reaction buffer (250 mM Tris-HCl, pH 7.6, 50 mM $MgCl_2$, 5 mM ATP, 5 mM DTT, 25% (w/v) polyethylene glycol-8000), digested plasmid vectors pBluescript or pcDNA3.1 (10-100 pg), and one or two digested DNA fragment inserts (~1 ng in total). Molar concentrations of inserts were normally 3-10 times higher than molar concentrations of the plasmid vectors. Samples were incubated at 4°C in fridge overnight for small inserts or 16°C overnight for long inserts.

2.4.3 *Transformation of E. coli*

Transformation was carried out using *E. coli* DH5α competent cells prepared by the Inoue method [Inoue, et al., 1990]. A single colony of DH5α was picked up and incubated in 25 mL of SOB (20 g of bacto tryptone, 5 g of bacto yeast extract, 0.5 g NaCl, 10 mL of 250 mM KCl, 0.2 mL of 5 M NaOH, 10 mL of 1 M $MgCl_2$, 10 mL of 1 M $MgSO_4$ and H_2O to 1 L) at 37°C 6-8 hours at 250 rpm shaking. Ten mL of this starter culture was added to 250 mL of SOB and incubated at 18-22°C overnight at 200 rpm shaking. After OD_{600} reached 0.4-0.8, cells were placed on ice. After pelleting, cells were resuspended in 80 mL of transformation buffer (55 mM $MnCl_2$, 15 mM $CaCl_2$, 250 mM KCl, 10 mM PIPES, pH6.7). Cells were pelleted again and resuspended in 20 mL transformation buffer and 1.5 mL of DMSO was added. Cells were aliquoted in 100 µL and freezed immediately in liquid nitrogen. Frozen tubes were stored under -70°C.

Five µL of the ligation mixture was mixed with 100 µL of competent DH5α cells for 20 minutes on ice. Sample mixtures were incubated at 42°C for 1 minute and then plunged in ice for 2 minutes. Samples were diluted with 900 µL of SOC (20 g of bacto tryptone, 5 g of bacto yeast extract, 0.5 g NaCl, 0.2 mL of 5 M NaOH, 10 mL of 1 M $MgCl_2$, 10 mL of 1 M $MgSO_4$, 20 mL of 1 M glucose and H_2O to 1 L) and were incubated at 37°C for 1 hour. Fifty to 200 µL of these diluted mixtures were streaked on LB agar plates containing 50 µg/mL ampicillin with 50 µL of 20 mg/mL X-gal and 20 µL of 0.1 M IPTG spread on the surface. Plates were incubated at 37°C overnight but not over 16 hours.

2.4.4 *Inoculation*

Single colonies were picked into 500 µL of super LB (SLB, LB with 20 mM glucose and 20 mM $MgCl_2$) for manual plasmid preparation, 2 mL of LB for miniprep or 50 mL of LB for midiprep. Solutions were incubated at 30-37°C for 12-16 hours with constant shaking. Inoculation using SLB was performed in duplicate to use one sample for the manual preparation and the other sample for preparation of glycerol stocks.

2.4.5 Manual plasmid preparation

After subcloning, manual plasmid preparations were performed initially to check that cloning was successful. Cells in 500 µL of SLB were pelleted by centrifugation. The other sample was mixed with 200 µL of 50% glycerol and stored at -80°C. Cell pellets were resuspended in 100 µL of Solution I (50 mM glucose, 25 mM Tris, 10 mM EDTA, pH 8.0) on ice. Two hundred µL of Solution II (0.2 M NaOH and 1% SDS) was added and incubated for 5 minutes on ice. One hundred and fifty µL of Solution III (3 M potassium acetate, 9.2 mL glacial acetic acid, H_2O to 80 mL) was added and incubated for 5 minutes on ice. After 5 minutes centrifugation at 12,000 g at 4°C, the supernatant was collected and mixed with 500 µL isopropanol. After 5-10 minutes, samples were centrifuged 10 minutes at 12,000 g at 4°C and DNA pellets were collected and then washed with 1 mL of 70% ethanol. DNA pellets were dried using a speedvac and redissolved in 30 µL of water and incubated at 37°C for 1 hour with 1 µL of RNase A (10 mg/mL) to dissolve the DNA completely and digest unwanted RNA. Yields were typically 100-130 ng/µL.

2.4.6 Mini or Midiprep

If the manual preparation showed that the subcloning was successful, cells from the same colony were used to inoculate 2 mL of LB and were incubated at 37°C overnight. A Quantum Prep® Plasmid Miniprep Kit (Bio-Rad) was used to purify plasmids of interest for restriction endonuclease digestion and further subcloning.

The full length WT or mutant *RYR1* cDNA clone was used to inoculate 50 mL of LB from colonies for midiprep using PureLink™ HiPure Plasmid Midiprep Kit (Invitrogen). The incubation time after inoculation of *RYR1* cDNA clone was strictly controlled. Over 12 hours of incubation at 37°C did not produce successful plasmid propagation in *E.coli* DH5α probably because the size of *RYR1* is too large for *E.coli* to carry the plasmid for a long length of time. Incubation was performed first at 30°C overnight (12-16 hours) and then at 37°C for 1-5 hours depending on the cell density observed visually in the glass flask. Manual plasmid preparation was performed first using 1 mL of the 50 mL culture to check that the inoculation had been successful and the condition of the *RYR1* cDNA clone was acceptable. Midipreps were performed

according to the manufacturer's instructions. Yields of plasmid DNA were typically 1 µg/µL in 100 µL TE.

2.5 Cell culture

HEK-293 cells were used for RYR1 expression. Transient transfection was performed using the purified *RYR1* cDNA. Procedures for cell cultures were performed in a class I or class II biohazard cabinet.

2.5.1 Starting frozen HEK-293 cells

Cell stocks of HEK-293 stored in liquid N_2 were placed on ice until thawed. Thawed cells were mixed with 5 mL of the medium (Dulbecco's Modified Eagle's Medium (DMEM) containing 10% fetal bovine serum and 1% penicillin/streptomycin). Cells were pelleted by centrifugation for 5 minutes at 4,000 g. Cell pellets were resuspended in 2 mL medium. One mL of cell suspension was transferred to a T75 flask containing 14 mL medium. Flasks were incubated for 2-3 days at 37°C and 5% CO_2.

2.5.2 Passage of HEK-293 cells

Cells became 80-90% confluent after 2-3 days. Spent medium was removed and adhered cells were washed with 0.5× trypsin in PBSE (PBS with 0.5 mM EDTA, PBS: phosphate buffered saline, 137 mM NaCl, 2.68 mM KCl, 8.1 mM Na_2HPO_4, 1.47 mM KH_2PO_4, pH 7.4) and incubated at 37°C for 10 minutes. Cells were removed from the plate and then pelleted and resuspended in 5-6 mL medium. One mL of cells was transferred to new T75 flasks with 14 mL medium.

2.5.3 Freezing HEK-293 cells

Ninety-100% confluent cells were used after 3-5 days from starting or passage. Cells were washed with trypsin as above and cell pellets were collected. Pellets were resuspended in fetal bovine serum containing 10% DMSO and placed in cryo tubes. Tubes were wrapped in tissue and placed at -80°C overnight. Tubes were then unwrapped and transferred to liquid N_2 for long term storage.

2.5.4 Transfection of HEK-293 cells

Transient transfection was performed for immunofluorescence and [^{3}H]ryanodine binding assays. HEK-293 cells were passaged in T75 flasks for [^{3}H]ryanodine binding assays and incubated until 90% confluent. Transient transfection was performed using FuGENE HD (Roche) according to the manufacturer's instructions. Eighteen µg of WT or mutant *RYR1* cDNA clones and 72 µL of FuGENE HD were used per flask. Detailed procedures for immunofluorescence are described in the section 2.6.3.

2.5.5 Harvesting transfected HEK-293 cells

Cells were harvested in PBS 72 hours after transfection. Pelleted cells were solubilised in cell lysis buffer (0.1 M Tris, 0.5% (v/v) Triton X-100, pH 7.8) for 15 minutes at 37°C for western blotting or in CHAPS buffer (150 mM NaCl, 50 mM Tris-Cl, pH 8.0, 1% CHAPS, 5 mg/mL L-α-phosphatidylcholine, 1× Complete mini, EDTA-free protease inhibitor cocktail tablets (Roche)) for 45 minutes on ice for [^{3}H]ryanodine binding assays. Approximately 1/100 of cell pellets were solubilised in cell lysis buffer and remaining cells were solubilised in CHAPS buffer. Samples were centrifuged at 10,000 g for 10 minutes at 4°C after incubation and supernatants were collected and stored at -20°C or -80°C for western blotting or immunofluorescence, respectively.

2.6 Protein handling

2.6.1 Bradford assay

Protein concentrations were determined by Bradford assay [Bradford, 1976] to calculate total protein concentrations in cell lysate. BSA (10 mg/mL) was diluted with water to obtain standard samples with concentrations of 0, 0.5, 1, 1.5, 2 and 2.5 µg/µL. Five µL of protein and BSA standard samples were placed in a 96-well microtiter plate and mixed with 195 µL of 5-fold diluted Bradford Reagent (Bio-Rad) with water for 10 minutes at room temperature. Absorbance at 595 nm was measured using a plate reader htII spectrometer (Sci Tech). A standard curve was obtained using BSA standard samples and concentrations of protein samples of interest were calculated using the standard curve.

2.6.2 Western blotting

Expressed RYR1 protein was analysed by immunoblotting using monoclonal antibody 34C (Sigma-Aldrich). Five to 20 µg of solubilised protein (16 µL) in cell lysis buffer was incubated with 4 µL of 5× sample buffer (60 mM Tris-Cl, pH 6.8, 25% glycerol, 2% SDS, 14.4 mM 2-mercaptoethanol, 0.1% bromophenol blue) for 10 minutes at room temperature. SDS-PAGE gels (7.5%, 0.75 mm) were prepared using the Bio-Rad mini gel system with components as listed in Table 2-1.

	7.5% Resolution gel	4% Stacking gel
H_2O	5.5 mL	3.15 mL
acrylamide-bis solution (40%, 29.1:0.9)	1.9 mL	500 µL
1.5 M Tris-Cl, pH 8.8	2.5 mL	-
0.5 M Tris-Cl, pH 6.8	-	1.25 mL
10% SDS	100 µL	50 µL
10% APS	50 µL	25 µL
TEMED	5 µL	5 µL

Table 2-1 Components for SDS-PAGE gel

Western blotting using an SDS-PAGE gel was performed to detect the expressed RYR1 protein. Gels were prepared in a pair using a mini gel kit and two gels were electrophoresed at the same time to analyse the maximum number of samples (10 wells per gel) in the same conditions.

Protein solutions including sample buffer were loaded into the wells and electrophoresed at 20 mA for 1-1.5 hours using protein gel running buffer (25 mM Tris, 190 mM glycine, 0.1% SDS). The gels were soaked in transfer buffer (15.6 mM Tris, 120 mM glycine, 10% methanol) for 10 minutes and then blotted onto a nitrocellulose membrane (Roche) at 30 V overnight at 4°C using transfer buffer. The membrane was washed with TBS (tris buffered saline, 50 mM Tris, 150 mM NaCl, pH 7.5) and was blocked using 1% blocking solution (Roche) for 1 hour at room temperature or 4°C overnight. The blots were then incubated with primary antibodies, 34C (mouse origin) for the RYR1 protein and anti-α-tubulin (mouse origin) for the control at a dilution of 1:5000 in TBS containing 0.5% Blocking Solution for 1 hour at room temperature or 4°C overnight. After washing four times for 10 minutes each with TBST (TBS containing 0.1% (v/v) Tween 20) the blots were incubated with secondary antibody, horseradish peroxidase-conjugated anti-mouse IgG at a dilution of 1:5000 in TBS containing 0.5% blocking solution for 1 hour at room temperature or 4°C overnight. Washing with TBST four times for 10 minutes each was carried out after incubation. The expressed RYR1 protein and tubulin as a control were detected on an X-ray film using BM Chemiluminescence Blotting Substrate (Roche) and an automated X-ray film processor according to the manufacturer's instructions.

2.6.3 Immunofluorescence

Transient transfection using 6-well plates was performed for immunofluorescence. A glass cover slip was placed in a well and 1 mL of 0.01% (w/v) poly-D-lysine was placed on top. The plate was left standing 1 hour under UV. This procedure prevents HEK-293 cells coming off the glass cover slip and helps them to remain adhered during washing procedures. Poly-D-lysine was removed and replaced by 2 mL of DMEM medium. Approximately 5×10^6 cells (50-100) µL of starting cell solution was added and the plate was incubated 1-2 days until 20-30% confluent. Transient transfection was performed using FuGENE 6 (Roche) according to the manufacturer's instructions. One µg of DNA and 3 µL of FuGENE 6 were used and the plate was incubated for 72 hours after transfection. After incubation, the medium was removed and the glass cover slip was briefly washed in PBS, and the cells were fixed with 1 mL of 3.7% (w/w) formaldehyde in PBS for 20 minutes at room temperature. Each slip

was then washed with PBS three times for 10 minutes each and incubated with 50 mM NH_4Cl in PBS for 10 minutes. The cells were permeabilised using 0.1% Triton X-100 in PBS for 5 minutes. The cover slips were then washed briefly with PBS and blocked using 1% blocking solution in PBS for 1 hour at room temperature. Each cover slip was then incubated overnight at 4°C with primary antibodies, 34C (1:1000) for the RYR1 protein and anti-protein disulfide isomerase (PDI) (rabbit origin, 1:1000) as the endoplasmic reticulum (ER) marker. After washing with PBS four times for 10 minutes each, the cover slips were incubated overnight at 4°C with secondary antibodies, fluorescein isothiocyanate (FITC)-labeled goat anti-mouse IgG (1:200) for 34C and tetramethylrhodamine isothiocyanate (TRITC)-labeled goat anti-rabbit IgG (1:200) for anti-PDI. The PBS solution with antibodies was then removed and the slips were incubated with 1 µL of 2 mg/mL 4',6-diamidino-2-phenylindole (DAPI) in 1 mL of PBS for 30 minutes at 30°C covered by aluminium foil to avoid unnecessary light exposure. The cover slips were washed with PBS four times for 10 minutes each and were observed under a fluorescence microscope (BX51, Olympus).

2.7 [^{3}H]ryanodine binding assay

2.7.1 Assay for 4-CmC activation

Harvested cells were analysed first by western blotting and if this showed that transient transfection was successful and expression levels of RYR1 proteins were sufficient for [^{3}H]ryanodine binding assays, the remaining cell pellets were solubilised in CHAPS buffer and stored at -80°C until use. Approximately 100 µg of crude proteins were incubated with binding buffer containing 25 mM PIPES, 1 M KCl, 0.5 mM EGTA, 100 nM free Ca^{2+}, 1× Complete mini, EDTA-free protease inhibitor cocktail tablets (Roche), pH 7.3, with 1 nM [^{3}H]ryanodine (PerkinElmer) and various concentrations of 4-C*m*C for 3 hours at 37°C. Concentrations of 4-C*m*C adopted for analyses were 0, 10, 50, 100, 200, 250, 300 and 500 µM. The concentrations of free Ca^{2+} adjusted by the amount of $CaCl_2$ in the binding solution were calculated using the computer software WINMAXC (v2.50, Chris Patton, Stanford University) [Patton, et al., 2004]. Binding reactions were quenched by rapid filtration through GB-140 glass fibre filters (ADVANTEC) using a Millipore manifold. The filters were washed twice with 10 mL

of ice-cold washing buffer (20 mM Tris, 250 mM KCl, 15 mM NaCl, pH 7.1) and were soaked in 1 mL of scintillation fluid (0.4% (w/v) PPO, 0.01% (w/v) POPOP, 30% Triton X-100 in toluene) overnight at room temperature. The radioactivity remaining on the filters was determined by liquid scintillation counting to quantify bound [^{3}H]ryanodine.

2.7.2 Assay for Mg^{2+} inhibition

Assays for Mg^{2+} were performed with 10 µM free Ca^{2+}, without 4-C*m*C and with various concentrations of Mg^{2+}. Concentrations of Mg^{2+} used were 0.5, 1, 3, 5, 10 and 30 mM. Concentrations of free Ca^{2+} and Mg^{2+} in the reaction solution were adjusted with $CaCl_2$ and $MgCl_2$, respectively and amounts of these to be added were calculated using WINMAXC.

2.7.3 Assay for [^{3}H]ryanodine

Assays for [^{3}H]ryanodine were performed with 10 µM Ca^{2+}, without 4-C*m*C and Mg^{2+} and with various concentrations of [^{3}H]ryanodine. Concentrations of [^{3}H]ryanodine used were 5, 10, 15, 20, 25 and 30 nM.

2.7.4 Data analysis

Results were obtained as mean ± standard error of the mean (SEM). Statistical significance (*$p<0.05$, **$p<0.001$) was determined using an unpaired Student's *t*-test. A p value, sigmoidal curve fitting for half maximal effective concentration (EC_{50}) and half maximal inhibitory concentration (IC_{50}), and linear fitting and Scatchard analyses for equilibrium binding parameters were determined using ORIGIN computer software (Microcal Software) [Thomsett-Scott, 2009].

CHAPTER THREE : RESULTS

3.1 Cloning of human *RYR1* cDNA

3.1.1 PCR for RYR1 cDNA fragments

The human *RYR1* cDNA was cloned for RYR1 protein expression and subsequent functional analyses. Total cellular RNA was extracted from blood or muscle samples of MHN individuals and reverse transcription produced the first strand cDNA from *RYR1* mRNA. Approximately 1 kb fragments were amplified using this first strand cDNA as a template to cover the entire *RYR1* cDNA. Figure 3-1 shows the strategy of *RYR1* amplification and the primers used are listed in Appendix 1. Each PCR fragment was subcloned into a general cloning vector, pBluescript II KS or SK. As *Pfx* DNA polymerase was used, PCR fragments had blunt ends. The pBluescript vector was digested with *Eco*RV to make blunt ends and each PCR fragment was inserted into this digested vector. After transformation of *E.coli*, several colonies were selected and restriction endonuclease digestion of plasmid preparations was performed to check that the PCR fragment of interest had been inserted successfully. The direction of inserted fragments was normally ignored except for some fragments such as pBSKS+817 (Figure 3-2) in order to utilise the cloning site of the vector. Purified plasmids were sequenced to ensure that the amplified fragments had no unwanted mutations. Plasmids were then digested by restriction endonucleases for subsequent ligation and subcloning to build the complete cDNA sequence.

3.1.2 Connecting individual fragments

PCR fragments were connected by ligation and subcloned as longer fragments. Figure 3-2 shows the basic concept of fragment connection. The nomenclature of subclones is based on the length of PCR products or the restriction endonucleases used for digestion. The subclone pBSKS+817 describes, for example, pBluescript II KS digested by *Eco*RV, with the 817 bp insert amplified by PCR using -7 and 248 primers. The name pBSXA+ indicates that the cloning vector was pBluescript (pBS) and XA+ indicates the inserted fragment lies between the unique *Xba*I and *Apa*I sites of the *RYR1* coding sequence. Figure 3-3 shows the enzyme map of *RYR1* cDNA used in this study.

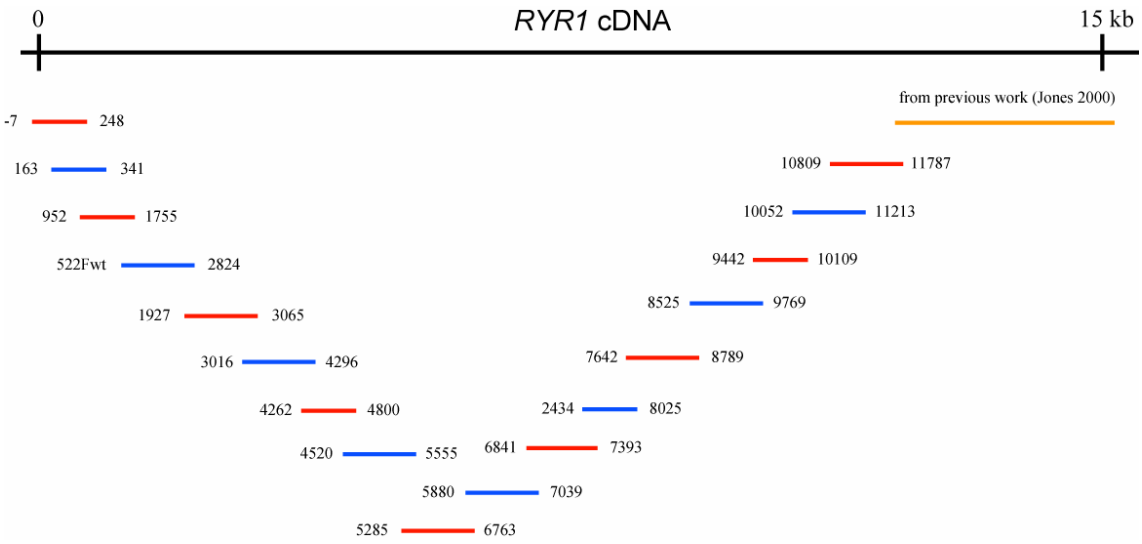

Figure 3-1 PCR strategy for *RYR1* cDNA

The template first strand cDNA was synthesised by reverse transcription from mRNA followed by PCR to amplify ~1 kb fragments (blue or red lines) using primers as shown. A total of 18 fragments was required to cover the complete coding sequence of *RYR1*. Each fragment was subcloned into pBluescript for subsequent restriction endonuclease digestion and fragment connection. The C-terminal region (orange line) was obtained from the pSVK3.5 vector constructed in previous work [Jones, 2000].

3.1.3 Cloning of the N-terminal region of RYR1 cDNA

The pBSXC+ subclone contains the N-terminal region of *RYR1* cDNA from the ATG start codon to the unique *Sac*I site (position at 2,635 bp). It consists of four PCR subclones and two connected fragment subclones described in Figure 3-4 and Table 3-1. The pBSXC+ subclone contains the N-terminal hotspot region 1 of *RYR1* mutations and hence it was later used as a template for site-directed mutagenesis to produce the R163C and G248R mutations.

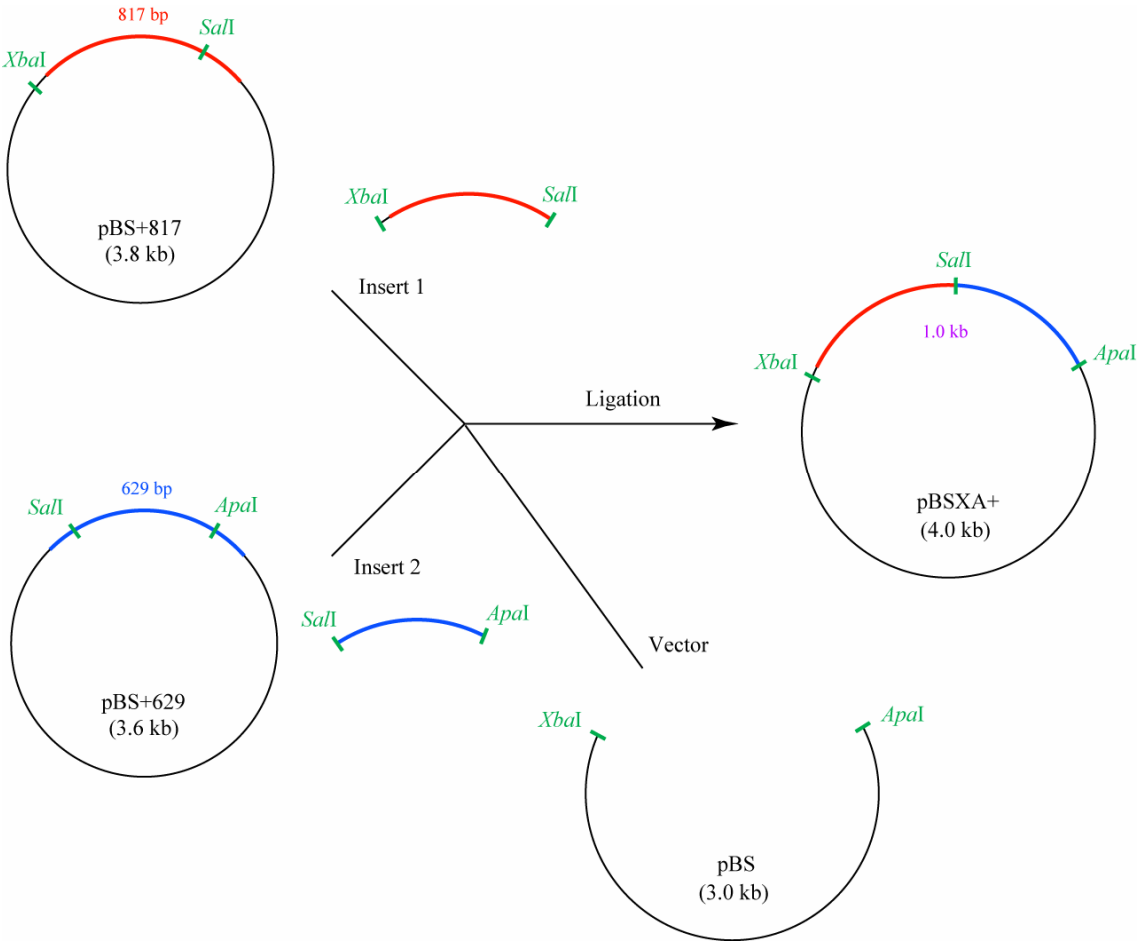

Figure 3-2 General strategy used to connect PCR fragments

PCR fragments were subcloned and the resultant plasmids were digested by two restriction endonucleases to obtain two insert fragments. These two fragments were connected by ligation at the enzyme site in the middle (*Sal*I in this figure). The connected fragments were subcloned for further digestion and subcloning to construct the entire *RYR1* cDNA. Cloning for fragment connections was carried out to connect two digested fragments into one cloning vector. Cloning of three fragments into one vector per ligation was not able to be used to obtain connected fragments after transformation. At later stages of cloning the *RYR1* cDNA fragments into vectors, only one fragment was used per ligation as larger (>7 kb) fragments proved too difficult to clone with more than one fragment.

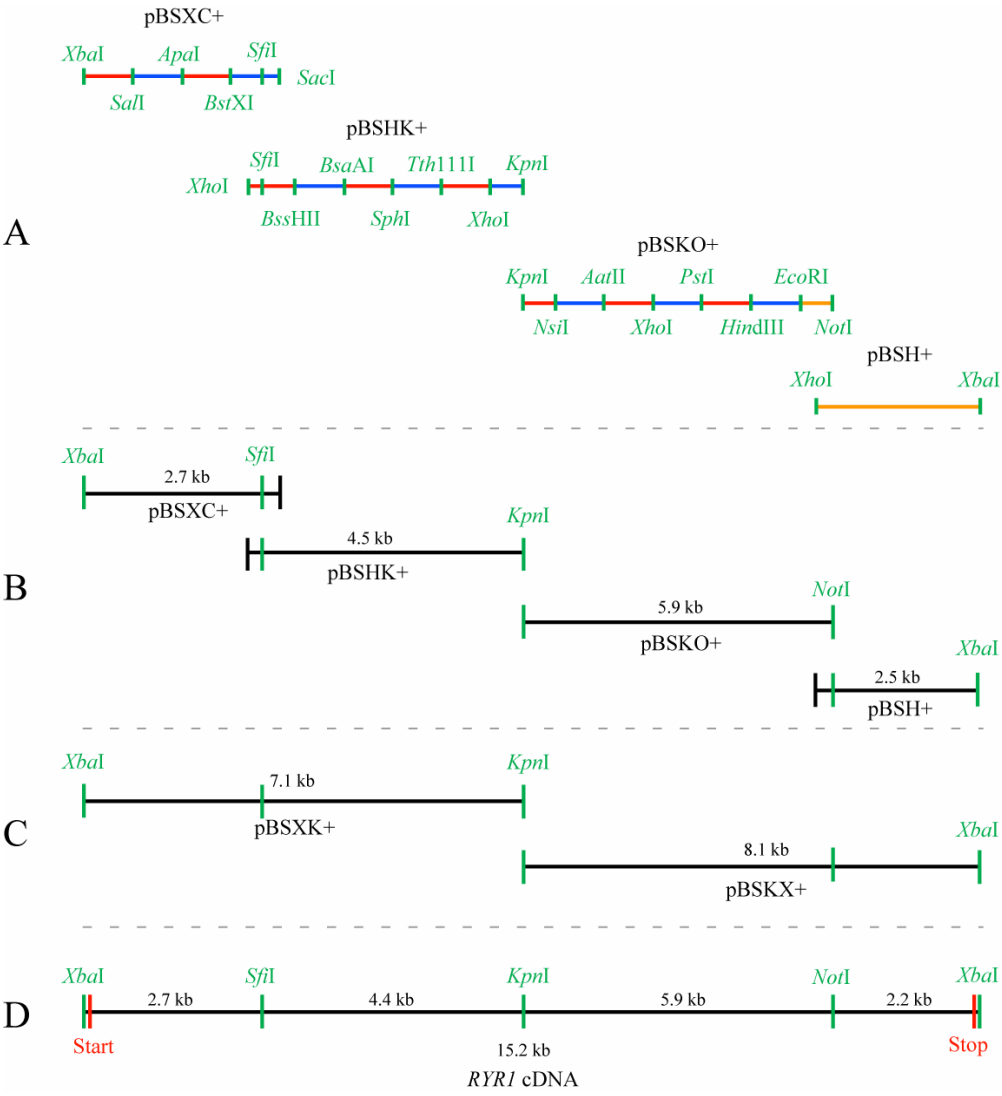

Figure 3-3 Enzyme map of *RYR1*

A subclone which has a PCR fragment (red or blue lines) was digested by the restriction enzyme shown and two fragments were connected at the enzyme site by ligation and subcloning to construct longer fragments of *RYR1* (A). The entire *RYR1* cDNA consists of four major subclones: pBSXC+, pBSHK+, pBSKO+ and pBSH+ (B). *Xba*I does not digest *RYR1* cDNA and hence it was used for both sides of the coding sequence. *Kpn*I digests only once in the middle of *RYR1*, therefore it was used for connection of the fragments from pBSXK+ and pBSKX+ (C), to complete the *RYR1* cDNA cloning. Available unique restriction endonucleases which digest *RYR1* only once were *Sal*I and *Kpn*I. As other restriction enzymes digest several times, enzyme selection and the order of fragment connections were carefully designed. Over 40 subclones were required to complete the 15.2 kb *RYR1* cDNA (D).

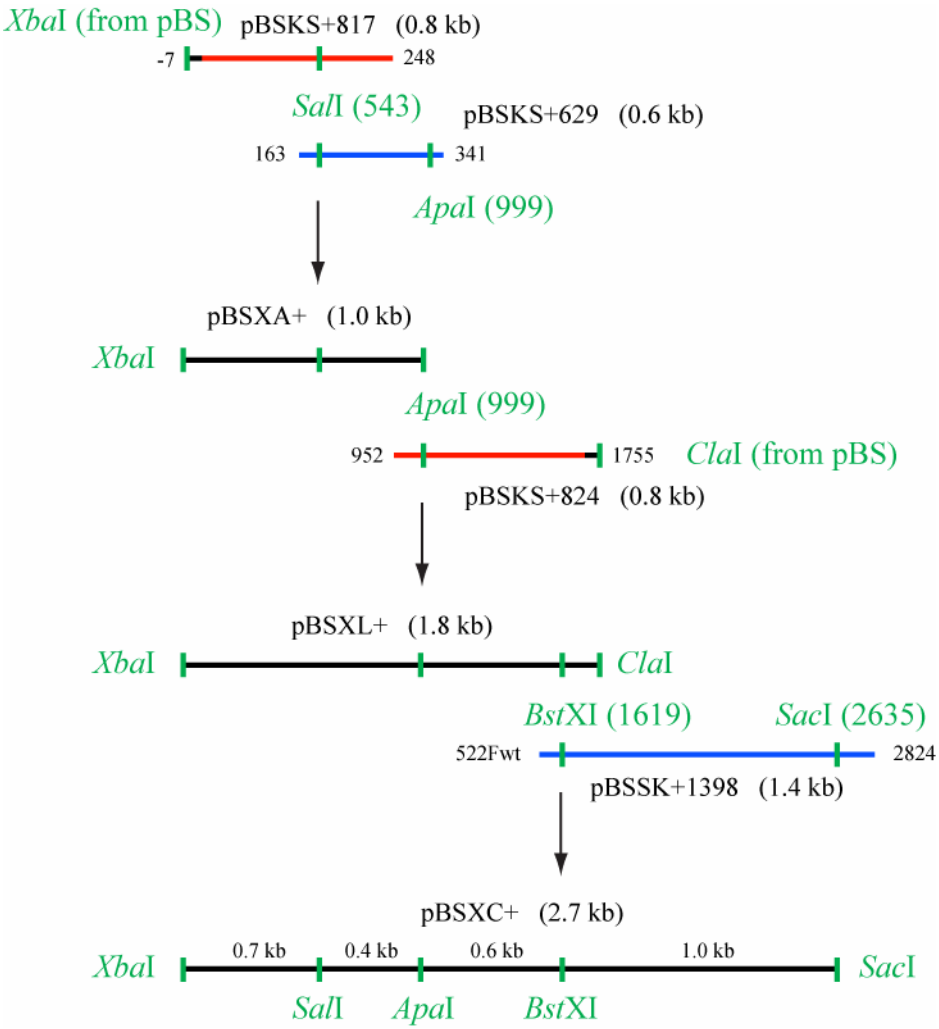

Figure 3-4 Construction of pBSXC+

This figure represents the order of fragment connection and the location of restriction endonuclease sites within the *RYR1* cDNA that were used in construction of the pBSXC+ subclone. Fragment sizes are given in kb. Blue and red lines indicate PCR fragments inserted in pBS with forward and reverse primers identified by number. The numbers of nucleotides are based on the *RYR1* sequence MIM# 180901. The pBSXC+ subclone consists of six subclones that make up the 5'-end of *RYR1* cDNA.

Target	Vector	Insert 1	Insert 2	5’ end	Middle	3’ end
pBSKS+817	pBS	PCR (F: -7, R: 248)				
pBSKS+629	pBS	PCR (F: 163, R: 341)				
pBSKS+824	pBS	PCR (F: 952, R: 1755)				
pBSSK+1398	pBS	PCR (F: 522Fwt, R: 2824)				
pBSXA+	pBS	pBSKS+817	pBSKS+629	*Xba*I	*Sal*I	*Apa*I
pBSXL+	pBS	pBSXA+	pBSKS+824	*Xba*I	*Apa*I	*Cla*I
pBSXC+	pBS	pBSXL+	pBSSK+1398	*Xba*I	*Bst*XI	*Sac*I

Table 3-1 Subclones for pBSXC+

This table shows a list of the subclones used for pBSXC+ construction and enzyme information. The pBSKS+817 subclone, for example, consisted of pBluescript as the cloning vector digested by *Eco*RV for blunt ends and a PCR fragment insert amplified using primers -7 and 248. The pBSXC+ subclone consists of pBluescript digested by two enzymes *Xba*I and *Sac*I (5’ and 3’ ends, respectively), and two inserts: the fragment from pBSXL+ digested by *Xba*I and *Bst*XI (5’ end and Middle), and the fragment from pBSSK+1398 digested by *Bst*XI and *Sac*I (Middle and 3’ end). The two inserts were connected at the *Bst*XI site. The pBSXC+ subclone was then used for further digestion and subcloning. F and R refer to the primers used in the initial PCR to obtain *RYR1* fragments. Primer names are based on nucleotide numbers of *RYR1* cDNA. Details of primers including the location in the *RYR1* sequence used in this study, MIM# 180901, are shown in Appendix 1.

3.1.4 Cloning of the central region of RYR1 cDNA

The central region of *RYR1* cDNA has a large number of restriction enzyme sites and has few unique sites such as *Kpn*I (position at 6,950 bp) which digest *RYR1* only once. Therefore, it was not feasible to simplify cloning of these regions using the available restriction endonucleases. Figure 3-5 and Table 3-2 show the details for construction of

subclones pBSHO+ and pBSOX+. The pBSHO+ subclone has a connected fragment from pBSKS+1159 and pBSKS+1304 and it was used at a later stage of pBSHK+ construction (Figure 3-6). The pBSKS+1304 subclone was used twice for construction of pBSHO+ and pBSOS+ (Table 3-2).

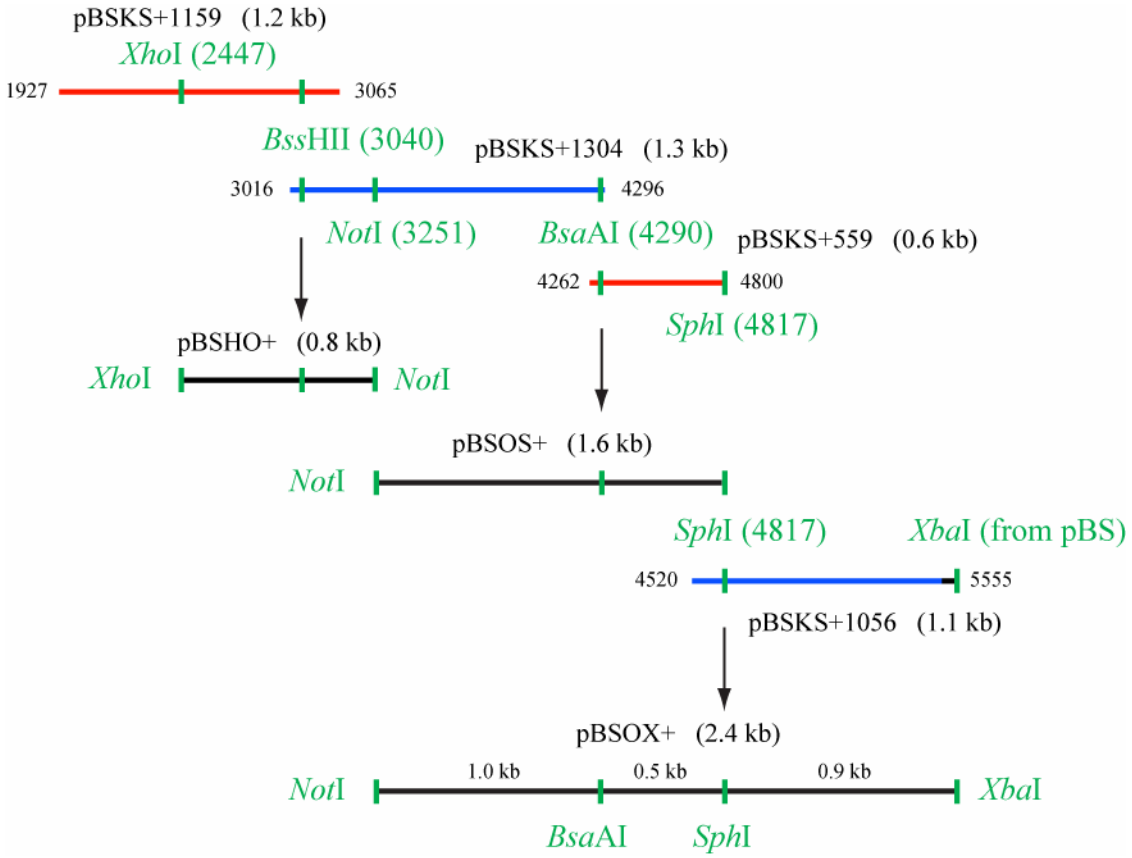

Figure 3-5 Construction of pBSHO+ and pBSOX+

The pBSHO+ and pBSOX+ subclones together contain the central region of *RYR1* cDNA. The order of ligation is indicated from top to bottom. These subclones were used later to construct pBSHK+.

Target	Vector	Insert 1	Insert 2	5’ end	Middle	3’ end
pBSKS+1159	pBS	PCR (F: 1927, R: 3065)				
pBSKS+1304	pBS	PCR (F: 3016, R: 4296)				
pBSKS+559	pBS	PCR (F: 4262, R: 4800)				
pBSKS+1056	pBS	PCR (F: 4520, R: 5555)				
pBSHO+	pBS	pBSKS+1159	pBSKS+1304	*Xho*I	*Bss*HII	*Not*I
pBSOS+	pBS	pBSKS+1304	pBSKS+559	*Not*I	*Bsa*AI	*Sph*I
pBSOX+	pBS	pBSOS+	pBSSK+1056	*Not*I	*Sph*I	*Xba*I

Table 3-2 Subclones for pBSHO+ and pBSOX+

Information of subclones for construction of pBSHO+ and pBSOX+ including names of subclones, primer names and restriction endonucleases is shown and follow the same pattern as described in Table 3-1.

The pBSHK+ subclone is one of two large central region subclones containing the fragment from 2,447 to 6,950 bp. Two subclones, pBSHO+ and pBSOX+ constructed as described previously were used at this stage for pBSHK+ construction (Figure 3-6 and Table 3-3). The pBSKS+1056 subclone was used twice for pBSOX+ and pBSCIIH+.

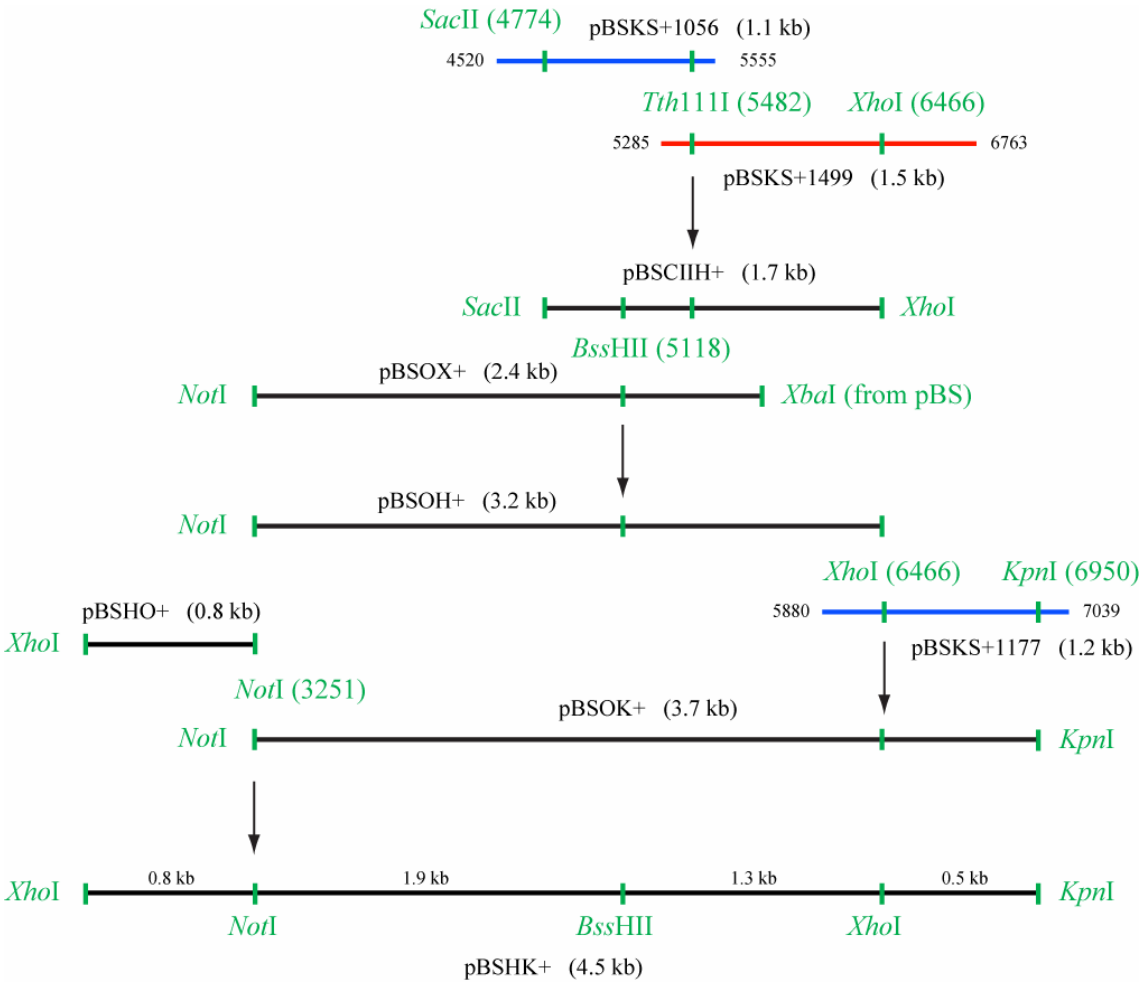

Figure 3-6 Construction of pBSHK+

The pBSHK+ subclone represents a quarter of the *RYR1* cDNA clone constructed in this study. The order of ligation is indicated from top to bottom. This subclone was used for the construction of pBSXK+ together with pBSXC+.

Target	Vector	Insert 1	Insert 2	5’ end	Middle	3’ end
pBSKS+1499	pBS	PCR (F: 5285, R: 6763)				
pBSKS+1177	pBS	PCR (F: 5880, R: 7039)				
pBSCIIH+	pBS	pBSKS+1056	pBSKS+1499	*Sac*II	*Tth*111I	*Xho*I
pBSOH+	pBS	pBSOX+	pBSCIIH+	*Not*I	*Bss*HII	*Xho*I
pBSOK+	pBS	pBSOH+	pBSKS+1177	*Not*I	*Xho*I	*Kpn*I
pBSHK+	pBS	pBSHO+	pBSOK+	*Xho*I	*Not*I	*Kpn*I

Table 3-3 Subclones for pBSHK+

Information of subclones for construction of pBSHK+ including names of subclones, primer names and restriction endonucleases is shown and follow the same pattern as described in Table 3-1.

The other large central region subclone is pBSKO+ (6,950 to 12,895 bp) consisting of inserts from pBSKCII+ and pBSCIIO+. Cloning of pBSKCII+ required a cloning vector which had an *Aat*II site for pBSKAII+ construction. As pBluescript II did not contain this site, a vector, pBSLA+ was constructed for pBSKAII+ subcloning. It was constructed by insertion of a 687 bp *RYR1* cDNA PCR fragment that contains the *Aat*II site. The pBSLA+ was then used as a cloning vector for pBSKAII+ construction. Figure 3-7 and Table 3-4 shows the details for pBSKCII+ construction.

The pBSKCII+ subclone was connected with pBSCIIO+ to construct pBSKO+. The pBSCIIV+ and pBSIIIO+ subclones were constructed with PCR fragment subclones and pSVK3.5 constructed in previous work, and then two subclones were digested and connected at the *Hin*dIII site to construct pBSCIIO+. The pBSKCII+ and pBSCIIO+ subclones were then connected at the *Sac*II site to construct pBSKO+. Figure 3-8 and Table 3-5 shows details for pBSKO+ construction.

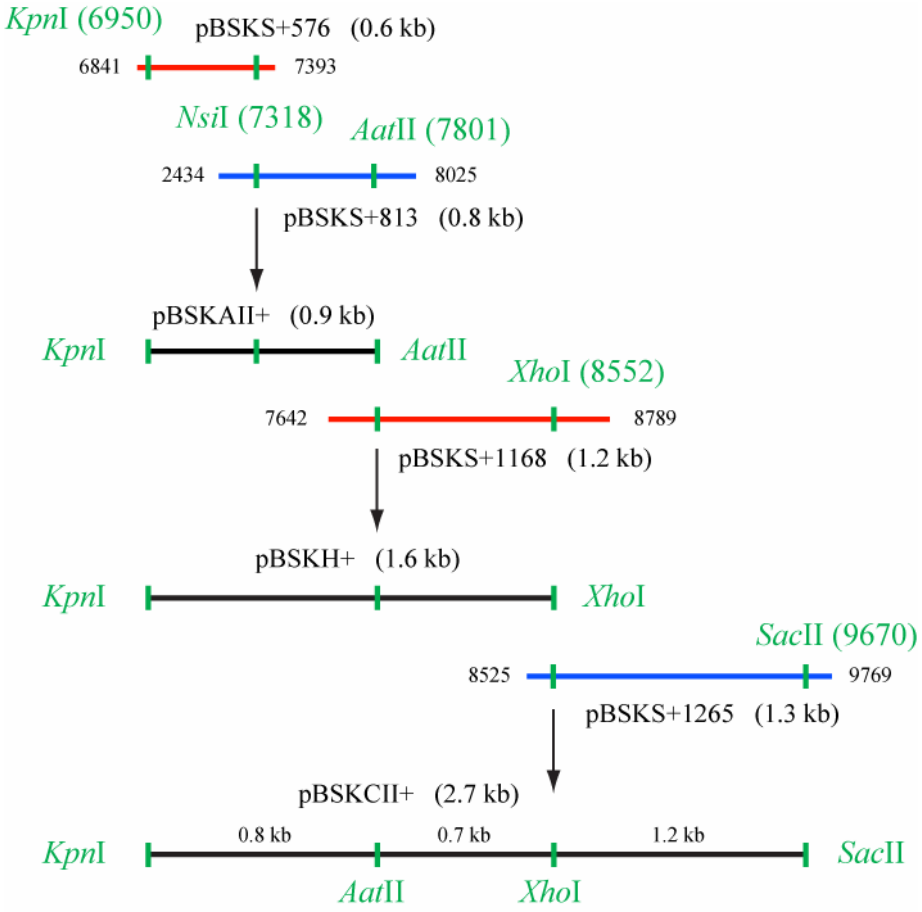

Figure 3-7 Construction of pBSKCII+

The pBSKCII+ subclone consists of four PCR fragment subclones and two connected fragment subclones. The order of ligation is indicated from top to bottom. This subclone was used for pBSKO+ construction at a later stage.

Target	Vector	Insert 1	Insert 2	5’ end	Middle	3’ end
pBSKS+576	pBS	PCR (F: 6841, R: 7393)				
pBSKS+813	pBS	PCR (F: 2434, R: 8025)				
pBSKS+1168	pBS	PCR (F: 7642, R: 8789)				
pBSKS+1265	pBS	PCR (F: 8525, R: 9769)				
pBSLA+	pBS	pBSKS+687		*Cla*I		*Apa*I
pBSKAII+	pBSLA+	pBSKS+576	pBSKS+813	*Kpn*I	*Nsi*I	*Aat*II
pBSKH+	pBS	pBSKAII+	pBSKS+1168	*Kpn*I	*Aat*II	*Xho*I
pBSKCII+	pBS	pBSKH+	pBSKS+1265	*Kpn*I	*Xho*I	*Sac*II

Table 3-4 Subclones for pBSKCII+

Information of subclones for construction of pBSKCII+ including names of subclones, primer names and restriction endonucleases is shown and follow the same pattern as described in Table 3-1.

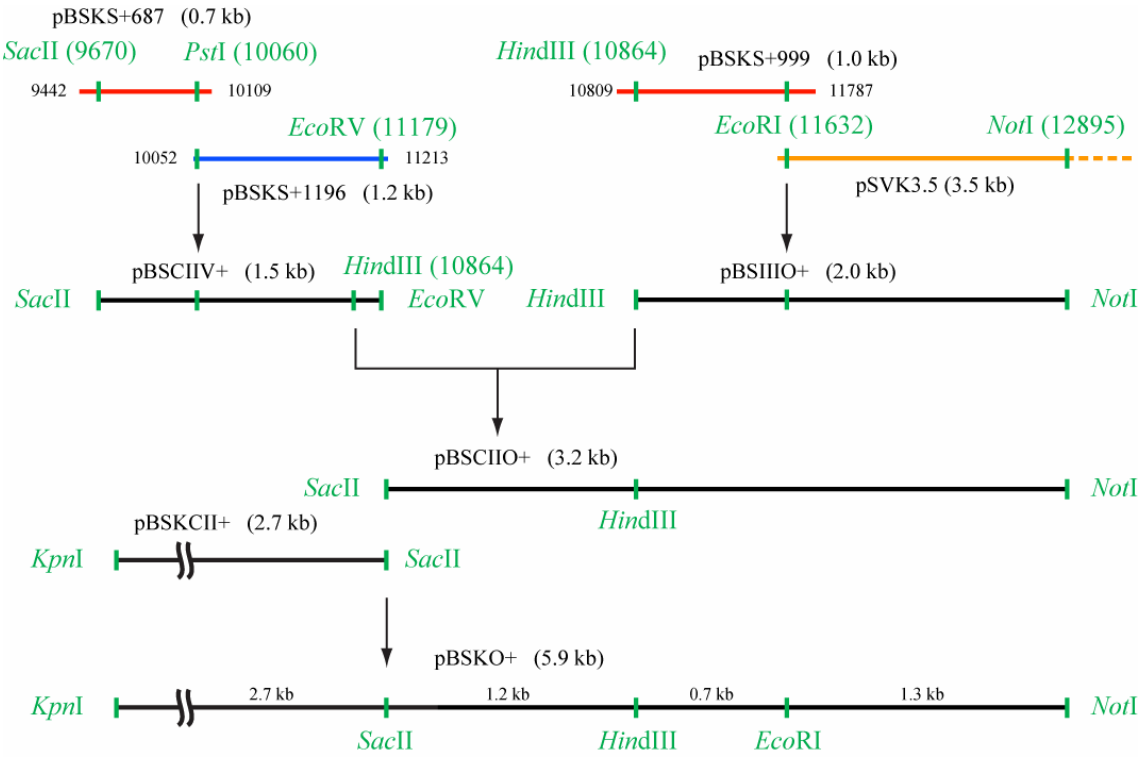

Figure 3-8 Construction of pBSKO+

The pBSKO+ subclone is a quarter of the complete *RYR1* cDNA clone. The order of ligation is indicated from top to bottom. This subclone was used to construct pBSKX+ together with pBSH+.

Target	Vector	Insert 1	Insert 2	5’ end	Middle	3’ end
pBSKS+687	pBS	PCR (F: 9442, R: 10109)				
pBSKS+1196	pBS	PCR (F: 10052, R: 11213)				
pBSKS+999	pBS	PCR (F: 10809, R: 11787)				
pBSCIIV+	pBS	pBSKS+687	pBSKS+1196	*Sac*II	*Pst*I	*Eco*RV
pBSIIIO+	pBS	pBSKS+999	pSVK3.5	*Hin*dIII	*Eco*RI	*Not*I
pBSCIIO+	pBS	pBSCIIV+	pBSIIIO+	*Sac*II	*Hin*dIII	*Not*I
pBSKO+	pBS	pBSKCII+	pBSCIIO+	*Kpn*I	*Sac*II	*Not*I

Table 3-5 Subclones for pBSKO+

Information of subclones for construction of pBSKO+ including names of subclones, primer names and restriction endonucleases is shown and follow the same pattern as described in Table 3-1.

3.1.5 Cloning of the C-terminal region of RYR1 cDNA

The pBSH+ clone contains the C-terminal region of *RYR1* cDNA from 12,895 bp to the stop codon and it was constructed from the pSVK3.5 subclone from previous work [Jones, 2000]. The fragment from pSVK3.5 was obtained by *Xho*I digestion and it was inserted into pBS (Figure 3-9, Table 3-6). The direction of insertion was confirmed in order to utilise the *Xba*I site in the pBS cloning site after the stop codon. The pBSH+ subclone contains C-terminal hotspot region 3 and hence it was used for site-directed mutagenesis for C-terminal mutations.

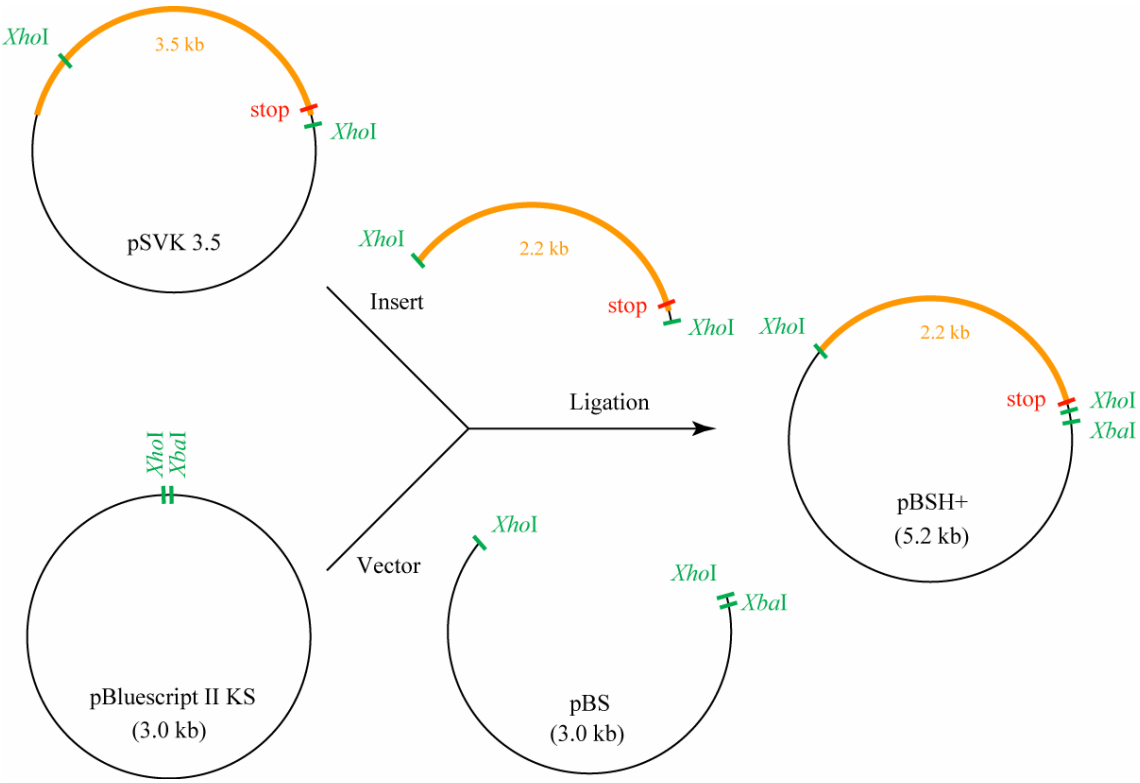

Figure 3-9 Construction of pBSH+

The pSVK3.5 subclone and the pBluescript II KS vector were digested by *Xho*I. The direction of the inserted fragment was noted so that the *Xba*I site of pBS could be used for subsequent digestion and subcloning to create pBSKX+.

3.1.6 Construction of the complete RYR1 cDNA

Four subclones had been prepared at this stage from which to create the complete *RYR1* cDNA: pBSXC+, pBSHK+, pBSKO+ and pBSH+ (Figure 3-3 B). The pBSXC+ subclone (section 3.1.3) was connected with pBSHK+ (section 3.1.4) to construct pBSXK+ (N-terminal half), and pBSKO+ (section 3.1.4) was connected with pBSH+ (section 3.1.5) to construct pBSKX+ (C-terminal half) (Figure 3-10 and Table 3-6). Both subclones have *Xba*I and *Kpn*I sites at their ends (Figure 3-3 C). *Xba*I does not digest *RYR1* cDNA and *Kpn*I is one of the few enzymes which digest the sequence only once.

The two subclones, pBSXK+ and pBSKX+ represent the complete *RYR1* coding

sequence. Each subclone was to be digested with *Xba*I and *Kpn*I, followed by ligation at the *Kpn*I site and *Xba*I site of pBS to construct pBSRYR1. It was intended to transfer the *RYR1* cDNA fragment from pBluescript to pcDNA3.1 by *Xba*I digestion to construct pcRYR1 (Figure 3-11).

This direct plan, however, was experimentally not feasible because the two inserts were too long (7.0 and 8.2 kb) to connect in a single ligation and pBSRYR1 was never actually constructed. An alternative cloning strategy was designed to ligate one insert into the vector instead of two inserts at the same time. There was however, no restriction endonuclease available that did not digest *RYR1*.

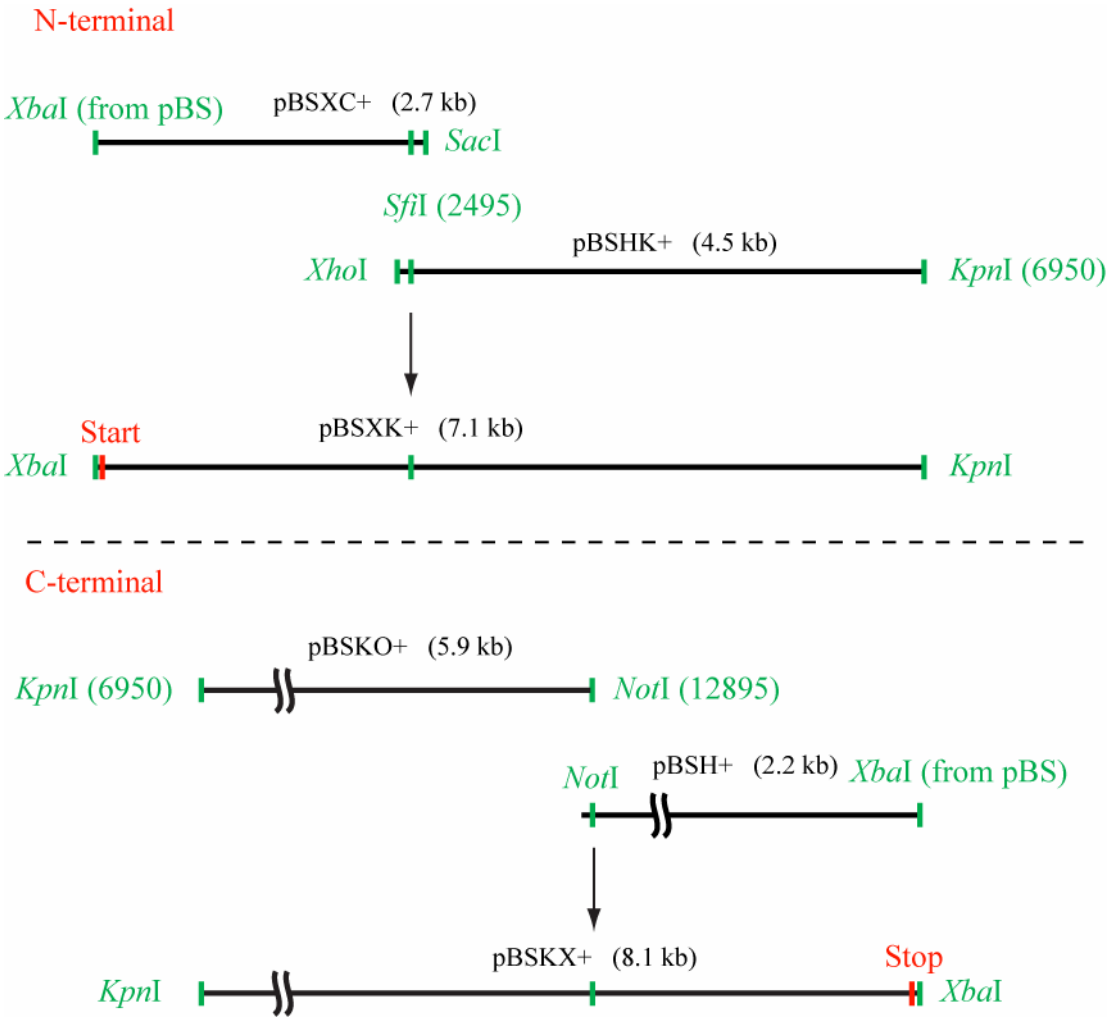

Figure 3-10 Construction of pBSXK+ and pBSKX+

The pBSXK+ subclone is the N-terminal half of *RYR1* cDNA from the start codon to 6,950 bp at the *Kpn*I site and the pBSKX+ subclone is the C-terminal half from the *Kpn*I site to the stop codon. Ligations were performed at 16°C overnight because of the size of inserts in an attempt to construct the full length of *RYR1* cDNA clone.

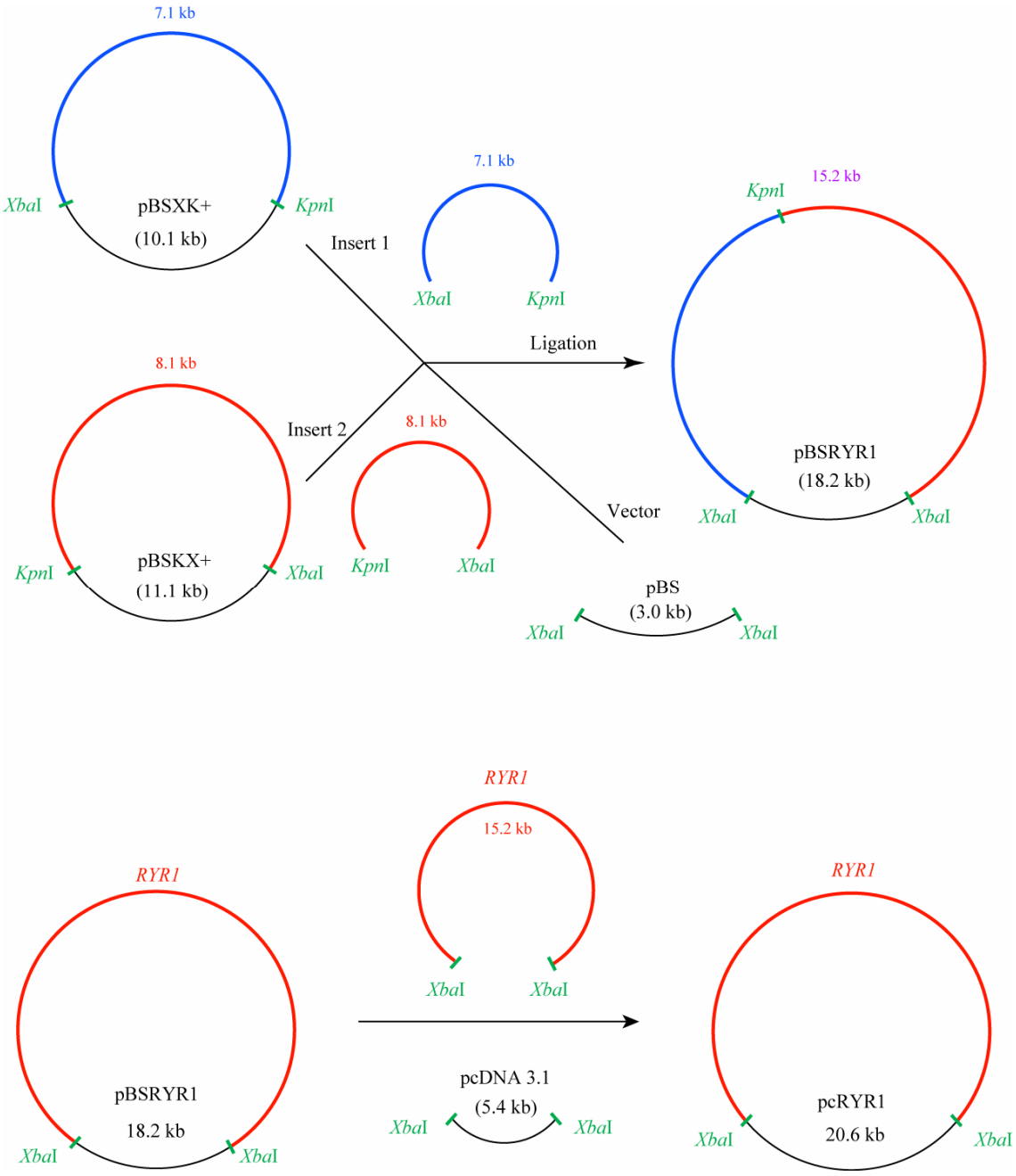

Figure 3-11 Direct plan for construction of *RYR1*

Two fragments digested with *Xba*I and *Kpn*I from pBSXK+ and pBSKX+ could be ligated and connected at the *Kpn*I site to construct pBSRYR1 (top). The complete *RYR1* cDNA could be cut out from pBSRYR1 by *Xba*I digestion to transfer into the expression vector pcDNA3.1 and construct pcRYR1 (bottom). This plan was not successful because of the large size of inserts.

The pcDNA3.1 (+) vector has an *Nhe*I site in the cloning site (Figure 3-12). The sequence for *Nhe*I is different from that for *Xba*I, but the sequence of sticky ends produced after digestion is identical for both enzymes (Figure 3-12). Therefore, it was feasible to use the *Nhe*I site for insertion of the fragment from pBSXK+ digested by *Xba*I and *Kpn*I (Figure 3-13).

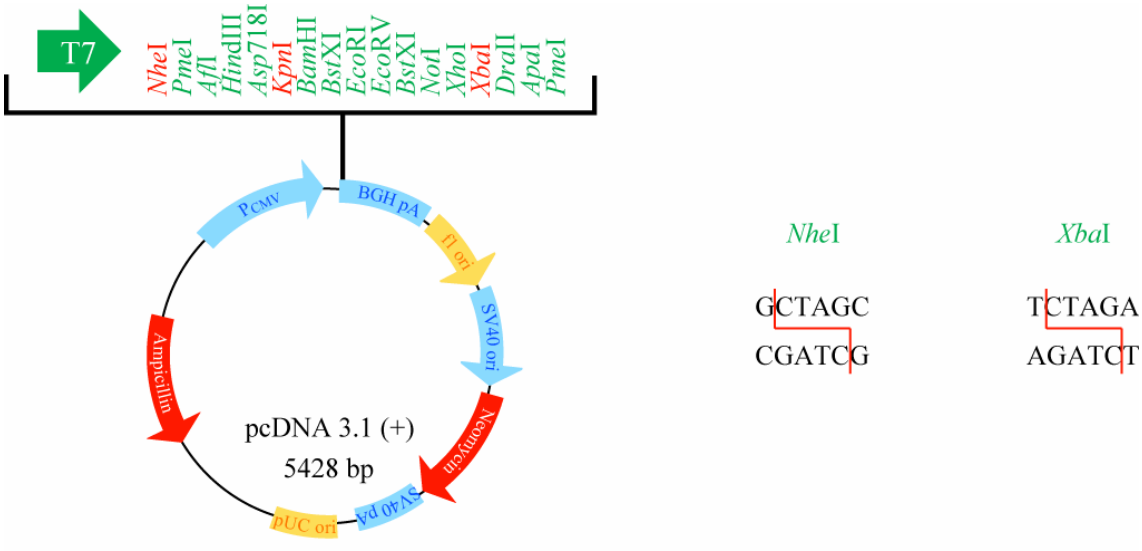

Figure 3-12 Cloning site of pcDNA3.1 (+)

Restriction endonuclease sites in the cloning site of pcDNA3.1 (+) are shown. Sequences of two enzyme sites, *Nhe*I and *Xba*I are also shown. Sequences of sticky ends digested by *Nhe*I or *Xba*I are identical and can be ligated. Figure adapted from the manufacturer's instructions (Invitrogen)

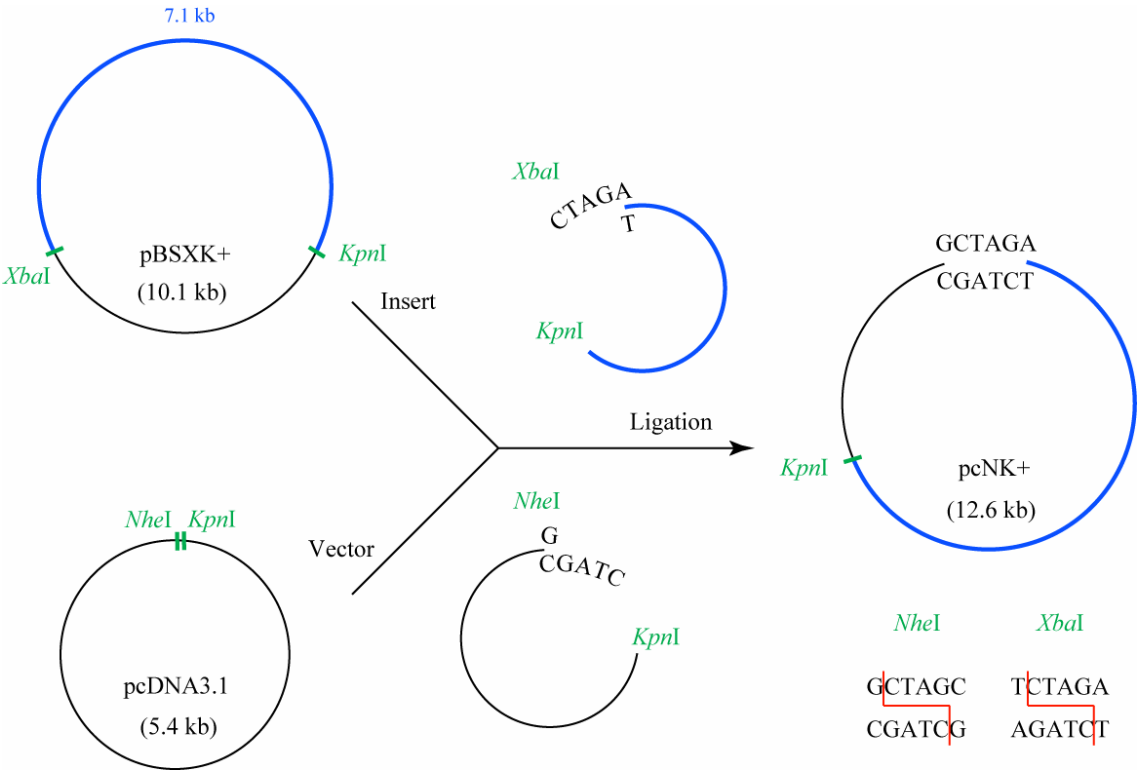

Figure 3-13 Cloning of pcNK+

Sequences of sticky ends after *Xba*I and *Nhe*I digestion are identical. The fragment from pBSXK+ digested by *Xba*I and *Kpn*I can be inserted into the vector digested by *Nhe*I and *Kpn*I. The sequence at the *Nhe*I site is changed after ligation and hence cannot be subsequently digested by either *Xba*I or *Nhe*I. Ligation was performed at 16°C overnight.

The modified method for *RYR1* cloning was to digest pBSXK+ with *Xba*I and *Kpn*I and insert this fragment into pcDNA digested by *Nhe*I and *Kpn*I to construct pcNK+. Ligation at the *Nhe*I site with the *Xba*I end changed the sequence at this site so that it could not be recognised by either *Xba*I or *Nhe*I (Figure 3-13). Therefore, *Xba*I digested pcNK+ only once at the cloning site of pcDNA and it was feasible to insert the fragment from pBSKX+ into pcNK+ at the *Kpn*I site of *RYR1* and *Xba*I site of the vector (Figure 3-14). The full length of *RYR1* cDNA was then constructed in the expression vector, pcDNA3.1 (Table 3-6). Although there was no method to cut *RYR1* out of the vector to transfer to another vector, *RYR1* cDNA was available in pcDNA and was sufficient to be used in transfections to assess expression.

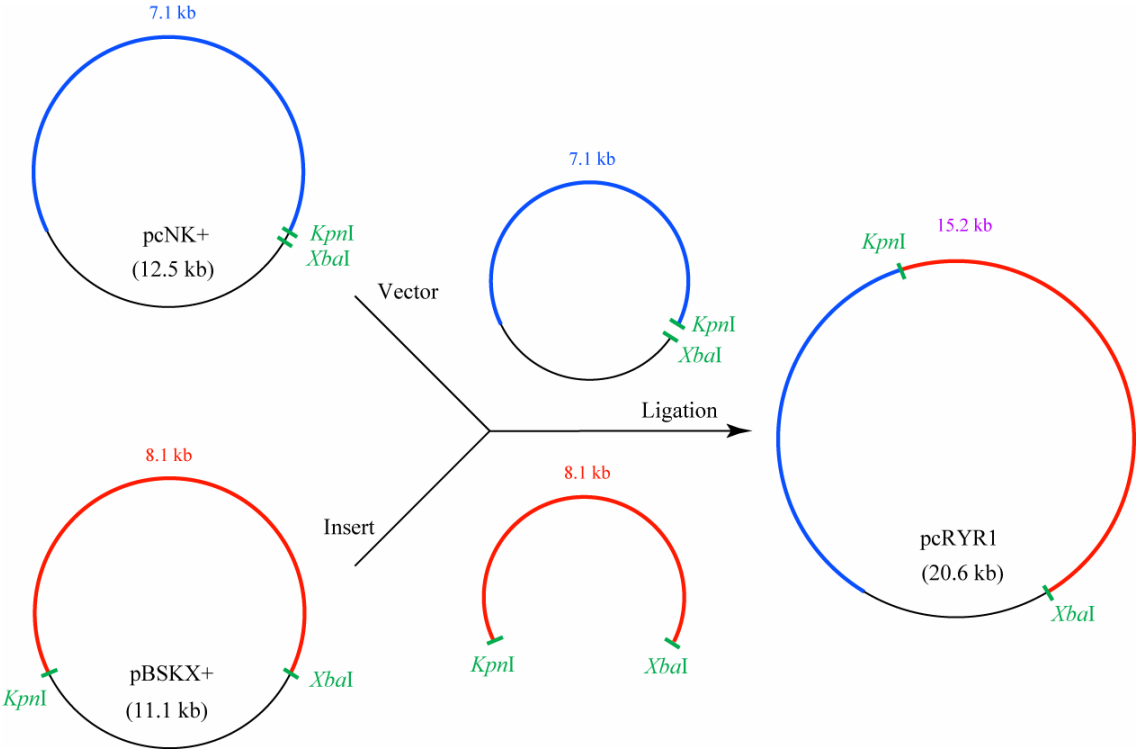

Figure 3-14 Cloning of pcRYR1

The entire region of *RYR1* cDNA was constructed in the expression vector pcDNA3.1. The pcNK+ and pBSKX+ subclones were digested by *Xba*I and *Kpn*I and ligated to construct pcRYR1. Ligation was performed at 16°C overnight and propagation of pcRYR1 in *E.coli* was carried out at carefully controlled temperature. The pcRYR1 was ready for use of transfection for *RYR1* protein expression.

Target	Vector	Insert 1	Insert 2	5’ end	Middle	3’ end
pBSH+	pBS	pSVK3.5		*Xho*I		
pBSXK+	pBS	pBSXC+	pBSHK+	*Xba*I	*Sfi*I	*Kpn*I
pBSKX+	pBS	pBSKO+	pBSH+	*Kpn*I	*Not*I	*Xba*I
pcNK+	pcDNA3.1	pBSXK+		*Nhe*I		*Kpn*I
pcRYR1	pcNK+	pBSKX+		*Kpn*I		*Xba*I

Table 3-6 Subclones for pcRYR1

Information of construction of the entire *RYR1* cDNA clone pcRYR1 including names of subclones, primer names and restriction endonucleases is shown and follows the same pattern as described in Table 3-1.

3.1.7 Confirmation of RYR1 cDNA

The *RYR1* cDNA was cloned into pcDNA3.1 successfully (pcRYR1) and it was directly sequenced on both strands. Although 17 silent polymorphisms that do not introduce an amino acid change were identified, sequencing both strands of pcRYR1 did not identify any unwanted mutation. The sequence of the *RYR1* cDNA in pcRYR1 is shown in Appendix 2 and silent polymorphisms identified from the *RYR1* coding region are listed in Appendix 3. This 20.6 kb vector was also confirmed for its identity by restriction endonuclease digestion. Four enzyme digestion experiments showed that the full length of *RYR1* was inserted in the vector successfully and the direction of the gene was correct and ready for transfection (Figure 3-15).

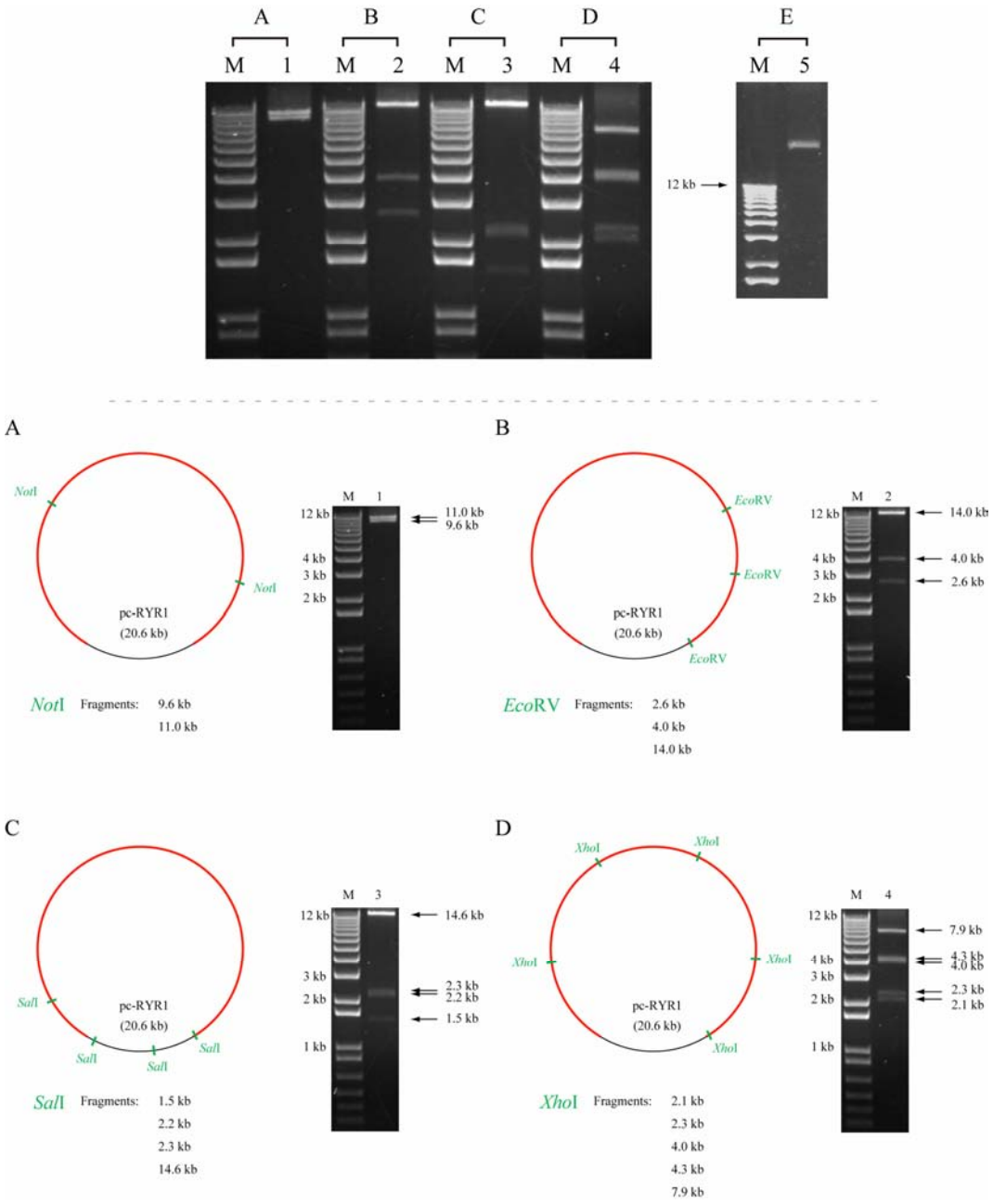

Figure 3-15 Confirmation of *RYR1* cDNA cloning

Purified pcRYR1 (~1 µg) was incubated with one of four restriction endonucleases (1 µL) 37°C overnight. Digested fragments were analysed on a 2% agarose gel at 100 V for 1 hour and were observed using ethidium bromide under UV light (top). *Not*I digests pcRYR1 twice producing two fragments of 9.6 and 11.0 kb (A, lane 1). *Eco*RV digests three times with 2.6, 4.0 and 14.0 kb fragments (B, lane 2). *Sal*I and *Xho*I digestion also showed correct numbers of fragments and fragment size (C, lane 3 and D, lane 4, respectively). The uncut pcRYR1 (20.6 kb) is also shown (E, lane 5).

3.2 Site-directed mutagenesis

The WT *RYR1* cDNA was cloned into pcDNA3.1 as pcRYR1 and several mutants were also constructed to study the functional effects of *RYR1* mutations. The nomenclature of mutants is simple with the addition of a mutation name such as pcRYR1+T4826I indicates that the mutant *RYR1* cDNA encodes the Thr4826Ile mutation. There is a large number of *RYR1* mutations reported to date, and only a small number of these were selected for mutant construction and functional analyses. Six *RYR1* mutations were selected according to different positions within the amino acid sequence and different associated phenotypes and were analysed in this study: two N-terminal mutations linked to MH, R163C and G248R, two C-terminal mutations linked to MH, T4826I and H4833Y, and two C-terminal mutations linked to CCD, I4898T and G4899R. As well as these mutations, other mutations were also selected and the corresponding full-length mutant clones were constructed. These mutations included R44C, R401C and R533C and each is associated with MH (Appendix 1). These mutants, however, were not used in [^{3}H]ryanodine binding assays because of lack of time and very weak signals in scintillation counting. Selection of *RYR1* mutations will be described in the discussion section.

Mutagenesis was performed by a PCR-based method described as MEGAWHOP, the modified technique of the QuikChange® method [Miyazaki and Takenouchi, 2002]. This technique amplifies megaprimers at the first PCR cycle and then elongates the whole template plasmid at the second cycle using these megaprimers followed by *Dpn*I digestion to select only amplified plasmids (Figure 3-16). This method helps plasmid amplification especially for large plasmids and it requires only one forward or reverse primer that contains a mutation, while QuikChange® requires the design of two primers bearing mutations. Plasmids were purified and sequenced after PCR to confirm that mutagenesis was successful without any accidental mutation.

A subclone containing an *RYR1* fragment was used as a template for PCR. It was not feasible to amplify a large plasmid such as pcRYR1 (20.6 kb), and therefore subclones which contain shorter *RYR1* fragments (~3 kb) were used as templates for PCR. The pBSXC+ subclone contains 2.7 kb of N-terminal *RYR1* and was used for R163C and

G248R mutagenesis. The C-terminal pBSH+ subclone (Figure 3-9) contains a 2.2 kb fragment and was used for the other four C-terminal mutations. Figure 3-17 shows an example of mutagenesis by PCR using megaprimers, Figure 3-18 shows *Xho*I digestion for plasmids after transformation, and Figure 3-19 shows an example of direct sequencing for detection of a mutation introduced by mutagenesis.

The successfully mutated plasmids were then used for construction of *RYR1* mutant clones. PCR was performed, for instance, using pBSH+ for the T4826I mutation to obtain pBSH+T4826I. This mutated plasmid was used for pBSKX+T4826I construction according to the strategy shown in Figure 3-10 and the fragment from pBSKX+T4826I was inserted into WT pcNK+ to construct pcRYR1+T4826I using the same strategy that was used to construct WT pcRYR1 (Figure 3-13 and 3-14).

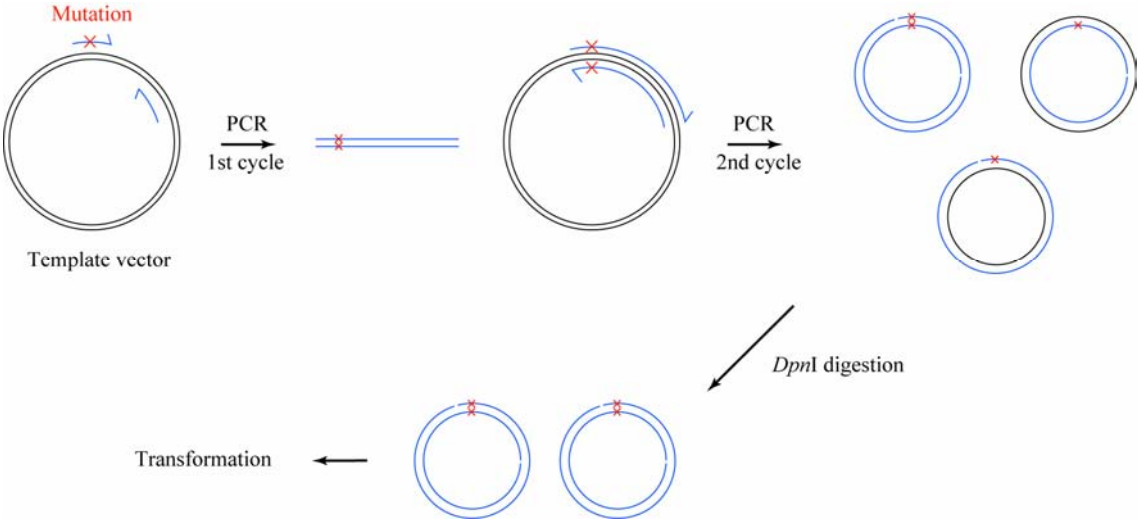

Figure 3-16 The MEGAWHOP technique

A ~1 kb megaprimer was amplified at the first PCR cycle and the whole plasmid was amplified at the second cycle using this megaprimer. *Dpn*I digests methylated template fragments and hence only mutated PCR fragments were obtained. Nicks were repaired in *E. coli* after transformation. The cloned vector was then sequenced for confirmation of the presence of the mutation of interest and the absence of any unwanted mutation. This MEGAWHOP method allows stable PCR amplification and high mutagenesis efficiency.

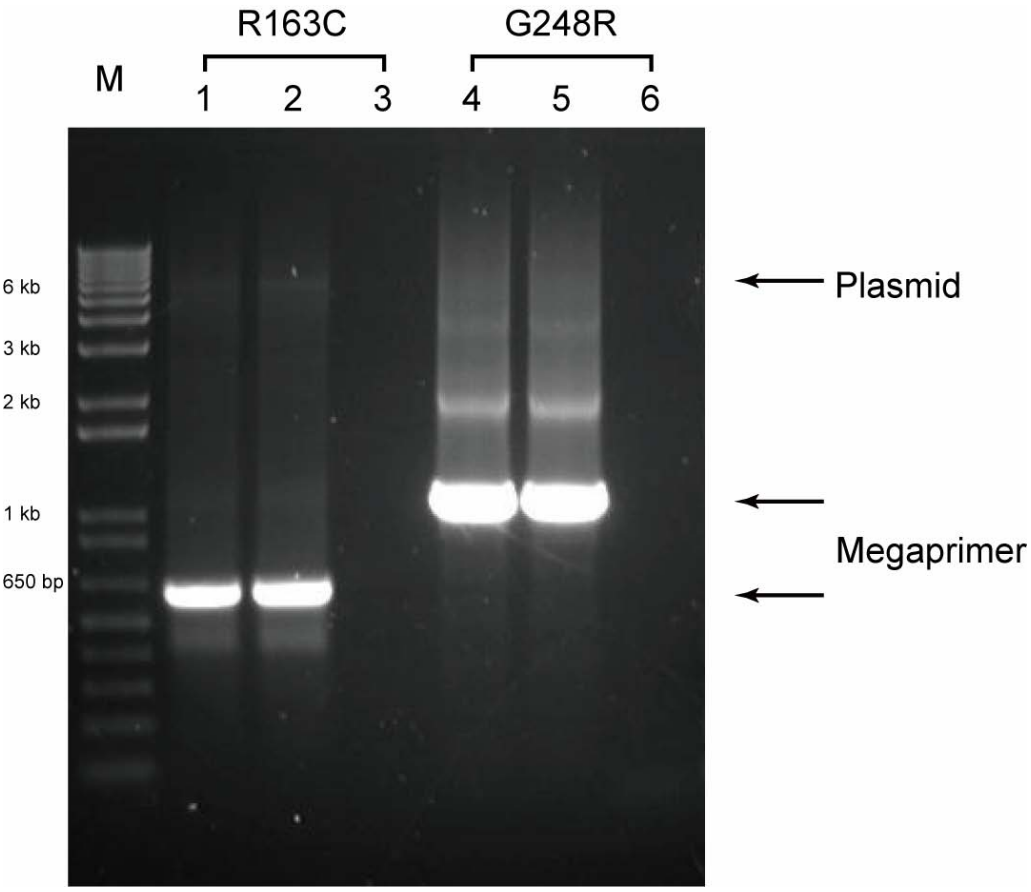

Figure 3-17 PCR example for mutagenesis

This figure shows an example of PCR for mutagenesis using the MEGAWHOP technique for the R163C and G248R mutations. Primer sets used were C487T and 341 (629 bp) for R163C (lane 1-3), and G742A and 1755 (1,046 bp) for G248R (lane 4-6). PCR reactions were performed using *Pfx* polymerase at 68°C, 30 seconds, 25 cycles for megaprimer amplification directly followed by 68°C, 10 minutes, 20 cycles for plasmid amplification. Lane 3 and 6 show negative controls without plasmid templates. The pBSXC+ subclone (5.7 kb) was used as a template for these two mutations. Amplified megaprimers and mutated plasmids were analysed by 2% agarose gel electrophoresis at 100 V for 1 hour and visualised by ethidium bromide under UV to check if reaction was successful by detecting megaprimers (629 or 1,046 bp) although amplified plasmids (5.7 kb) were not detectable on the gel. The remaining PCR reaction mixtures were treated with *Dpn*I 37°C overnight and were then used directly for transformation. Extra bands detected on the gel were ignored. M indicates the 1 kb DNA ladder used as a marker. Primer sequences are listed in Appendix 1.

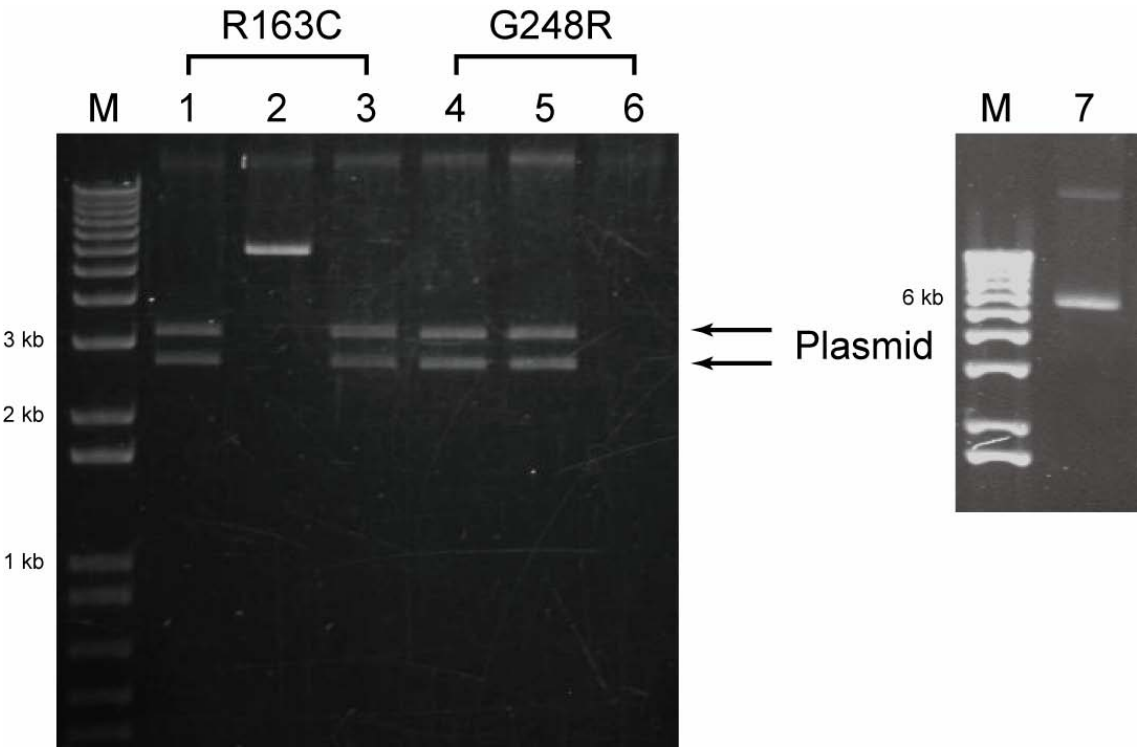

Figure 3-18 Restriction enzyme digestion for mutated plasmids

Plasmids were incubated with a restriction endonuclease and were analysed on a gel to check if transformation was successful by detecting digested fragments. *Xho*I was used for the N-terminal plasmid pBSXC+. This enzyme digests the plasmid two times producing two fragments (2.6 and 3.1 kb). Several colonies were selected after transformation. In this case, two colonies for R163C (lane 1 and 3) and two colonies for G248R (lane 4 and 5) carried plasmids of interest. Direct sequencing was carried out after plasmid purification to distinguish amplified plasmids with the mutation of interest from WT pBSXC+ used as a template. The uncut WT pBSXC+ plasmid (5.7 kb) is also shown (lane 7).

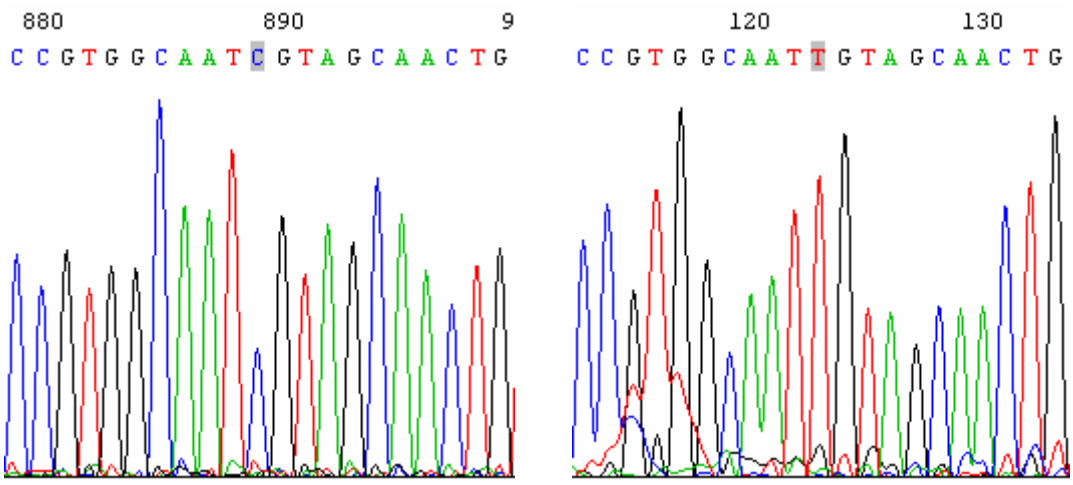

Figure 3-19 Example of direct sequencing for *RYR1* mutations

Plasmids were directly sequenced after transformation and plasmid purification to detect the *RYR1* mutation introduced by mutagenesis and any other unwanted mutation. This example shows sequence comparison for the R533C mutation. The plasmid carried this mutation for both strands (homozygous) and hence only one signal was detected (C for WT on the left and T for the mutant on the right) at the nucleotide position 1,597. The R533C mutation was used for mutant *RYR1* cDNA cloning but not for functional analysis and hence data for this mutation are not included in this study. The details and future applications for mutant selection and functional studies respectively are described in the discussion section.

3.3 Western blotting for expressed RYR1

The cloned WT and mutant human *RYR1* cDNAs were used for transient transfection using FuGENE HD in HEK-293 cells as described in section 2.5.4. After harvesting, partial cell pellets were solubilised in cell lysis buffer for western blotting to detect the expressed RYR1 protein. The WT and six mutant RYR1 proteins were detected by western blotting using the monoclonal antibody 34C as well as the positive control tubulin using the anti-α-tubulin antibody (Figure 3-20). No differences were detected on the blot for WT and mutants.

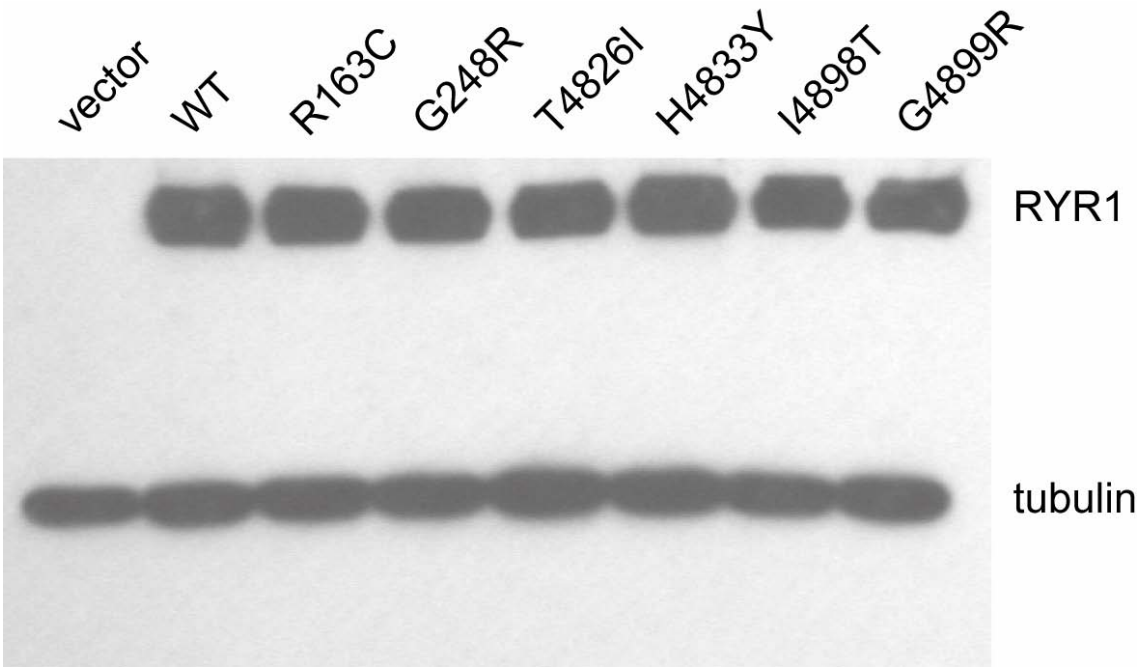

Figure 3-20 Western blotting for RYR1

Total proteins harvested from HEK-293 cells (100-200 µL) solubilised in cell lysis buffer were analysed using 7.5% SDS-PAGE. The WT and mutant RYR1 (565 kDa) was detected using the 34C antibody (mouse origin) and tubulin (50 kDa) was detected using an anti-α-tubulin antibody (mouse origin) for a positive control using the horseradish peroxidise-conjugated anti-mouse IgG secondary antibody. The negative control (vector only without *RYR1* cDNA) shows that there is no endogenous RYR1 protein in HEK-293 cells. The sample proteins were intentionally overloaded for ease of detection because the RYR1 proteins are large and can be unstable during electrophoresis often producing extra bands and smears. No other bands were detected indicating that transfection was successful for WT and the six mutants. No suitable size marker was available for the RYR1 proteins because of their size. No differences were detected for all RYR1 samples.

3.4 Immunofluorescence in transfected HEK-293

Immunofluorescence was also performed to detect expressed RYR1. Western blotting showed that the RYR1 protein was expressed by transfection, and immunofluorescence showed the location of the RYR1 protein expressed in HEK-293 cells after transfection. HEK-293 cells were grown on a glass slide and transfected with WT or mutant *RYR1* cDNAs using FuGENE 6 as described in section 2.6.3. The 34C antibody against the RYR1 protein was used as the primary antibody and a FITC-conjugated secondary anti-mouse antibody was used to detect bound 34C. The expressed RYR1 protein was observed as green under a fluorescence microscope.

The RYR1 is a calcium channel located on the membrane of the SR in skeletal muscle and when expressed in HEK-293 cells, the RYR1 is thought to localise to the membrane of the endoplasmic reticulum (ER). To confirm this, the ER was also detected using a common ER marker, protein disulfide isomerase (PDI). The PDI is a protein specifically expressed in the ER, and hence an anti-PDI antibody detects the location of the ER in HEK-293 cells. The anti-PDI primary antibody was detected by a TRITC-conjugated secondary antibody which could be observed as red. If the location of green fluorescence (RYR1) is identical to that of red (ER), it indicates that the RYR1 and the ER co-localise in HEK-293 cells. DAPI was also used to stain nuclei in blue for ease of observation of cell shape. Figure 3-21 shows the strategy for immunofluorescence used in this study.

This experiment showed clearly that the RYR1 co-localised with the ER in HEK-293 cells (Figure 3-22). Transfection for this particular application was performed at very low confluence (20-30%) to control cell density after 72-hour-incubation. Therefore, transfection was successful in only a limited number of cells. As HEK-293 cells do not express the RYR1 without pcRYR1, green fluorescence was observed in only a few cells when transfection was successful. Every HEK-293 cell, on the other hand, has the endogenous ER, and hence red fluorescence was observed in every cell. Figure 3-22 clearly shows the difference between normal and transfected cells with or without green fluorescence. As in western blotting, no differences in immunofluorescence were observed between WT and mutants.

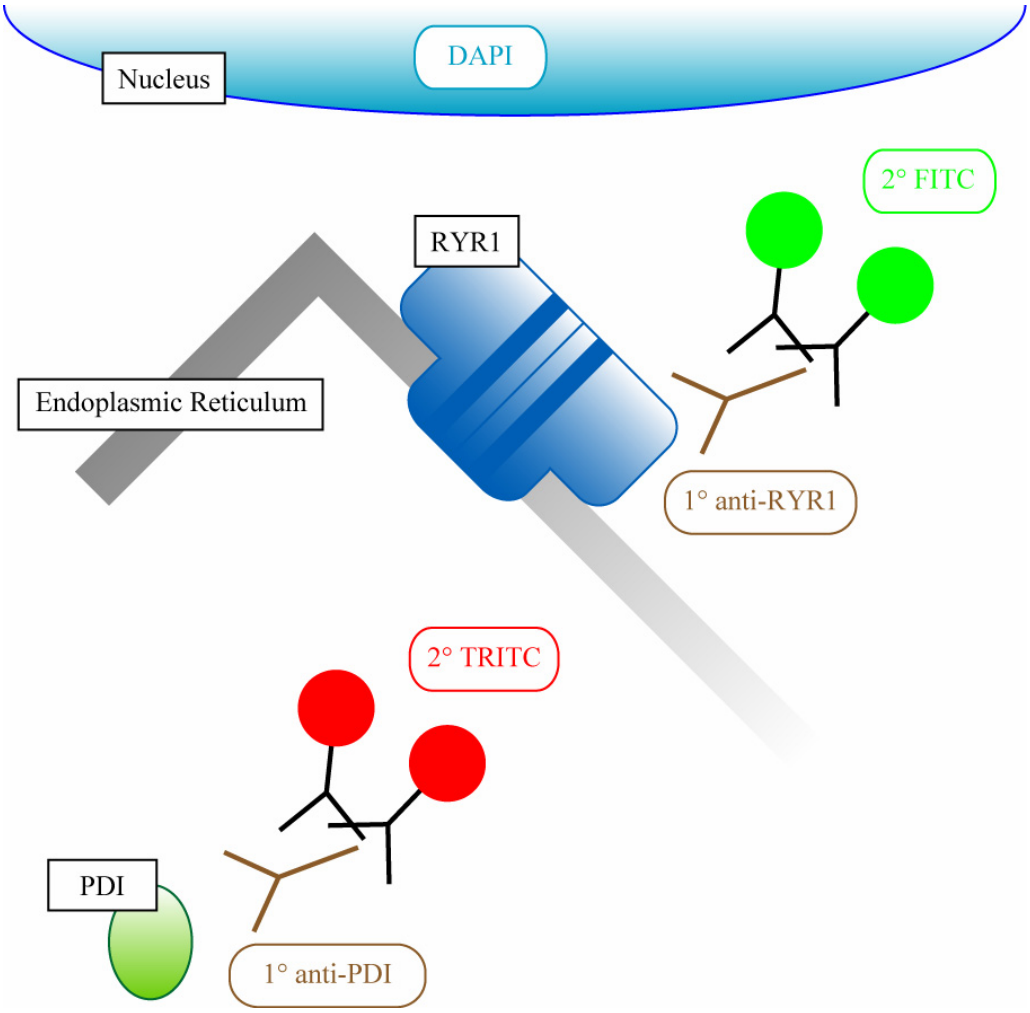

Figure 3-21 Immunofluorescence strategy

Immunofluorescence was designed to observe co-localisation of the RYR1 and the ER. The RYR1 protein was detected by mouse anti-RYR1 (34C) and FITC-conjugated secondary anti-mouse (goat origin). The PDI was detected by rabbit anti-PDI and TRITC-conjugated secondary anti-rabbit (goat origin). As there was no conflict between two secondary antibodies, incubation was performed for both antibodies at the same time. The RYR1 and PDI were observed under a fluorescent microscope as green and red, respectively showing co-localisation of these two proteins. DAPI was used for nuclear staining in blue and assisted in recognition of cells and cell shape.

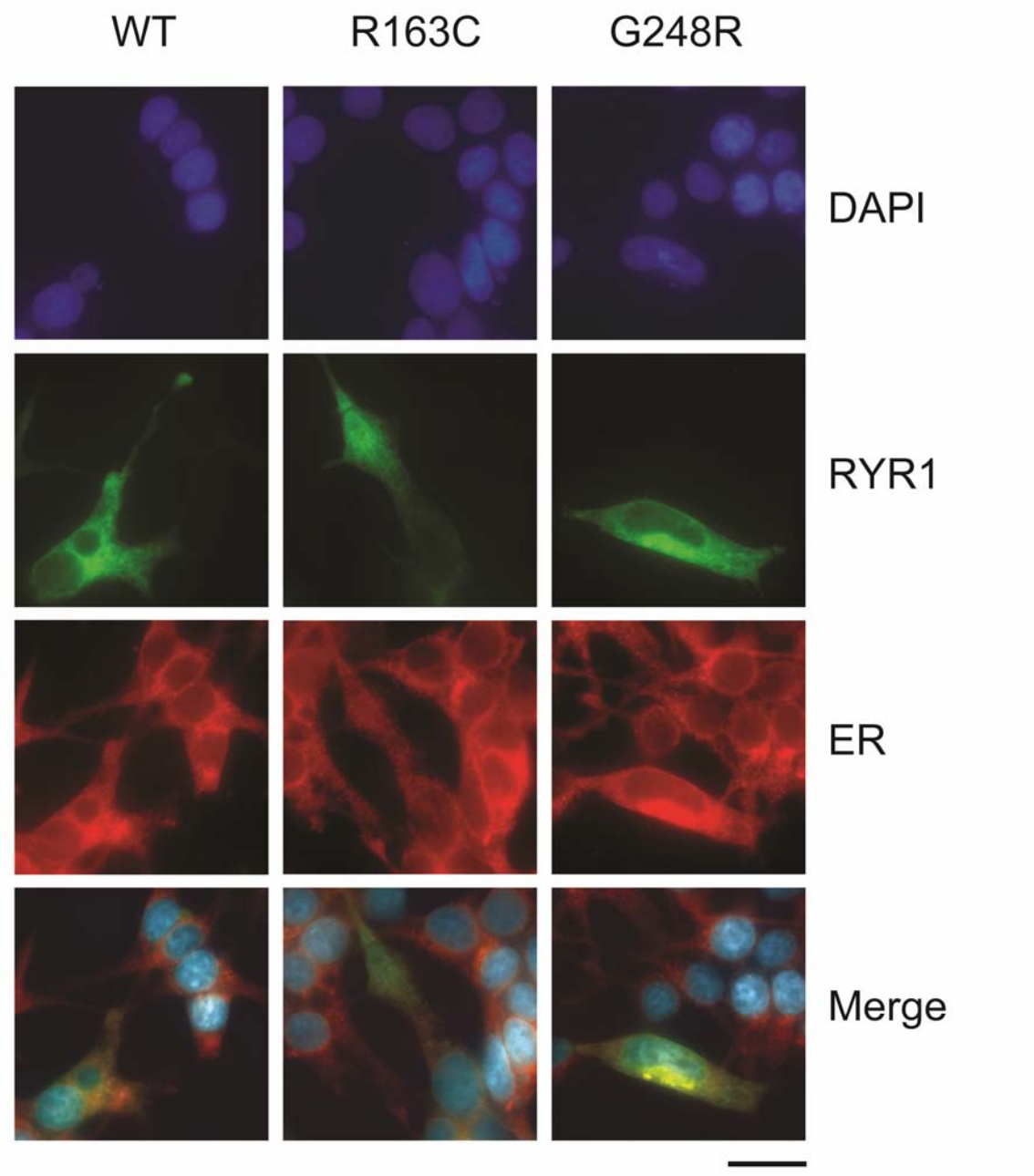

Figure 3-22 Immunofluorescence for transfected HEK-293 cells

HEK-293 cells on a glass slide were transfected with WT or two N-terminal *RYR1* mutants, R163C or G248R. The expressed RYR1 was detected by 34C and FITC-conjugated secondary antibody (green). The PDI was detected by anti-PDI and TRITC-conjugated secondary antibody (red) for the ER marker. Nuclei were also stained by DAPI (blue). Fluorescence was observed using a BX51 fluorescence microscope (Olympus) using the 100× objective and filter cubes, U-MWU2, U-MWIBA2, U-MWIG2 or U-61000V2. The scale bar represents 50 μm. Transfection was successful only for a limited number of cells and hence the RYR1 was observed only from these cells.

3.5 [^{3}H]ryanodine binding assay

After western blotting confirmed that transfection was successful and gave sufficient RYR1 expression, the remaining cell pellets were solubilised in CHAPS buffer for [^{3}H]ryanodine binding assays. This assay analysed Ca^{2+} release indirectly by detecting [^{3}H]ryanodine bound to the open state of the RYR1 protein. Higher binding indicates larger amounts of the opened RYR1 protein suggesting higher Ca^{2+} release from the SR in skeletal muscle leading to MH.

3.5.1 Activation by 4-chloro-m-cresol

4-chloro-*m*-cresol (4-C*m*C) is a specific agonist for the RYR1 protein. [^{3}H]ryanodine binding assays were performed with various concentrations of 4-C*m*C to calculate half maximal effective concentration (EC_{50}). Concentrations of free Ca^{2+} in the reaction mixture were controlled at 100 nM so that the RYR1 was not activated by Ca^{2+}. [^{3}H]ryanodine binding was determined as counts per minute (cpm) using a scintillation counter. Assays were performed for 0 to 500 µM of 4-C*m*C, and a cpm value at 500 µM was set as 100% binding for each sample. Values at other concentrations were calculated as percentages compared to that at 500 µM.

[^{3}H]ryanodine binding is highly dependent on RYR1 concentrations in the reaction mixture. It was not feasible, however, to obtain reliable data for RYR1 quantification as western blotting was used to detect expressed RYR1. RYR1 quantification based on western blotting cannot be used to estimate RYR1 concentrations in [^{3}H]ryanodine binding assays as the signal detected is above the very narrow linear range for autoradiography and thus is only qualitative. Therefore, cpm values could not be compared between WT and mutants directly, and hence data were analysed independently for each sample to calculate EC_{50} and then each mutant was compared to the WT EC_{50} value. Figure 3-23 shows the sigmoidal fitted curves generated for WT and four MH mutants for 4-C*m*C activation. Curves for mutants were shifted to the left from WT showing a lower EC_{50} for 4-C*m*C activation than WT. This indicates that mutant RYR1 proteins open the channel at the significantly lower concentrations of 4-C*m*C than do WT RYR1 proteins. Two C-terminal *RYR1* mutants linked to MH, T4826I and H4833Y showed extremely strong sensitivity to 4-C*m*C and very

significantly lower EC_{50} values ($p<0.001$) compared to WT. The EC_{50} of these two mutants were also significantly lower ($p<0.05$) than those of the N-terminal *RYR1* mutants, R163C and G248R. T4826I and H4833Y mutants also showed very significant ($p<0.001$) ryanodine binding even without 4-C*m*C (Table 3-7) indicating that they may cause the channel to be leaky.

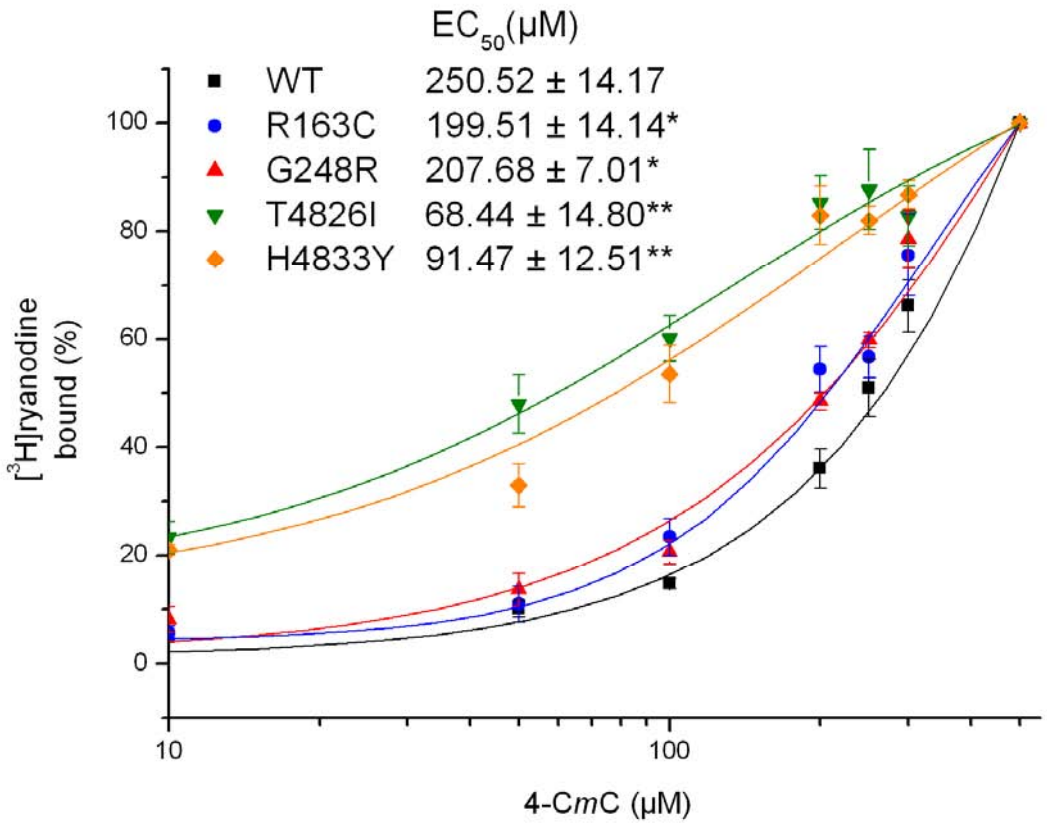

Figure 3-23 [^{3}H]ryanodine binding after 4-C*m*C activation

HEK-293 cell pellets after transfection were solubilised in CHAPS buffer and [^{3}H]ryanodine binding was performed to calculate EC_{50} of 4-C*m*C activation. Binding reactions were performed with 100 nM free Ca^{2+}, 1 nM [^{3}H]ryanodine and 0-500 μM 4-C*m*C. Sigmoidal fitted curves and EC_{50} were calculated using ORIGIN software. Normalized [^{3}H]ryanodine binding is shown as mean ± SEM (n=6). The scale is shown in log 10 for the x axis and hence binding at 0 μM is not shown. These data for binding without 4-C*m*C are shown in Table 3-7. All MH mutants showed significantly lower EC_{50} for 4-C*m*C activation compared to WT (*$p<0.05$, **$p<0.001$).

Sample	Mean (%)	SEM	p value
WT	0.83604	0.37405	-
R163C	1.55444	0.77413	0.42291
G248R	2.80489	1.32671	0.18368
T4826I	14.10054	2.59623	4.94207×10^{-4} **
H4833Y	11.72774	1.17066	4.75137×10^{-6} **

Table 3-7 [^{3}H]ryanodine binding without 4-C*m*C

[^{3}H]ryanodine binding reactions were performed six times with 100 nM free Ca^{2+} without 4-C*m*C. Data are shown as mean ± SEM. The p value was calculated by unpaired Student's *t*-test using ORIGIN. Without agonists, N-terminal *RYR1* mutants R163C and G248R remain closed and did not show significant binding ($p>0.1$) compared to WT while two C-terminal mutants T4826I and H4833Y showed very significant binding (**$p<0.01$) without 4-C*m*C. This result suggests that these two mutants may always be opened without any signals or agonists.

[^{3}H]ryanodine binding reaction for 4-C*m*C activation was also performed for two C-terminal *RYR1* mutants linked to CCD, I4898T and G4899R. These mutants, however, did not show any binding for any concentration of 4-C*m*C (Figure 3-24). 4-C*m*C is a strong and specific RYR1 agonist and the RYR1 proteins including WT should be opened at high concentrations of 4-C*m*C such as 500 µM. It was not feasible to detect cpm for these mutants and therefore EC_{50} could not be calculated. No [^{3}H]ryanodine binding indicates that the RYR1 protein is not opened. This result suggests that these CCD mutants may not be sensitive to 4-C*m*C and cannot be opened by agonists.

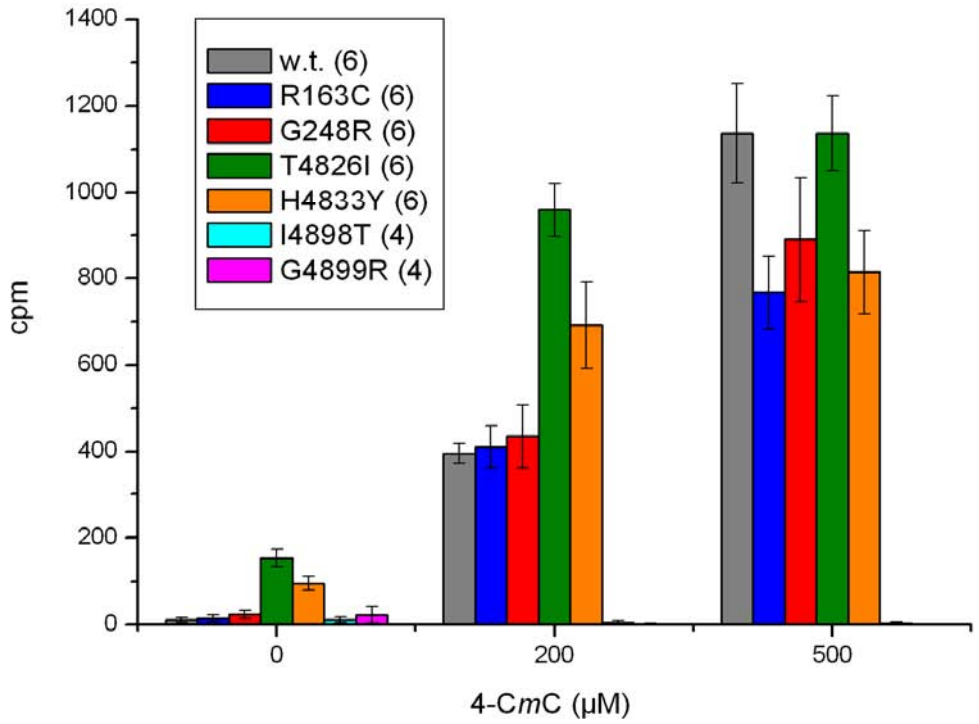

Figure 3-24 4-C*m*C activation for CCD mutants

Data are shown in cpm values and are not normalised because it was not feasible to do this for the two mutants linked to CCD, I4898T and G4899R. Reactions were performed 4-6 times (shown in brackets). WT and four mutants linked to MH showed binding with 4-C*m*C especially at high concentrations (500 µM). Two mutants linked to CCD did not show any binding to enable plotting a graph or calculation of EC_{50} indicating that these mutants may be hyposensitive to 4-C*m*C. Note that two C-terminal MH mutants, T4826I and H4833Y showed binding without 4-C*m*C (green and orange, respectively) indicating that these mutants may constitute a leaky channel. It is also notable that WT showed similar binding to R163C and G248R at 200 µM of 4-C*m*C. This could be because the WT had higher concentrations of RYR1 in reaction mixtures than did the mutants. WT tended to give higher RYR1 expression in transfections and often gave higher cpm in binding assays than mutants although the reason for higher expression for WT *RYR1* cDNA is unknown. Quantification of RYR1 in solubilisation buffer was not successful or reliable. Therefore, data needed to be normalised using cpm values at 500 µM as 100% binding and are shown in percentages for EC_{50} calculation (Figure 3-23).

3.5.2 Inhibition by Mg^{2+}

Binding reactions were also performed with various concentrations of the RYR1 antagonist, Mg^{2+}. High concentrations of Mg^{2+} inhibit channel opening and Ca^{2+} release. Binding reactions were performed with 10 µM free Ca^{2+}, without 4-C*m*C and 0.5-30 mM free Mg^{2+}. The RYR1 is activated to be opened by high concentrations (10 µM) of free Ca^{2+}. 4-C*m*C was not used because of its strong activation effect. Reactions were performed six times and sigmoidal fitted curves were used to calculate sensitivity to Mg^{2+} inhibition (half maximal inhibitory concentration, IC_{50}) (Figure 3-25). The cpm value at 0.5 mM Mg^{2+} was set as 100% binding. This assay was carried out for WT and four *RYR1* mutants linked to MH because the mutants linked to CCD could not be activated by 10 µM free Ca^{2+}. Curves from all mutants linked to MH were shifted to the right indicating that they were less sensitive to Mg^{2+} inhibition with significantly ($p<0.05$) higher IC_{50} than WT.

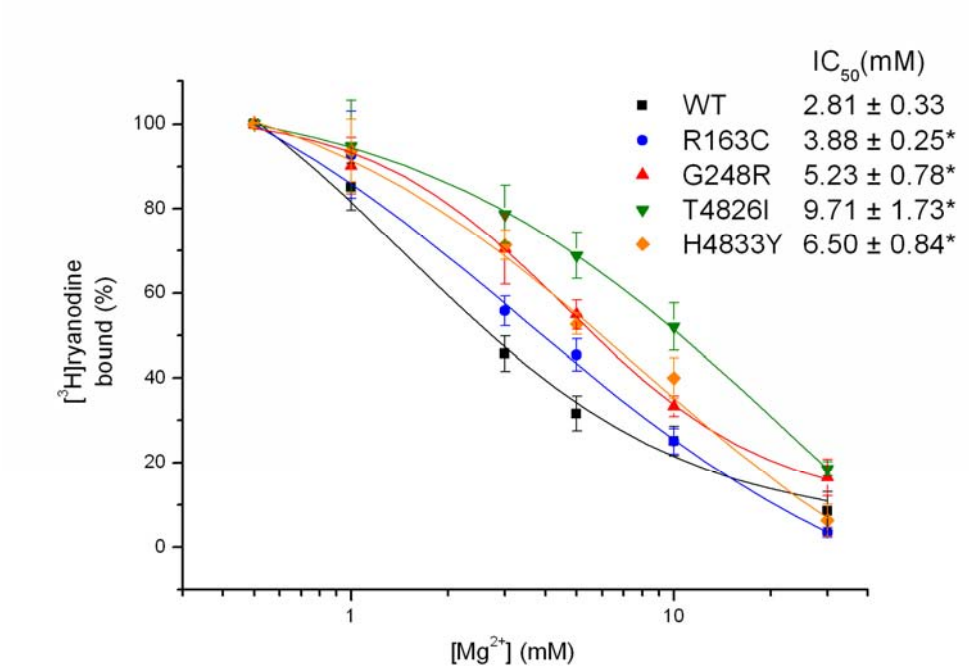

Figure 3-25 [^{3}H]ryanodine binding after Mg^{2+} inhibition

Reactions were performed with 10 µM free Ca^{2+} and 0.5-30 mM free Mg^{2+}. Normalised [^{3}H]ryanodine binding is shown as mean ± SEM (n=6) using values at 0.5 mM as 100%. All MH mutants were shifted to right showing less sensitivity to Mg^{2+}. IC_{50} for these mutants were also significantly higher than WT (*$p<0.05$).

3.5.3 Equilibrium binding parameters

The equilibrium binding parameters, dissociation constant K_d and maximal binding capacity B_{max} were obtained by reactions with various concentrations of [^{3}H]ryanodine. Reactions were performed with 10 µM free Ca^{2+} to activate the RYR1 protein and without any agonist or antagonist, 4-C*m*C or Mg^{2+}. [^{3}H]ryanodine binding increased depending on concentrations of [^{3}H]ryanodine in the reaction solution (Figure 3-26). The C-terminal mutants linked to MH T4826I and H4833Y showed higher binding ability and the two mutants linked to CCD showed lower binding compared to WT. Data were analysed by Scatchard analysis to calculate K_d and B_{max} (Figure 3-27). K_d and B_{max} for the two N-terminal RYR1 MH-linked mutants was not significantly different from WT RYR1 although they showed significantly different sensitivity or insensitivity against 4-C*m*C or Mg^{2+}, respectively. The two C-terminal RYR1 mutants linked to MH showed higher affinity and binding capacity to [^{3}H]ryanodine and both were statistically significantly ($p<0.05$) different to WT RYR1. In contrast, the two RYR1 mutants linked to CCD, I4898T and G4899R, showed very low significantly different B_{max} values compared to WT ($p<0.001$ and $p<0.05$, respectively) although binding affinity was not significantly different indicating their poor ability to bind [^{3}H]ryanodine. Data for the [^{3}H]ryanodine binding assay are shown in Table 3-8.

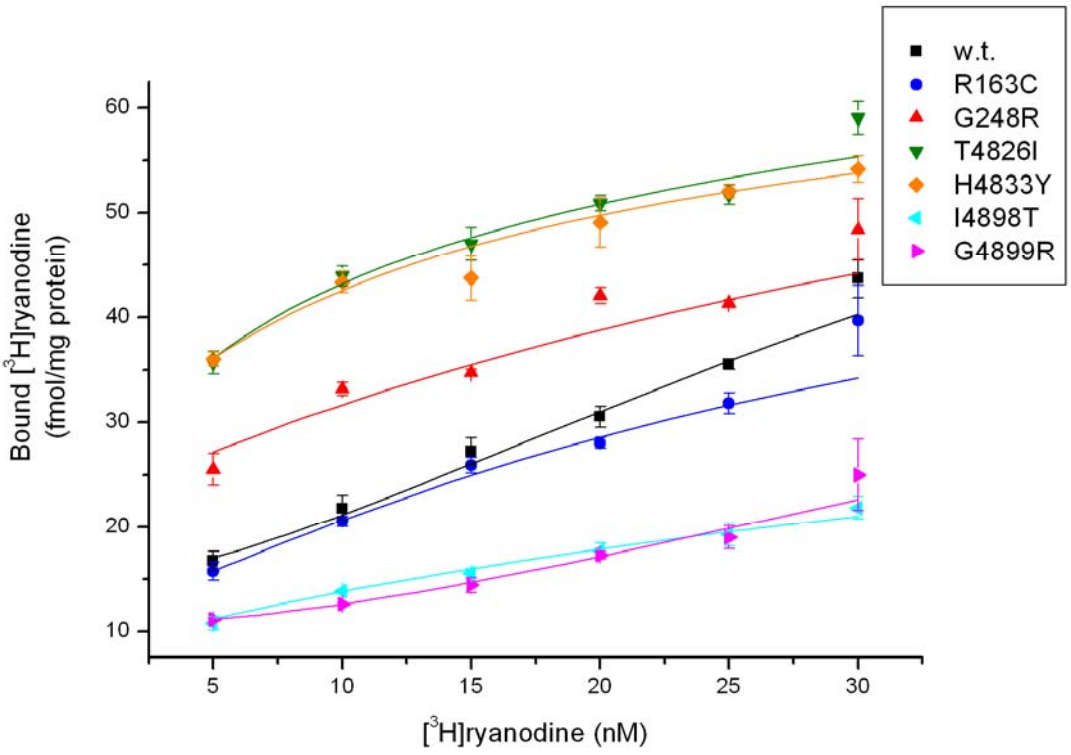

Figure 3-26 [^{3}H]ryanodine binding ability for the RYR1 proteins

[^{3}H]ryanodine binding was performed with 10 µM free Ca^{2+} and 5-30 nM [^{3}H]ryanodine for WT and six mutants linked to either MH or CCD to calculate equilibrium binding parameters K_d and B_{max}. Assays were performed only three times to conserve [^{3}H]ryanodine.

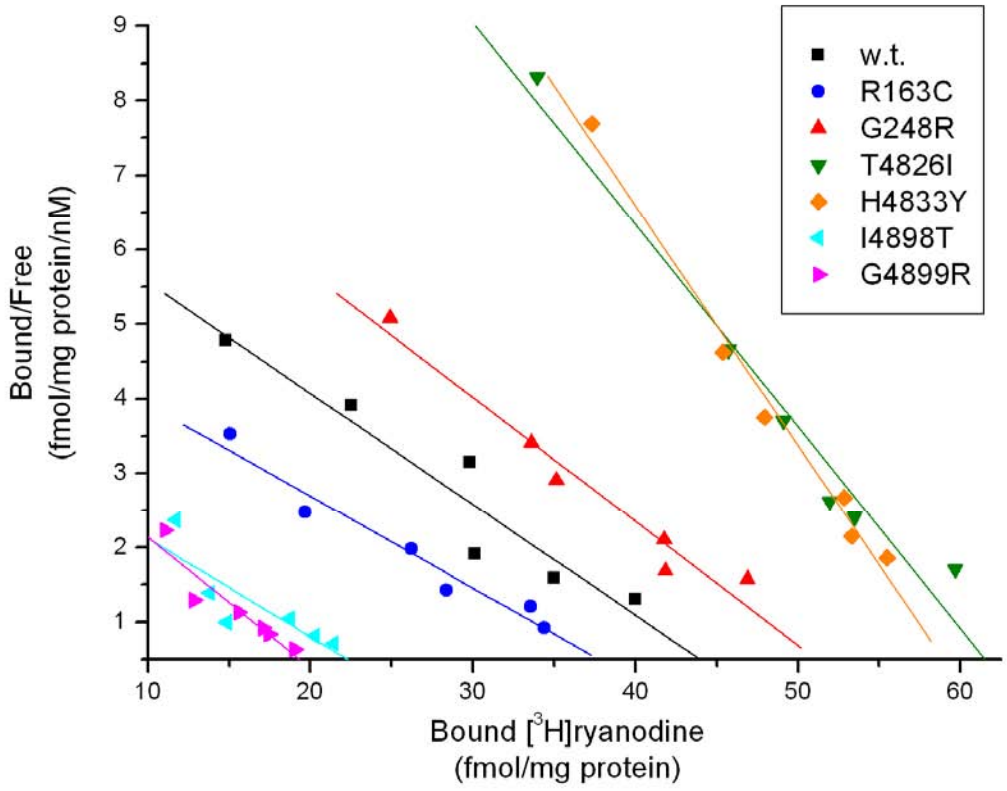

Figure 3-27 Scatchard analysis of [^{3}H]ryanodine binding

Scatchard analyses were performed to calculate K_d and B_{max}. K_d was calculated using slopes of each graph (K_d = -1/slope) showing the affinity between ryanodine and RYR1 proteins. Low K_d indicates high affinity. B_{max} was calculated using intercepts of the x axis showing how much ryanodine is required to saturate RYR1 proteins. Data analyses and graph plotting were carried out using ORIGIN software.

Mutations	EC_{50} for Ca^{2+} activation (μM)	IC_{50} for Mg^{2+} inhibition (mM)	K_d (nM)	B_{max} (fmol/mg)
WT	250.52 ± 14.17 (6)	2.81 ± 0.33 (6)	9.95 ± 1.62 (3)	51.92 ± 2.37 (3)
R163C	199.51 ± 14.14 (6)*	3.88 ± 0.25 (6)*	8.60 ± 1.58 (3)	45.21 ± 3.25 (3)
G248R	207.68 ± 7.01 (6)*	5.23 ± 0.78 (6)*	6.05 ± 1.22 (3)	54.75 ± 3.85 (3)
T4826I	68.44 ± 14.80 (6)**	9.71 ± 1.73 (6)*	3.91 ± 0.26 (3)*	62.47 ± 1.35 (3)*
H4833Y	91.47 ± 12.51 (6)**	6.50 ± 0.84 (6)*	3.58 ± 0.25 (3)*	59.26 ± 1.05 (3)*
I4898T	0 (4)**	N/A	8.40 ± 0.69 (3)	26.38 ± 1.40 (3)**
G4899R	0 (4)**	N/A	10.72 ± 2.81 (3)	29.32 ± 3.72 (3)*

Table 3-8 Data of [^{3}H]ryanodine binding assay in this study

Data are shown in mean ± SEM (numbers of experiments) calculated from sigmoidal or linear curve fitting. *p<0.05, **p<0.001 in unpaired Student's *t*-test compared with WT. The C-terminal *RYR1* mutants linked to CCD, I4898T and G4899R showed too little response to perform sigmoidal curve fitting and to calculate EC_{50} in 4-C*m*C activation and hence zero was obtained for these mutants. Binding reactions for Mg^{2+} inhibition were not feasible for these mutants because they could not be activated by 10 μM free Ca^{2+} and cpm values at 0.5 mM of Mg^{2+} to be set as 100% binding could not be obtained.

CHAPTER FOUR : DISCUSSION

4.1 Cloning strategy

This study is the first report of functional analyses using cloned human *RYR1* cDNA while previous studies have used *RYR1* cDNA from rabbit. A previous study has described the cloning strategy of rabbit *RYR1* cDNA amplifying small fragments of cDNA by PCR and subcloning the connected fragments by ligation [Tong, et al., 1997]. A similar strategy was adopted in this study for human *RYR1* cDNA. RT-PCR was performed to amplify ~1 kb fragments and 17 initial PCR reactions were required. The number of PCR reactions may be able to be reduced by amplifying longer fragments (2 to 3 kb) and thus simplify cloning steps. PCR primer sets for 1 kb fragments were selected by previous personal experience in RT-PCR of *RYR1* cDNA.

The previous study also described the restriction endonucleases used for cloning [Tong, et al., 1997]. For cloning of human *RYR1* cDNA, however, these restriction endonucleases described could not be used because of the different DNA sequences and absence of unique restriction endonuclease sites for digestion and ligation. The only available restriction endonuclease which does not digest the *RYR1* cDNA coding region was *Xba*I. Therefore, both ends of the coding region were necessarily *Xba*I. The use of the same enzyme site for both ends prevented a simple strategy to obtain the complete coding region in pBS as pBSRYR1. On the other hand, two enzymes *Xba*I and *Hin*dIII were used for rabbit *RYR1* cDNA simplifying the final fragment connection and excision of the entire coding region after subcloning to transfer it to another vector. An extra step was required for human *RYR1* using *Nhe*I for the final subcloning step to obtain pcRYR1 and this made excision of the entire coding region impossible. The pcRYR1 vector was, however sufficient for this study, but if the entire *RYR1* coding region is needed to be cloned into another vector, connection of fragments from pBSXK+ and pBSKX+ into the vector of interest using *Nhe*I and *Xba*I will be required. The vector should contain enzyme sites for *Nhe*I and *Xba*I in the correct orientation for expression (transcriptional start → *Nhe*I →*Xba*I).

Unique restriction endonuclease sites which digest *RYR1* only once are also limited for the human *RYR1* cDNA. These enzymes include *Sal*I and *Kpn*I. This limitation

prevents not only simplification of cloning steps but also of mutagenesis steps. *Kpn*I is an essential enzyme for cloning human *RYR1* cDNA with the strategy described in this thesis. Unfortunately, this enzyme site is located in the middle of hotspot region 2 and necessitates additional cloning steps after mutagenesis of this region. *RYR1* mutations within this region were not selected in this study because of lack of time. A subclone which contains the small fragment (2 to 3 kb) covering hotspot region 2 could be constructed for mutagenesis using PCR, but cloning after mutagenesis may still be difficult. Modifications of cloning steps may be required to introduce mutations within region 2, or cloning with extra steps may result in the fastest and most successful strategies.

4.2 Mutation selection

There are a large number of *RYR1* mutations reported that are linked to MH and/or CCD although functional studies have been performed for only a limited number of mutations. A major objective in this study was to construct the human *RYR1* cDNA clone and perform functional analyses using this cDNA. Functional studies using human cDNA had not been reported at the outset of this study or when this thesis was submitted. Although it was uncertain if cloning of *RYR1* cDNA was feasible, western blotting clearly showed the expressed RYR1 protein. As the cloning and expression was successful, it was then necessary to select *RYR1* mutations for mutant construction and subsequent functional studies.

Six *RYR1* mutations were selected and mutants were constructed for these mutations: two N-terminal mutations linked to MH, R163C and G248R, two C-terminal mutations linked to MH, T4826I and H4833Y, and two C-terminal mutations linked to CCD, I4898T and G4899R. As human *RYR1* cDNA had not been used previously in functional studies, mutations that had been used in previous work using rabbit *RYR1* cDNA were selected in order to test the use of human *RYR1* cDNA in functional analyses. The R163C and G248R mutations are two of the most common *RYR1* mutations identified widely throughout the world. The rabbit *RYR1* cDNA mutant clones had been constructed for these mutations and functional analyses had been performed showing their hypersensitivity against agonists such as halothane and

caffeine using HEK-293 cells in transient transfections [Tong, et al., 1997; Yang, et al., 2003]. This work suggested that they should make sound positive controls for functional studies using human *RYR1* cDNA. They should also be useful in establishing the experimental procedures for other *RYR1* mutations that are either currently unknown or uncommon with unpredictable responses against drugs.

Two C-terminal *RYR1* mutations linked to MH were also selected: T4826I and H4833Y. Both have been identified in New Zealand Maori MH families and clearly co-segregate in MHS patients who showed strong positive reactions during the IVCT [Anderson, et al., 2008; Brown, et al., 2000]. Functional studies have also been performed for the T4826I mutation using rabbit *RYR1* cDNA and for the H4833Y mutation using human B lymphocytes showing their hypersensitivity to agonists [Anderson, et al., 2008; Yang, et al., 2003]. At the time the H4833Y mutation was selected for the current work, the functional study using B lymphocytes had not been started. These four mutations are located in the N-terminal hotspot region 1 or C-terminal region 3, respectively. Comparison of several *RYR1* mutations from each hotspot region using the same experimental conditions may be of use in showing that *RYR1* mutations linked to MH have similar hypersensitivity against drugs regardless of the location of the mutations. Mutants with *RYR1* mutations from hotspot region 2, however, were not constructed because of the difficulties associated with cloning after mutagenesis. Site-directed mutagenesis using the MEGAWHOP technique [Miyazaki and Takenouchi, 2002] requires PCR amplification using a plasmid as a template. An *RYR1* fragment insert in the template plasmid should not be larger than 3 kb for successful and correct elongation. The pBSXC+ (2.7 kb insert) and pBSH+ (2.2 kb) subclones were used as templates for N-terminal (hotspot region 1) or C-terminal (hotspot region 3) mutations, respectively. It was not feasible, however, to design a subclone which contained a ~3 kb fragment covering the central hotspot region 2 because of unavailability of unique restriction enzyme sites. The pBSHK+ (4.5 kb) and pBSKO+ (5.8 kb) subclones cover region 2, but each is too large for use as a PCR template. The pBSKS+1177 (1.2 kb) or pBSKCII+ (2.7 kb) may be suitable to be used for mutagenesis of mutations located on region 2 although there are many subsequent steps of subcloning to construct pcRYR1+mutation after mutagenesis. Hence, MH mutations located only in either

region 1 or region 3 were selected in this study.

Functional studies for CCD mutations have recently been reported using the rabbit cDNA or transgenic mice [Durham, et al., 2008; Lynch, et al., 1999]. Two C-terminal CCD mutations I4898T and G4898R were selected in this study to compare with MH mutations under the same experimental conditions. Both mutations are common CCD mutations which have been identified only in CCD patients and not in MH families.

All mutations selected in this study have been used for previous functional studies. While the work carried out may not have produced new data, this is the first study using human *RYR1* cDNA. Nevertheless it is important to establish experimental procedures for cloning, mutagenesis, and protein expression for future work using other novel or uncharacterised *RYR1* mutations. Some other *RYR1* mutations including R44C, R401C and R533C were also selected but were not used for functional analyses in this study because of lack of time. Only mutagenesis was completed for some mutations such as G341R and mutagenesis and cloning was completed but [^{3}H]ryanodine binding assays were not performed for some mutations such as R44C. These mutations have been identified previously, but functional analyses have not yet been reported. The common mutations used in previous studies such as R163C were intended as positive controls to validate the human *RYR1* cDNA clone and establish its utility prior to analysing uncharacterised mutations. Further analyses of the other mutations already prepared by mutagenesis and cloned into the full-length human *RYR1* cDNA may be of interest for future work. This study provides a positive control for future studies using human *RYR1* cDNA.

4.3 Experimental design

Functional studies have been performed previously using several methods with three major methods used to date. The most direct method is to use cells obtained from MHS patients. This method includes studies using cultured skeletal muscle cells and B lymphocytes. Cultured skeletal muscle cells provide the most physiological *ex vivo* experimental environment for functional studies although surgery is required to obtain a skeletal muscle biopsy. B lymphocytes do not require surgery and can be obtained from blood samples. Both methods, however, require MHS patients and MHN

individuals for negative controls, for appropriate samples and these are not always readily available. These methods are also limited for mutation selection. Some mutations have been identified from only a few families and this limited sample availability prevents data comparison for several mutations under the same experimental conditions at the same time. Cultured muscle cells have several proteins associated with calcium homeostasis including calsequestrin and DHPR, and hence results cannot be considered specific for a functional defect of the RYR1 protein if drug treatment shows an abnormal response in calcium release. Therefore, it is difficult to trace the cause of abnormality in calcium homeostasis during functional studies. B lymphocytes do not express the DHPR or associated skeletal muscle triad proteins, so any abnormality in calcium release should be able to be attributed to the RYR1 but patient samples are still required.

Another method is to generate transgenic knock-in mice carrying an *RYR1* mutation. This technique has been established recently and can be used to monitor clinical conditions and physiological responses *in vivo* of mutation-carrying mice. This method has revealed that many mitochondria in muscle cells of transgenic mice that contain the Y522S mutation have been damaged [Durham, et al., 2008]. Although this technique also allows mutation selection, it requires establishment of transgenic mice. It generally takes a few years before functional analyses can be attempted and a specific facility for housing mice is needed during this period. The difficulties involved in establishing transgenic knock-in mice prevent wide-spread adoption of this method and hence limited numbers of reports have been published to date. These are generally limited to well-funded laboratories or collaborations.

The most common approach for functional studies of RYR1 proteins is *in vitro* analysis using *RYR1* cDNA clones. This system allows mutation selection and design, free access to samples, unsophisticated facilities, and a relatively short time for establishment and optimisation of experimental conditions. There are also some choices to make when using this approach: origin of *RYR1* cDNA, rabbit or human, and cells for RYR1 expression, COS-1, HEK-293 or dyspedic myotubes.

In this study, human *RYR1* cDNA and HEK-293 cells were used. This was the only accessible system available at the outset of this study. Although dyspedic myotubes,

RYR1-knockout skeletal muscle cells, may mimic *in vivo* conditions of MHS patients, HEK-293 cells were sufficient to express RYR1 proteins. Cells were solubilised after harvesting and RYR1 proteins were analysed in solubilised solutions except for the immunofluorescence assays. Calcium assays that detect intracellular calcium concentrations in cells use live cells on a plate, whereas [^{3}H]ryanodine binding assays use solubilised RYR1 proteins in CHAPS buffer no matter which cells were used for RYR1 protein expression.

The [^{3}H]ryanodine binding assay is an old method for RYR1 analyses established in 1998 [Du, et al., 1998]. This assay detects the open or closed state of the RYR1 channel and it can be used to analyse the response of RYR1 proteins to various agents. This technique, however, is not often used for functional studies compared with calcium release assays because it detects calcium release indirectly by scintillation counting for bound [^{3}H]ryanodine in the open state of RYR1 proteins while calcium assays detect intracellular Ca^{2+} concentrations ($[Ca^{2+}]_i$) directly released in response to agonists. Calcium assays can monitor $[Ca^{2+}]_i$ in real-time during drug treatments and they can provide strong evidence for hypersensitivity if cells show abnormally high $[Ca^{2+}]_i$ with agonists and this can also allow data plotting in real-time. The [^{3}H]ryanodine binding assay, however, is still used in some studies to calculate K_d and B_{max}. These binding parameters can measure properties of RYR1 proteins although they are omitted in many functional studies because RYR1 mutants often do not show significant differences in these parameters compared with WT.

In this study, calcium assays were not performed because of the unavailability of a spectrofluorometer or microscope required for the analysis. Ca^{2+} release from actively loaded cells using ^{45}Ca was also not performed due to lack of time. The [^{3}H]ryanodine binding assay, however, can be used to detect the response of RYR1 proteins to agonists and antagonists and can compare ryanodine binding characteristics between WT and mutant proteins. Therefore, this study focused on the characterisation of solubilised RYR1 proteins showing responses to 4-C*m*C and Mg^{2+} and measured binding parameters. Experimental conditions may not mimic environments in MHS patients or myotubes and any response against 4-C*m*C is necessarily an indirect measurement of channel opening properties. Calcium assays are required to confirm

that MH mutations cause abnormally high Ca^{2+} release to the cytosol leading to MH reactions in MHS patients. Nevertheless this study showed that RYR1 mutants have different ryanodine binding characteristics depending on the mutation introduced. These results imply different channel properties associated with different mutations.

The [^{3}H]ryanodine binding assay, however, may not be suitable or reliable for every mutant to be characterised by functional analyses. Prior to [^{3}H]ryanodine binding assay, several other *RYR1* cDNA mutants linked to MH were constructed including R401C and R533C as previous functional studies had not been reported. Western blotting detected RYR1 expression for these mutants although these data are not shown in this thesis. These mutants, however, did not show significantly different responses in the [^{3}H]ryanodine binding assay compared with WT. The number of experiments carried out for each of these was limited, however, and it cannot be concluded that these mutations cause no functional effects as patients carrying these mutations have shown clear MHS in the IVCT. The six mutants used in this study showed significant differences from WT in preliminary assays, and hence they were selected as mutants of interest to be analysed in a complete set of experiments.

The [^{3}H]ryanodine binding assay may be less sensitive than calcium assays and therefore may not be able to distinguish *RYR1* mutations linked to MH that cause weak MH reactions compared to those that cause strong MH reactions. The R163C mutations is one of the most common MH mutations identified worldwide with clear co-segregation with MHS phenotype and patients carrying this mutation have shown strong responses against agonists. This hypersensitivity to agonists including halothane, caffeine and 4-C*m*C has been observed in the IVCT, cultured skeletal muscle cells, transfected cells with cloned *RYR1* cDNAs of rabbit or human (this study), and transgenic knock-in mice [Censier, et al., 1998; Tong, et al., 1997; Yang, et al., 2006]. Some *RYR1* mutations may lead to strong sensitivity and MH susceptibility without any other trait or factor, and some *RYR1* mutations may have a minor effect on MH susceptibility and/or they require other traits or factors to induce strong MH susceptibility. It may be difficult for some mutations linked to minor MH susceptibility to conclude that the mutation shows significant abnormality to lead to the disorder using only one technique for functional studies. Therefore, several different functional

analyses may be required to confirm that a particular *RYR1* mutation leads to the disorder.

Four MH mutations used in this study showed a significantly high response or low response to 4-C*m*C or Mg^{2+}, respectively. These may be *RYR1* mutations linked to strong MH susceptibility and hence there are previous studies reported probably because of their strong hypersensitivity detectable in several different experimental systems. This study alone cannot conclude that these *RYR1* mutations lead to MH susceptibility, although results suggest that functions of RYR1 proteins are changed by a *RYR1* mutation and the functional effects are dependent on the mutation. Nevertheless the [^{3}H]ryanodine binding assay results presented do confirm causality of these mutations as shown by others [Lynch, et al., 1999; Yang, et al., 2003].

4.4 Expression and quantification

During transfection and subsequent western blotting, it was observed that WT RYR1 proteins were expressed at higher levels than the mutant proteins. The same experimental conditions always gave higher expression for WT. Figure 3-20 shows similar expression levels for each of the WT and six mutants, but total proteins to be analysed on the gel were intentionally overloaded for clarification of bands. In addition, the transfections with FuGENE HD in T75 flasks were carried out at high cell density for subsequent [^{3}H]ryanodine binding assays which require high RYR1 concentrations in the solution. The expression level of WT was observed more highly than mutants by western blotting on a smaller scale using 6-well plates and FuGENE 6 although these data were omitted from this thesis. Although the reason for this observation is unknown, it prevented comparison of cpm data directly between samples because the expression levels for all WT and mutant samples could not be controlled.

Protein quantification was attempted but was not used because reliable data could not be obtained as this necessarily measures total proteins not just RYR1. Quantification based on western blotting uses strength of signal from the bands on the blot. This requires that the protein of interest be located in a single band on the blot. The RYR1 protein, however, is a large protein and was often not stable during electrophoresis. It often gave two, sometimes three bands which were located very close together and

could be detected by the monoclonal 34C antibody. These bands may be different forms of RYR1 proteins changed in structure during electrophoresis or degradation products. Bands were often observed near the top of the well suggesting that some RYR1 proteins did not advance very far through the acrylamide gel. Some solubilised RYR1 proteins may aggregate with each other or with other proteins to form an insoluble protein complex which cannot be separated by the SDS-PAGE method used in this study.

Therefore, RYR1 concentrations in the solubilised solutions could not be determined. As control of expression levels for all samples could not be achieved because of the higher expression for WT, quantification of expressed RYR1 was abandoned and normalisation of data from the [^{3}H]ryanodine binding assays was carried out to calculate EC_{50} for 4-C*m*C activation and IC_{50} for Mg^{2+} inhibition ignoring the expression levels for each sample. Calculation of equilibrium binding parameters, K_d and B_{max} required protein concentrations in the binding solution to be known. As it was not feasible to calculate RYR1 concentrations, concentrations of total proteins in the solution calculated by the Bradford assay [Bradford, 1976] were used. Although the results showed significant differences for some mutants, the problems associated with determining protein concentrations may cause an inherent unreliability of data. Binding reactions for these parameters were performed only three times because these reactions consume a large volume of expensive [^{3}H]ryanodine and this limited number of experiments also decreases reliability. The [^{3}H]ryanodine binding assay has not always been performed in previous functional studies and this technique has been adopted for specific studies such as the first report of hyposensitive RYR1 mutants linked to CCD [Lynch, et al., 1999]. This assay may generally not be suitable for the production of reliable, reproducible results and may be omitted in functional studies when a large number of RYR1 mutants are compared. Alternatively, it may be performed in some situations for specific mutants with a reliably large number of experiments.

4.5 Hypersensitive RYR1

MH reactions are believed to be caused by abnormally high Ca^{2+} release from the SR triggered by agonists. It has therefore been suggested that RYR1 mutants linked to MH may show higher responses to triggering drugs in functional studies leading to higher Ca^{2+} release. Hypersensitivity, against triggering agents, of RYR1 mutants linked to MH has been observed in previous studies using the rabbit *RYR1* cDNA and transgenic knock-in mice [Chelu, et al., 2006; Yang, et al., 2003].

Four MH mutations were analysed in this study and each of them showed hypersensitivity to 4-C*m*C. This result supports previous studies using the rabbit cDNA and the suggested mechanism of MH reactions [Tong, et al., 1997; Yang, et al., 2003]. These RYR1 mutants linked to MH also showed a lower sensitivity to the antagonist Mg^{2+}, indicating that these mutants may not be closed readily during EC coupling. The WT RYR1 channel releases Ca^{2+} triggered by a signal but it can also be closed readily triggered by released Ca^{2+} in the sarcoplasm. On the other hand, it is thought that MH-linked RYR1 mutant channels cannot be induced to close as readily by high concentrations of released Ca^{2+} during MH reactions. A previous report has shown that low concentrations (10-100 µM) of free Ca^{2+} induce WT RYR1 opening, and high concentrations (> 1 mM) inhibit opening *in vitro* [Du, et al., 1998]. In this study, 10 µM of free Ca^{2+} was used as an agonist and Mg^{2+} was used as an antagonist for Mg^{2+} inhibition analyses. A lower sensitivity of MH-linked RYR1 mutants to antagonists supports previous studies and hypotheses developed to explain MH mechanisms [Yang, et al., 2003].

Two C-terminal RYR1 mutants linked to MH, T4826I and H4833Y showed very strong sensitivity. A low EC_{50} for 4-C*m*C activation was statistically very significant ($p< 0.001$) compared to WT and also significant ($p<0.05$) when compared to the two N-terminal RYR1 mutants R163C and G248R linked to MH. The T4826I and H4833Y mutations may be very strong MH mutations although the reason for their strong sensitivity is unknown and there are no clinical reports showing that MHS patients carrying these mutations show significantly more severe MH reactions or stronger responses in the IVCT compared with other MH mutations. Previous functional studies

using the rabbit cDNA has also shown significantly less sensitivity of the T4826I RYR1 mutant (T4825I in rabbit) to antagonists, Ca^{2+} and Mg^{2+} [Yang, et al., 2003]. These observations indicate that *RYR1* mutations which can lead to MH may cause higher sensitivity to agonists and less sensitivity to antagonists than WT, and the functional effects of mutations may differ depending on the mutation.

The N-terminal mutants, R163C and G248R showed no difference from WT in equilibrium binding parameters showing similar affinity and capacity for [^{3}H]ryanodine binding to WT. This observation indicates that these mutants may not exhibit any differences in properties of the channel, abilities in channel opening or performance as a calcium channel in normal conditions during EC coupling compared with WT, and they may only be hypersensitive to triggering anaesthetics leading to MH reactions.

4.6 Leaky RYR1

The C-terminal mutants, T4826I and H4833Y showed significantly ($p<0.05$) higher values for affinity (K_d) and maximal binding capacity (B_{max}). The N-terminal R163C and G248R mutations affect only sensitivity of the channel to agonists and the C-terminal T4826I and H4833Y mutations affect sensitivity and binding properties of the protein to ryanodine. These two C-terminal mutants may have not only high sensitivity but also high affinity to agonists and high binding ability to ryanodine. These mutants also showed significantly higher binding than WT in the absence of 4-C*m*C. Over 10% of [^{3}H]ryanodine binding without 4-C*m*C suggests that these mutants may always be opened and hence they may cause a leaky channel that releases Ca^{2+} continuously. Previous work using the rabbit cDNA containing the rabbit T4825I (T4826I in humans) mutation has also shown very significantly high binding in the presence of 4-C*m*C and high binding without 4-C*m*C [Yang, et al., 2003]. Although the effect of these mutations on the structure of the channel is unknown, they may be localised in the pore region of the channel and may severely influence channel opening. This result suggests that a single mutation may be able to change RYR1 function differently depending on both its location and the amino acid involved.

Leaky channels have been reported previously using rabbit cDNA. The Y523S

mutation (Y522S in humans) resulted in high resting cytosolic Ca^{2+} concentrations and reduced agonist-dependent Ca^{2+} release [Brini, et al., 2005; Tong, et al., 1999]. Y522S is a CCD-causing mutation and it is thought that a leaky channel depletes Ca^{2+} stores in the SR and the consequently reduced Ca^{2+} release during EC-coupling may cause muscle weakness which is one of the most common clinical symptoms of CCD. Transgenic knock-in mice have also shown that the Y522S mutation causes Ca^{2+} leakage and CCD-like characteristics such as abnormal mitochondria [Durham, et al., 2008]. Therefore, leaky RYR1 is one of the explanations for the mechanism underlying CCD.

The C-terminal MH mutations in this study, T4826I and H4833Y showed increased [^{3}H]ryanodine binding in the presence and absence of agonists suggesting leakage and hypersensitivity to 4-C*m*C at the same time. Although the [^{3}H]ryanodine binding assay shows only that the channel is opened and measurement of resting intracellular Ca^{2+} concentrations is required to confirm that these mutations cause leaky channels, these result indicates that the RYR1 channel could have both leaky and hypersensitive characteristics at the same time.

Previous studies have also shown co-existence of leakage and hypersensitivity. Cultured muscle cells from individuals who carry a CCD mutation I2453T have shown Ca^{2+} leakage (high resting $[Ca^{2+}]_i$) and hypersensitivity to 4-C*m*C [Wehner, et al., 2003]. Individuals have been clinically diagnosed with CCD and have also been diagnosed as MHS by the IVCT. Cultured muscle cells with the A2350T mutation have also shown a similar co-existence of these two disorders, MH and CCD and the two abnormalities, leakage and hypersensitivity [Wehner, et al., 2004]. These observations suggest that some *RYR1* mutations can cause both leaky and hypersensitive channels. The T4826I and H4833Y mutations have been identified only in MH patients and there have been no previous data showing that these mutations are associated with CCD. It may be possible, however, that they may result in both leaky and hypersensitive channels, and may result only in MH as a “compensated” leaky channel [Dirksen and Avila, 2004].

Although the H4833Y mutant showed both leakage and hypersensitivity in this study, a previous study using B lymphocytes isolated from affected patients has shown

hypersensitivity but no leakage [Anderson, et al., 2008]. It should be noted however that the mutation is present in homozygous form in transfected HEK-293 cells, and is heterozygous in B lymphocytes. As results may differ in different experimental systems and methods of functional analyses, it is important to investigate functional effects of *RYR1* mutations using several techniques to confirm the function of mutant proteins. Further investigation is required using resting $[Ca^{2+}]_i$ analysis in isolated cell systems and analysis of EC-coupling in membrane systems or myotubes isolated from knock-in mice.

4.7 Hyposensitive RYR1

The other description for the mechanism of CCD pathology is that the channel is hyposensitive and thus EC is uncoupled. The rabbit RYR1 mutant protein which carries the I4897T mutation (I4898T in humans), has shown no response to caffeine [Lynch, et al., 1999]. Other studies have also reported similar observations that some CCD mutants have been less or not sensitive to any triggering agents including drugs and electrical stimulation [Avila, et al., 2003; Ducreux, et al., 2004; Lyfenko, et al., 2007]. A leaky RYR1 channel which is a less sensitive channel to electrical signals during EC coupling is thought to cause decreased Ca^{2+} release and muscle weakness leading to CCD. Two common CCD mutations I4898T and G4899R that have been identified only in CCD families were analysed in this study. These mutants showed no response to any concentration of 4-C*m*C and this hyposensitivity supports a previous study using B lymphocytes from affected patients [Tilgen, et al., 2001]. The binding assay also showed that these mutants had similar affinity to [^{3}H]ryanodine (K_d) but significantly ($p<0.001$ and $p<0.05$ for I4898T and G4899R, respectively) reduced binding capacity (B_{max}) compared with WT. Although the effects of these mutations on the structure of the RYR1 are unknown, they may lose their ability to open the channel. Further analyses are required to detect resting $[Ca^{2+}]_i$ and to confirm that these mutants are leaky because these mutations may simply occlude a ryanodine binding site and hence they showed no binding in this study.

The I4898T and G4899R mutations have been identified only from CCD patients and there have been no reports showing the co-existence of hypersensitivity and

hyposensitivity.

4.8 Co-existence of MH and CCD

The co-existence of MH and CCD is observed phenotypically and diagnostically but is still controversial [Robinson, et al., 2002]. Functional studies for *RYR1* mutations sometimes provide inconsistent data. The R163C mutation, for example, is one of the most common MH mutations but it is also associated with CCD. Previous studies using rabbit *RYR1* cDNA containing the rabbit R164C mutation have shown hypersensitivity of the mutant to drugs including halothane and 4-C*m*C [Tong, et al., 1997; Yang, et al., 2003]. Another study, however, has reported that the rabbit RYR1 mutant with R164C shows low Ca^{2+} release because of leakage in myotubes [Avila and Dirksen, 2001]. The reason for this inconsistency is unclear: the results may differ in different experimental conditions or methodology; the R163C mutation may give the channel variable characteristics; or hypersensitivity and leakage can simply co-exist. This study using human *RYR1* cDNA and [^{3}H]ryanodine binding assay showed hypersensitivity for the R163C mutation but no evidence for leakage was found for this mutation. A previous report has tried to explain a mechanism of co-existence suggesting that a "compensated" leaky channel causes both hypersensitivity and leakage and a "decompensated" leaky channel causes Ca^{2+} store depletion and insufficient Ca^{2+} release leading to CCD [Dirksen and Avila, 2004]. The level of Ca^{2+} store depletion may depend on the level of the leakage. The mutant channel which has a low level of Ca^{2+} leakage and low sensitivity to triggering agents may show both leakage and hypersensitivity leading to MH, and the mutant which has large Ca^{2+} leakage and Ca^{2+} store depletion may show little Ca^{2+} release triggered by signals leading to CCD although more functional and detailed data are required to support this hypothesis.

Transient transfection was performed using only the R163C mutant cDNA clone, and hence the expressed protein was a homozygous mutant. The channel function may differ in homozygous and heterozygous conditions. A previous report using Y522S knock-in mice has shown that heterozygous mutant mice were hypersensitive to triggering agents and in contrast, homozygous knock-in mice were hyposensitive probably because of the leaky Y522S mutant channel and Ca^{2+} store depletion [Chelu,

et al., 2006]. Although the R163C knock-in mouse has shown hypersensitivity to triggering agents in both homozygous and heterozygous conditions [Yang, et al., 2006], results are likely to differ between homozygous and heterozygous mutant proteins and hence the genotype of the mutation may be important for the phenotype and channel functions.

The Y522S mutation is associated with both MH and CCD, and another study has reported that heterozygous Y522S knock-in mouse have shown MH-like symptoms (muscle contracture upon overheating) as well as CCD-like symptoms (swollen and misshapen mitochondria) [Durham, et al., 2008]. Previous observations suggest that the mutant RYR1 with Y522S is associated with both MH and CCD, and the single mutation leads to a leaky and hypersensitive channel.

In EC coupling, a depolarizing signal from nerves is detected by a voltage sensor protein, the dihydropyridine receptor (DHPR) and the DHPR transmits this signal to the RYR1 through a conformational change. Although a defined region of the DHPR plays a critical role in transmission of the signal [Kugler, et al., 2004], it is still not clear which RYR1 region is important in receiving the signalling that is allosteric from the DHPR. The N-terminal region of the RYR1 including hotspot region 1 is exposed in the sarcoplasm and some amino acids in this region may be important for contact with the DHPR (or other protein/s) and signal detection. Some N-terminal mutations such as Y522S may cause the functional defect in signal detection or transmission and hence this may cause hyposensitivity to the signal and insufficient Ca^{2+} release leading to CCD. These mutations may also cause hypersensitivity to triggering drugs such as halothane and abnormal Ca^{2+} release leading to MH because the pore region of the channel and the ability of channel opening is normal and Ca^{2+} stores are not completely depleted if the leakage is reasonably small.

There are some previous functional studies showing co-existence of leakage and hypersensitivity but there is no report so far showing co-existence of hypersensitivity and hyposensitivity. It is unlikely that the mutant RYR1 is sensitive to drugs releasing Ca^{2+} and insensitive without Ca^{2+} release at the same time. This study showed that CCD mutations I4898T and G4899R result in the RYR1 protein having no sensitivity to 4-C*m*C and the mutant channels may lose the ability of channel opening with less

[^{3}H]ryanodine binding. If the mutant RYR1 cannot open the channel pore and cannot release sufficient Ca^{2+} leading to CCD, then these mutations would be unlikely to cause MH reactions releasing abnormal Ca^{2+} release through the channel. A previous study, however, has reported a CCD family which has the I4898T mutation co-segregating with the phenotype of affected family members. Some members have the mutation, have shown CCD symptoms and been diagnosed as MHS by the IVCT [Lynch, et al., 1999]. It is not clear whether the mutation is responsible for both MH and CCD or the patients have another trait for MH susceptibility. Alternatively, the IVCT is not specific for MH so an *RYR1* mutation may result in a positive IVCT but not cause clinical MH. Further analyses are required to understand functional effects of CCD mutations and the mechanism of co-existence of MH and CCD.

4.9 Conclusions

In this study, human *RYR1* cDNA was cloned in a mammalian expression vector as pcRYR1. Mutant clones were also constructed containing the *RYR1* mutations R163C, G248R, T4826I, H4833Y, T4898I or G4899R. Western blotting detected expressed WT and mutant RYR1 proteins showing that transient transfection was successful. Immunofluorescence showed that expressed RYR1 proteins were co-localised with the ER in HEK-293 cells. [^{3}H]ryanodine binding assays showed that RYR1 mutants linked to MH were more sensitive to the agonist 4-C*m*C and less sensitive to the antagonist Mg^{2+}, compared with WT. The C-terminal mutants T4826I and H4833Y also showed high [^{3}H]ryanodine binding without 4-C*m*C suggesting that these mutants may cause leaky channels. The RYR1 mutants linked to CCD showed hyposensitivity to 4-C*m*C. This study showed that a mutation in *RYR1* can cause a different functional effect on the RYR1 protein depending on the position and amino acid residue that is altered.

4.10 Future directions

Only [^{3}H]ryanodine binding assays were carried out in this study because of limited availability of experimental apparatus. This technique is useful for analyses of channel opening and binding parameters but it cannot detect Ca^{2+} concentrations in cytosol directly. Therefore, it is still possible that mutations used in this study may alter the binding sites for [^{3}H]ryanodine or 4-C*m*C of the RYR1 mutants leading to significantly

different binding compared with WT. Ca^{2+} imaging using fluorescence microscope are hence the prime objective for future work. The T4826I and H4833Y mutants showed high [^{3}H]ryanodine binding without 4-C*m*C for [^{3}H]ryanodine binding assays in this study, and if they also show high intracellular resting Ca^{2+} concentrations ($[Ca^{2+}]_i$), it will strongly suggest that these mutations lead to leaky RYR1 channels. Ca^{2+} imaging can monitor $[Ca^{2+}]_i$ in real-time allowing visualisation of Ca^{2+} release responses to incremental doses of triggering agents in living cells and to compare the amplitudes of the Ca^{2+} release in the cytosol. Studies such as these may increase further understanding of RYR1 channel functions and functional effects of *RYR1* mutations. To spare expensive [^{3}H]ryanodine and reduce experimental cost, it may be useful to perform Ca^{2+} assays to determine the sensitivity to drugs for EC_{50} or IC_{50} calculation, and perform [^{3}H]ryanodine binding assays to establish binding parameters K_d and B_{max}.

HEK-293 cells were used in this study because of their availability, but dyspedic myotubes may be more useful and more suitable especially for Ca^{2+} assays. Origin of cells does not influence results in [^{3}H]ryanodine binding assays after cell lysis and protein solubilisation, but Ca^{2+} assays detect $[Ca^{2+}]_i$ in living cells. As dyspedic myotubes are likely to provide the most physiological experimental conditions *in vitro*, results of assays using these cells may be the most reliable. Although procedures including transfection using myotubes are more difficult compared with those for HEK-293 cells, functional studies using myotubes may distinguish functional effects of *RYR1* mutations associated with strong or weak MH or CCD.

Dyspedic myotubes or cultured skeletal muscle cells from MHS or MHN individuals may be necessary, especially for studies addressed at understanding the mechanism underlying EC coupling and ECCE. If an *RYR1* mutation does not influence channel function directly but does affect binding with other proteins and consequently EC coupling, or if abnormal calcium homeostasis in MHS patients is caused by proteins involved in ECCE not by RYR1 or DHPR, functional studies using HEK-293 cells may miss abnormal reactions caused by mutant RYR1 or other proteins. Although both dyspedic myotubes and cultured human myotubes are associated with difficulties in availability, handling and experimental procedures, it may be useful to attempt to use

them if they can be obtained.

Several other proteins are involved in calcium homeostasis in skeletal muscle cells. As for mutations in DHPR, a mutation may be identified in the future within a gene encoding a skeletal muscle protein involved in calcium homeostasis that binds to the RYR1 channel. The pcRYR1 vector and expressed RYR1 proteins may be useful for functional studies for these mutations within other calcium-related proteins. The RYR1 channel plays a central role in calcium release in skeletal muscle cells and studies of other proteins may also require recombinant RYR1 protein and the pcRYR1 vector.

Only known *RYR1* mutations for which there are previous functional studies were selected. Results of the study indicated the efficacy of using human *RYR1* cDNA in functional [^{3}H]ryanodine binding assays. This suggests that the same experimental procedures could be used to analyse functional effects of other *RYR1* mutations using the complete pcRYR1 vector. As the total number of *RYR1* mutations functionally analysed has been limited thus far, studies of other novel or relatively uncommon mutations may be worthwhile.

A recent study, reporting the three-dimensional structure of a specific region of the RYR1 protein (1-210 amino acids), indicated that N-terminal mutations associated with MH are clustered and localised in a specific outside loop of the channel [Amador, et al., 2009]. A random mutation series within this loop may be used for functional analyses to pin-point the amino acids which are involved in hypersensitivity to agonists.

Recent studies have reported that multi-minicore disease (MmD) is also thought to be associated with *RYR1* mutations [Jungbluth, 2007b]. MmD is a non-progressive congenital myopathy with an autosomal recessive trait. It is characterised by neonatal hypotonia, muscle weakness and presence of core lesions in muscle biopsies. MmD is distinguished from CCD by inheritance pattern, the different length of the histological lesions in skeletal muscle and different clinical symptoms. Although some homozygous mutations have been identified in the C-terminal region of *RYR1*, there are very few case reports and clinical studies reported for this rare myopathy [Ferreiro, et al., 2002; Monnier, et al., 2003]. As a single mutation within *RYR1* may cause

various functional defects and various disorders depending on the individual mutation, functional studies for a number of *RYR1* mutations to compare their effects may provide important and novel data to understand the mechanisms of these disorders as well as EC coupling and RYR1 channel functions. The complete vector pcRYR1 containing the human *RYR1* coding region could be a powerful tool for studies of MH, CCD and MmD, and calcium homeostasis including EC coupling and signaling as long as cells appropriate to the application are used.

CHAPTER FIVE : REFERENCES

Allen GC, Larach MG, Kunselman AR. 1998. The sensitivity and specificity of the caffeine-halothane contracture test: a report from the North American Malignant Hyperthermia Registry. The North American Malignant Hyperthermia Registry of MHAUS. Anesthesiology 88(3):579-88.

Amador FJ, Liu S, Ishiyama N, Plevin MJ, Wilson A, MacLennan DH, Ikura M. 2009. Crystal structure of type I ryanodine receptor amino-terminal beta-trefoil domain reveals a disease-associated mutation "hot spot" loop. Proc Natl Acad Sci U S A 106(27):11040-4.

Anderson AA, Brown RL, Polster B, Pollock N, Stowell KM. 2008. Identification and biochemical characterization of a novel ryanodine receptor gene mutation associated with malignant hyperthermia. Anesthesiology 108(2):208-15.

Avila G. 2005. Intracellular Ca2+ dynamics in malignant hyperthermia and central core disease: established concepts, new cellular mechanisms involved. Cell Calcium 37(2):121-127.

Avila G, Dirksen RT. 2001. Functional effects of central core disease mutations in the cytoplasmic region of the skeletal muscle ryanodine receptor. J Gen Physiol 118(3):277-90.

Avila G, O'Brien JJ, Dirksen RT. 2001. Excitation--contraction uncoupling by a human central core disease mutation in the ryanodine receptor. Proc Natl Acad Sci U S A 98(7):4215-20.

Avila G, O'Connell KMS, Dirksen RT. 2003. The pore region of the skeletal muscle ryanodine receptor is a primary locus for excitation-contraction uncoupling in central core disease. J Gen Physiol 121(4):277-286.

Bannister RA, Grabner M, Beam KG. 2008. The alpha(1S) III-IV loop influences 1,4-dihydropyridine receptor gating but is not directly involved in excitation-contraction coupling interactions with the type 1 ryanodine receptor. J Biol Chem 283(34):23217-23.

Beard NA, Wei L, Dulhunty AF. 2009. Ca(2+) signaling in striated muscle: the elusive roles of triadin, junctin, and calsequestrin. Eur Biophys J 39(1):27-36.

Bellah JR, Robertson SA, Buergelt CD, McGavin AD. 1989. Suspected malignant hyperthermia after halothane anesthesia in a cat. Vet Surg 18(6):483-8.

Berridge MJ, Lipp P, Bootman MD. 2000. The versatility and universality of calcium signalling. Nat Rev Mol Cell Biol 1(1):11-21.

Bethlem J, van Wijngaarden GK, Meijer AE, Fleury P. 1971. Observations on central core disease. J Neurol Sci 14(3):293-9.

Bradford MM. 1976. A rapid and sensitive method for the quantitation of microgram quantities of protein utilizing the principle of protein-dye binding. Anal Biochem 72:248-54.

Brini M, Manni S, Pierobon N, Du GG, Sharma P, MacLennan DH, Carafoli E. 2005. Ca^{2+} signaling in HEK-293 and skeletal muscle cells expressing recombinant

ryanodine receptors harboring malignant hyperthermia and central core disease mutations. J Biol Chem 280(15):15380-15389.

Brinkmeier H, Kramer J, Kramer R, Iaizzo PA, Baur C, Lehmann-Horn F, Rudel R. 1999. Malignant hyperthermia causing Gly2435Arg mutation of the ryanodine receptor facilitates ryanodine-induced calcium release in myotubes. Br J Anaesth 83(6):855-61.

Brown RL, Pollock AN, Couchman KG, Hodges M, Hutchinson DO, Waaka R, Lynch P, McCarthy TV, Stowell KM. 2000. A novel ryanodine receptor mutation and genotype-phenotype correlation in a large malignant hyperthermia New Zealand Maori pedigree. Hum Mol Genet 9(10):1515-1524.

Carpenter D, Ringrose C, Leo V, Robinson RL, Booms P, Iles DE, Steele D, Halsall PJ, Hopkins P, Shaw M-A. 2008. New mutatin in the dihydropyridine receptor gene, *CACNA1S* predisposing to Malignant Hyperthermia. The EMHG Meeting. p 15.

Carrier L, Villaz M, Dupont Y. 1991. Abnormal rapid Ca^{2+} release from sarcoplasmic reticulum of malignant hyperthermia susceptible pigs. Biochim Biophys Acta 1064(2):175-83.

Censier K, Urwyler A, Zorzato F, Treves S. 1998. Intracellular calcium homeostasis in human primary muscle cells from malignant hyperthermia-susceptible and normal individuals. Effect of overexpression of recombinant wild-type and Arg163Cys mutated ryanodine receptors. J Clin Invest 101(6):1233-42.

Chelu MG, Goonasekera SA, Durham WJ, Tang W, Lueck JD, Riehl J, Pessah IN, Zhang P, Bhattacharjee MB, Dirksen RT and others. 2006. Heat- and anesthesia-induced malignant hyperthermia in an RyR1 knock-in mouse. FASEB J 20(2):329-30.

Chen SR, Vaughan DM, Airey JA, Coronado R, MacLennan DH. 1993. Functional expression of cDNA encoding the Ca^{2+} release channel (ryanodine receptor) of rabbit skeletal muscle sarcoplasmic reticulum in COS-1 cells. Biochemistry 32(14):3743-53.

Cherednichenko G, Ward CW, Feng W, Cabrales E, Michaelson L, Samso M, Lopez JR, Allen PD, Pessah IN. 2008. Enhanced excitation-coupled calcium entry in myotubes expressing malignant hyperthermia mutation R163C is attenuated by dantrolene. Mol Pharmacol 73(4):1203-12.

Chomczynski P, Sacchi N. 1987. Single-step method of RNA isolation by acid guanidinium thiocyanate-phenol-chloroform extraction. Anal Biochem 162(1):156-9.

Coronado R, Morrissette J, Sukhareva M, Vaughan DM. 1994. Structure and function of ryanodine receptors. Am J Physiol 266(6 Pt 1):C1485-504.

Davis M, Brown RL, Dickson A, Horton H, James D, Laing N, Marston R, Norgate M, Perlman D, Stowell KM. 2002. Malignant hyperthermia associated with exercise-induced rhabdmyolysis or congenital abnormalities and a novel *RYR1* mutation in New Zealand and Australian pedigrees. Br J Anaesth 88(4):508-515.

Denborough M. 1998. Malignant hyperthermia. Lancet 352(9134):1131-1136.

Denborough M, Lovell R. 1960. Anaesthetic deaths in a family. Lancet 2:45.

Denborough MA. 1982. Heat stroke and malignant hyperpyrexia. Med J Aust 1(5):204-5.

Denborough MA, Dennett X, Anderson RM. 1973. Central-core disease and malignant hyperpyrexia. Br Med J 1(5848):272-3.

Denborough MA, Forster JF, Lovell RR, Maplestone PA, Villiers JD. 1962. Anaesthetic deaths in a family. Br J Anaesth 34:395-6.

Deufel T, Golla A, Iles D, Meindl A, Meitinger T, Schindelhauer D, DeVries A, Pongratz D, MacLennan DH, Johnson KJ and others. 1992. Evidence for genetic heterogeneity of malignant hyperthermia susceptibility. Am J Hum Genet 50(6):1151-61.

Dirksen RT. 2009. Checking your SOCCs and feet: the molecular mechanisms of Ca2+ entry in skeletal muscle. J Physiol 587(Pt 13):3139-47.

Dirksen RT, Avila G. 2002. Altered ryanodine receptor function in central core disease: leaky or uncoupled Ca(2+) release channels? Trends Cardiovasc Med 12(5):189-97.

Dirksen RT, Avila G. 2004. Distinct effects on Ca^{2+} handling caused by malignant hyperthermia and central core disease mutations in *RyR1*. Biophys J 87(5):3193-204.

Du GG, Imredy JP, MacLennan DH. 1998. Characterization of recombinant rabbit cardiac and skeletal muscle Ca^{2+} release channels (ryanodine receptors) with a novel [^{3}H]ryanodine binding assay. J Biol Chem 273(50):33259-66.

Du GG, Oyamada H, Khanna VK, MacLennan DH. 2001. Mutations to Gly(2370), Gly(2373) or Gly(2375) in malignant hyperthermia domain 2 decrease caffeine and cresol sensitivity of the rabbit skeletal-muscle Ca^{2+} -release channel (ryanodine receptor isoform 1). Biochem J 360:97-105.

Dubowitz V, Pearse AG. 1960. Oxidative enzymes and phosphorylase in central-core disease of muscle. Lancet 2(7140):23-4.

Ducreux S, Zorzato F, Muller C, Sewry C, Muntoni F, Quinlivan R, Restagno G, Girard T, Treves S. 2004. Effect of ryanodine receptor mutations on interleukin-6 release and intracellular calcium homeostasis in human myotubes from malignant hyperthermia-susceptible individuals and patients affected by central core disease. J Biol Chem 279(42):43838-46.

Duke AM, Hopkins PM, Halsal JP, Steele DS. 2004. Mg^{2+} dependence of halothane-induced Ca^{2+} release from the sarcoplasmic reticulum in skeletal muscle from humans susceptible to malignant hyperthermia. Anesthesiology 101(6):1339-46.

Durham WJ, Aracena-Parks P, Long C, Rossi AE, Goonasekera SA, Boncompagni S, Galvan DL, Gilman CP, Baker MR, Shirokova N and others. 2008. RyR1 S-nitrosylation underlies environmental heat stroke and sudden death in Y522S RyR1 knockin mice. Cell 133(1):53-65.

Ellis FR, Harriman DG, Keaney NP, Kyei-Mensah K, Tyrrell JH. 1971. Halothane-induced muscle contracture as a cause of hyperpyrexia. Br J Anaesth 43(7):721-2.

European Malignant Hyperpyrexia Group. 1984. A Protocol for the Investigation of Malignant Hyperpyrexia (MH) Susceptibility. Br J Anaesth 56(11):1267-1269.

Fagerlund TH, Ording H, Bendixen D, Islander G, Ranklev Twetman E, Berg K. 1997. Discordance between malignant hyperthermia susceptibility and *RYR1* mutation C1840T in two Scandinavian MH families exhibiting this mutation. Clin Genet 52(6):416-21.

Feng W, Tu JC, Yang TZ, Vernon PS, Allen PD, Worley PF, Pessah IN. 2002. Homer regulates gain of ryanodine receptor type 1 channel complex. J Biol Chem 277(47):44722-44730.

Ferreiro A, Monnier N, Romero NB, Leroy JP, Bonnemann C, Haenggeli CA, Straub V, Voss WD, Nivoche Y, Jungbluth H and others. 2002. A recessive form of central core disease, transiently presenting as multi-minicore disease, is associated with a homozygous mutation in the ryanodine receptor type 1 gene. Ann Neurol 51(6):750-759.

Fill M, Coronado R, Mickelson JR, Vilven J, Ma JJ, Jacobson BA, Louis CF. 1990. Abnormal ryanodine receptor channels in malignant hyperthermia. Biophys J 57(3):471-475.

Fletcher JE, Calvo PA, Rosenberg H. 1993. Phenotypes associated with malignant hyperthermia susceptibility in swine genotyped as homozygous or heterozygous for the ryanodine receptor mutation. Br J Anaesth 71(3):410-7.

Fletcher JE, Tripolitis L, Hubert M, Vita GM, Levitt RC, Rosenberg H. 1995. Genotype and phenotype relationships for mutations in the ryanodine receptor in patients referred for diagnosis of malignant hyperthermia. Br J Anaesth 75(3):307-10.

Frank JP, Harati Y, Butler IJ, Nelson TE, Scott CI. 1980. Central core disease and malignant hyperthermia syndrome. Ann Neurol 7(1):11-7.

Friesen CM, Brodsky JB, Dillingham MF. 1979. Successful use of dantrolene sodium in human malignant hyperthermia syndrome: a case report. Can Anaesth Soc J 26(4):319-21.

Gillard EF, Otsu K, Fujii J, Duff C, de Leon S, Khanna VK, Britt BA, Worton RG, MacLennan DH. 1992. Polymorphisms and deduced amino acid substitutions in the coding sequence of the ryanodine receptor (RYR1) gene in individuals with malignant hyperthermia. Genomics 13(4):1247-54.

Gillard EF, Otsu K, Fujii J, Khanna VK, de Leon S, Derdemezi J, Britt BA, Duff CL, Worton RG, MacLennan DH. 1991. A substitution of cysteine for arginine 614 in the ryanodine receptor is potentially causative of human malignant hyperthermia. Genomics 11(3):751-5.

Girard T, Cavagna D, Padovan E, Spagnoli G, Urwyler A, Zorzato F, Treves S. 2001. B-lymphocytes from malignant hyperthermia-susceptible patients have an increased sensitivity to skeletal muscle ryanodine receptor activators. J Biol

Chem 276(51):48077-82.

Girard T, Treves S, Voronkov E, Siegemund M, Urwyler A. 2004. Molecular genetic testing for malignant hyperthermia susceptibility. Anesthesiology 100(5):1076-1080.

Grabner M, Dirksen RT, Suda N, Beam KG. 1999. The II-III loop of the skeletal muscle dihydropyridine receptor is responsible for the Bi-directional coupling with the ryanodine receptor. J Biol Chem 274(31):21913-9.

Hackl W, Mauritz W, Schemper M, Winkler M, Sporn P, Steinbereithner K. 1990. Prediction of malignant hyperthermia susceptibility: statistical evaluation of clinical signs. Br J Anaesth 64(4):425-9.

Hakamata Y, Nakai J, Takeshima H, Imoto K. 1992. Primary structure and distribution of a novel ryanodine receptor/calcium release channel from rabbit brain. FEBS Lett 312(2-3):229-35.

Hall LW, Woolf N, Bradley JW, Jolly DW. 1966. Unusual reaction to suxamethonium chloride. Br Med J 2(5525):1305.

Hamilton SL, Serysheva, II. 2009. Ryanodine receptor structure: progress and challenges. J Biol Chem 284(7):4047-51.

Harbitz I, Chowdhary B, Thomsen PD, Davies W, Kaufmann U, Kran S, Gustavsson I, Christensen K, Hauge JG. 1990. Assignment of the porcine calcium release channel gene, a candidate for the malignant hyperthermia locus, to the 6p11----q21 segment of chromosome 6. Genomics 8(2):243-8.

Healy JM, Quane KA, Keating KE, Lehane M, Heffron JJ, McCarthy TV. 1996. Diagnosis of malignant hyperthermia: a comparison of the in vitro contracture test with the molecular genetic diagnosis in a large pedigree. J Med Genet 33(1):18-24.

Herrmann-Frank A, Richter M, Lehmann-Horn F. 1996. 4-Chloro-m-cresol: a specific tool to distinguish between malignant hyperthermia-susceptible and normal muscle. Biochem Pharmacol 52(1):149-55.

Hopkins PM, Ellis FR, Halsall PJ. 1991. Evidence for related myopathies in exertional heat-stroke and malignant hyperthermia. Lancet 338(8781):1491-1492.

Iles DE, Lehmann-Horn F, Scherer SW, Tsui LC, Olde Weghuis D, Suijkerbuijk RF, Heytens L, Mikala G, Schwartz A, Ellis FR and others. 1994. Localization of the gene encoding the alpha 2/delta-subunits of the L-type voltage-dependent calcium channel to chromosome 7q and analysis of the segregation of flanking markers in malignant hyperthermia susceptible families. Hum Mol Genet 3(6):969-75.

Iles DE, Segers B, Sengers RCA, Monsieurs K, Heytens L, Halsall PJ, Hopkins PM, Ellis FR, Hallcurran JL, Stewart AD and others. 1993. Genetic-mapping of the beta(1)-subunit and gamma-subunit of the human skeletal-muscle L-type voltage-dependent calcium-channel on chromosome-17q and exclusion as candidate genes for malignant hyperthermia Susceptibility. Hum Mol Genet 2(7):863-868.

Inoue H, Nojima H, Okayama H. 1990. High efficiency transformation of *Escherichia coli* with plasmids. Gene 96(1):23-8.

Islander G, Ording H, Bendixen D, Twetman ER. 2002. Reproducibility of in vitro contracture test results in patients tested for malignant hyperthermia susceptibility. Acta Anaesthesiol Scand 46(9):1144-1149.

Jiang D, Xiao B, Yang D, Wang R, Choi P, Zhang L, Cheng H, Chen SR. 2004. RyR2 mutations linked to ventricular tachycardia and sudden death reduce the threshold for store-overload-induced Ca^{2+} release (SOICR). Proc Natl Acad Sci U S A 101(35):13062-7.

Jones AM. 2000. Preliminary investigation of the C-terminal mutations that cause malignant hyperthermia [MSc thesis]. Palmerston North: Massey University. 142 p.

Jungbluth H. 2007a. Central core disease. Orphanet J Rare Dis 2:25.

Jungbluth H. 2007b. Multi-minicore Disease. Orphanet J Rare Dis 2:31.

Kalow W, Britt BA. 1973. Drugs causing rigidity in malignant hyperthermia. Lancet 2(7825):390-1.

Kalow W, Britt BA, Chan FY. 1979. Epidemiology and inheritance of malignant hyperthermia. Int Anesthesiol Clin 17(4):119-39.

Kalow W, Britt BA, Terreau ME, Haist C. 1970. Metabolic error of muscle metabolism after recovery from malignant hyperthermia. Lancet 2(7679):895-8.

Keating KE, Quane KA, Manning BM, Lehane M, Hartung E, Censier K, Urwyler A, Klausnitzer M, Muller CR, Heffron JJ and others. 1994. Detection of a novel RYR1 mutation in four malignant hyperthermia pedigrees. Hum Mol Genet 3(10):1855-8.

Kim DH, Sreter FA, Ohnishi ST, Ryan JF, Roberts J, Allen PD, Meszaros LG, Antoniu B, Ikemoto N. 1984. Kinetic studies of Ca^{2+} release from sarcoplasmic reticulum of normal and malignant hyperthermia susceptible pig muscles. Biochim Biophys Acta 775(3):320-7.

Kobayashi S, Yamamoto T, Parness J, Ikemoto N. 2004. Antibody probe study of Ca^{2+} channel regulation by interdomain interaction within the ryanodine receptor. Biochem J 380:561-569.

Kraev N, Loke JCP, Kraev A, MacLennan DH. 2003. Protocol for the sequence analysis of ryanodine receptor subtype 1 gene transcripts from human leukocytes. Anesthesiology 99(2):289-296.

Kugler G, Weiss RG, Flucher BE, Grabner M. 2004. Structural requirements of the dihydropyridine receptor alpha(1S) II-III loop for skeletal-type excitation-contraction coupling. J Biol Chem 279(6):4721-4728.

Larach MG. 1989. Standardization of the caffeine halothane muscle contracture test. Anesthesia and Analgesia 69(4):511-515.

Lee JM, Rho SH, Shin DW, Cho CH, Park WJ, Eom SH, Ma JJ, Kim DH. 2004. Negatively charged amino acids within the intraluminal loop of ryanodine

receptor are involved in the interaction with triadin. J Biol Chem 279(8):6994-7000.

Levano S, Vukcevic M, Singer M, Matter A, Treves S, Urwyler A, Girard T. 2009. Increasing the number of diagnostic mutations in malignant hyperthermia. Hum Mutat 30(4):590-8.

Litman RS, Rosenberg H. 2005. Malignant hyperthermia - Update on susceptibility testing. JAMA 293(23):2918-2924.

Lopez JR, Alamo L, Caputo C, Wikinski J, Ledezma D. 1985. Intracellular ionized calcium concentration in muscles from humans with malignant hyperthermia. Muscle Nerve 8(5):355-8.

Lopez JR, Contreras J, Linares N, Allen PD. 2000. Hypersensitivity of malignant hyperthermia-susceptible swine skeletal muscle to caffeine is mediated by high resting myoplasmic [Ca^{2+}]. Anesthesiology 92(6):1799-806.

Lyfenko AD, Ducreux S, Wang Y, Xu L, Zorzato F, Ferreiro A, Meissner G, Treves S, Dirksen RT. 2007. Two central core disease (CCD) deletions in the C-terminal region of *RYR1* alter muscle excitation-contraction (EC) coupling by distinct mechanisms. Hum Mutat 28(1):61-8.

Lynch PJ, Krivosic-Horber R, Reyford H, Monnier N, Quane K, Adnet P, Haudecoeur G, Krivosic I, McCarthy T, Lunardi J. 1997. Identification of heterozygous and homozygous individuals with the novel RYR1 mutation Cys35Arg in a large kindred. Anesthesiology 86(3):620-6.

Lynch PJ, Tong J, Lehane M, Mallet A, Giblin L, Heffron JJ, Vaughan P, Zafra G, MacLennan DH, McCarthy TV. 1999. A mutation in the transmembrane/luminal domain of the ryanodine receptor is associated with abnormal Ca^{2+} release channel function and severe central core disease. Proc Natl Acad Sci U S A 96(7):4164-9.

MacLennan DH, Duff C, Zorzato F, Fujii J, Phillips M, Korneluk RG, Frodis W, Britt BA, Worton RG. 1990. Ryanodine receptor gene is a candidate for predisposition to malignant hyperthermia. Nature 343(6258):559-561.

Magee KR, Shy GM. 1956. A new congenital non-progressive myopathy. Brain 79(4):610-21.

Manning BM, Quane KA, Lynch PJ, Urwyler A, Tegazzin V, Krivosic-Horber R, Censier K, Comi G, Adnet P, Wolz W and others. 1998a. Novel mutations at a CpG dinucleotide in the ryanodine receptor in malignant hyperthermia. Hum Mutat 11(1):45-50.

Manning BM, Quane KA, Ording H, Urwyler A, Tegazzin V, Lehane M, O'Halloran J, Hartung E, Giblin LM, Lynch PJ and others. 1998b. Identification of novel mutations in the ryanodine-receptor gene (RYR1) in malignant hyperthermia: genotype-phenotype correlation. Am J Hum Genet 62(3):599-609.

Marks AR, Tempst P, Hwang KS, Taubman MB, Inui M, Chadwick C, Fleischer S, Nadal-Ginard B. 1989. Molecular cloning and characterization of the ryanodine receptor/junctional channel complex cDNA from skeletal muscle sarcoplasmic reticulum. Proc Natl Acad Sci U S A 86(22):8683-7.

McCarthy TV, Healy JMS, Heffron JJA, Lehane M, Deufel T, Lehmannhorn F, Farrall M, Johnson K. 1990. Localization of the malignant hyperthermia susceptibility locus to human-chromosome 19q12-13.2. Nature 343(6258):562-564.

McCarthy TV, Mackrill JJ. 2004. Unravelling calcium-release channel gating: clues from a 'hot' disease. Biochem J 380:e1-e3.

McCarthy TV, Quane KA, Lynch PJ. 2000. Ryanodine receptor mutations in malignant hyperthermia and central core disease. Human Mutation 15(5):410-417.

McPherson PS, Campbell KP. 1993. The ryanodine receptor/Ca^{2+} release channel. J Biol Chem 268(19):13765-8.

Melzer W, Dietze B. 2001. Malignant hyperthermia and excitation-contraction coupling. Acta Physiol Scand 171(3):367-78.

Melzer W, Herrmannfrank A, Luttgau HC. 1995. The role of Ca^{2+} Ions in excitation-contraction coupling of skeletal-muscle fibers. Biochim Biophys Acta 1241(1):59-116.

Mickelson JR, Gallant EM, Litterer LA, Johnson KM, Rempel WE, Louis CF. 1988. Abnormal sarcoplasmic reticulum ryanodine receptor in malignant hyperthermia. J Biol Chem 263(19):9310-5.

Mickelson JR, Knudson CM, Kennedy CF, Yang DI, Litterer LA, Rempel WE, Campbell KP, Louis CF. 1992. Structural and functional correlates of a mutation in the malignant hyperthermia-susceptible pig ryanodine receptor. FEBS Lett 301(1):49-52.

Miyazaki K, Takenouchi M. 2002. Creating random mutagenesis libraries using megaprimer PCR of whole plasmid. Biotechniques 33(5):1033-1038.

Monnier N, Ferreiro A, Marty I, Labarre-Vila A, Mezin P, Lunardi J. 2003. A homozygous splicing mutation causing a depletion of skeletal muscle RYR1 is associated with multi-minicore disease congenital myopathy with ophthalmoplegia. Hum Mol Genet 12(10):1171-1178.

Monnier N, Procaccio V, Stieglitz P, Lunardi J. 1997. Malignant-hyperthermia susceptibility is associated with a mutation of the alpha(1)-subunit of the human dihydropyridine-sensitive L-type voltage-dependent calcium-channel receptor in skeletal muscle. Am J Hum Genet 60(6):1316-1325.

Nelson TE. 1983. Abnormality in calcium release from skeletal sarcoplasmic-reticulum of pigs susceptible to malignant hyperthermia. J Clin Invest 72(3):862-870.

Nelson TE, Sweo T. 1988. Ca^{2+} uptake and Ca^{2+} release by skeletal muscle sarcoplasmic reticulum: differing sensitivity to inhalational anesthetics. Anesthesiology 69(4):571-7.

Otsu K, Willard HF, Khanna VK, Zorzato F, Green NM, MacLennan DH. 1990. Molecular cloning of cDNA encoding the Ca2+ release channel (ryanodine receptor) of rabbit cardiac muscle sarcoplasmic reticulum. J Biol Chem 265(23):13472-83.

Patton C, Thompson S, Epel D. 2004. Some precautions in using chelators to buffer metals in biological solutions. Cell Calcium 35(5):427-31.

Protasi F, Paolini C, Dainese M. 2009. Calsequestrin-1: a new candidate gene for malignant hyperthermia and exertional/environmental heat stroke. J Physiol 587(Pt 13):3095-100.

Quane KA, Healy JM, Keating KE, Manning BM, Couch FJ, Palmucci LM, Doriguzzi C, Fagerlund TH, Berg K, Ording H and others. 1993. Mutations in the ryanodine receptor gene in central core disease and malignant hyperthermia. Nat Genet 5(1):51-5.

Quane KA, Keating KE, Healy JM, Manning BM, Krivosic-Horber R, Krivosic I, Monnier N, Lunardi J, McCarthy TV. 1994. Mutation screening of the RYR1 gene in malignant hyperthermia: detection of a novel Tyr to Ser mutation in a pedigree with associated central cores. Genomics 23(1):236-9.

Rempel WE, Lu M, Elkandelgy S, Kennedy CFH, Irvin LR, Mickelson JR, Louis CF. 1993. Relative accuracy of the halothane challenge test and a molecular-genetic test in detecting the gene for porcine stress syndrome. J Anim Sci 71(6):1395-1399.

Roberts MC, Mickelson JR, Patterson EE, Nelson TE, Armstrong PJ, Brunson DB, Hogan K. 2001. Autosomal dominant canine malignant hyperthermia is caused by a mutation in the gene encoding the skeletal muscle calcium release channel (*RYR1*). Anesthesiology 95(3):716-25.

Robinson R, Carpenter D, Shaw MA, Halsall J, Hopkins P. 2006. Mutations in *RYR1* in malignant hyperthermia and central core disease. Hum Mutat 27(10):977-89.

Robinson RL, Brooks C, Brown SL, Ellis FR, Halsall PJ, Quinnell RJ, Shaw MA, Hopkins PM. 2002. *RYR1* mutations causing central core disease are associated with more severe malignant hyperthermia in vitro contracture test phenotypes. Hum Mutat 20(2):88-97.

Robinson RL, Monnier N, Wolz W, Jung M, Reis A, Nuernberg G, Curran JL, Monsieurs K, Stieglitz P, Heytens L and others. 1997. A genome wide search for susceptibility loci in three European malignant hyperthermia pedigrees. Hum Mol Genet 6(6):953-961.

Romero NB, Monnier N, Viollet L, Cortey A, Chevallay M, Leroy JP, Lunardi J, Fardeau M. 2003. Dominant and recessive central core disease associated with RYR1 mutations and fetal akinesia. Brain 126:2341-2349.

Rosenberg H, Davis M, James D, Pollock N, Stowell K. 2007. Malignant hyperthermia. Orphanet J Rare Dis 2:21.

Rueffert H, Olthoff D, Deutrich C, Froster UG. 2001. Determination of a positive malignant hyperthermia (MH) disposition without the *in vitro* contracture test in families carrying the *RYR1* Arg614Cys mutation. Clin Genet 60(2):117-24.

Sambrook J, Fritsch EF, Maniatis T. 1989. Molecular Cloning: A Laboratory Manual. 2nd edn. Cold Spring Harbor, NY, USA: Cold Spring Harbor Laboratory Press.

Sei Y, Brandom BW, Bina S, Hosoi E, Gallagher KL, Wyre HW, Pudimat PA, Holman SJ, Venzon DJ, Daly JW and others. 2002. Patients with malignant hyperthermia demonstrate an altered calcium control mechanism in B lymphocytes. Anesthesiology 97(5):1052-8.

Sei Y, Gallagher KL, Basile AS. 1999. Skeletal muscle type ryanodine receptor is involved in calcium signaling in human B lymphocytes. J Biol Chem 274(9):5995-6002.

Serfas KD, Bose D, Patel L, Wrogemann K, Phillips MS, MacLennan DH, Greenberg CR. 1996. Comparison of the segregation of the *RYR1* C1840T mutation with segregation of the caffeine/halothane contracture test results for malignant hyperthermia susceptibility in a large Manitoba Mennonite family. Anesthesiology 84(2):322-9.

Sewry CA, Muller C, Davis M, Dwyer JSM, Dove J, Evans G, Schroder R, Furst D, Helliwell T, Laing N and others. 2002. The spectrum of pathology in central core disease. Neuromuscul Disord 12(10):930-938.

Stowell KM. 2008. Malignant hyperthermia: a pharmacogenetic disorder. Pharmacogenomics 9(11):1657-72.

Sudbrak R, Procaccio V, Klausnitzer M, Curran JL, Monsieurs K, van Broeckhoven C, Ellis R, Heyetens L, Hartung EJ, Kozak-Ribbens G and others. 1995. Mapping of a further malignant hyperthermia susceptibility locus to chromosome 3q13.1. Am J Hum Genet 56(3):684-91.

Takeshima H, Nishimura S, Matsumoto T, Ishida H, Kangawa K, Minamino N, Matsuo H, Ueda M, Hanaoka M, Hirose T and others. 1989. Primary structure and expression from complementary DNA of skeletal muscle ryanodine receptor. Nature 339(6224):439-45.

Thompson JD, Higgins DG, Gibson TJ. 1994. CLUSTAL W: improving the sensitivity of progressive multiple sequence alignment through sequence weighting, positions-specific gap penalties and weight matrix choice. Nucleic Acids Res 22:4673-4680.

Thomsett-Scott B. 2009. Software Review of Origin 8 Origin 8 . OriginLab Corporation, One Roundhouse Plaza, Suite 303, Northampton, MA 01060. J Chem Inf Model.

Tilgen N, Zorzato F, Halliger-Keller B, Muntoni F, Sewry C, Palmucci LM, Schneider C, Hauser E, Lehmann-Horn F, Muller CR and others. 2001. Identification of four novel mutations in the C-terminal membrane spanning domain of the ryanodine receptor 1: association with central core disease and alteration of calcium homeostasis. Hum Mol Genet 10(25):2879-87.

Tiso N, Stephan DA, Nava A, Bagattin A, Devaney JM, Stanchi F, Larderet G, Brahmbhatt B, Brown K, Bauce B and others. 2001. Identification of mutations in the cardiac ryanodine receptor gene in families affected with arrhythmogenic right ventricular cardiomyopathy type 2 (ARVD2). Hum Mol Genet 10(3):189-94.

Tong J, Oyamada H, Demaurex N, Grinstein S, McCarthy TV, MacLennan DH. 1997. Caffeine and halothane sensitivity of intracellular Ca^{2+} release is altered by 15 calcium release channel (ryanodine receptor) mutations associated with malignant hyperthermia and/or central core disease. J Biol Chem 272(42):26332-9.

Tong JF, McCarthy TV, MacLennan DH. 1999. Measurement of resting cytosolic Ca^{2+} concentrations and Ca^{2+} store size in HEK-293 cells transfected with malignant hyperthermia or central core disease mutant Ca^{2+} release channels. J Biol Chem 274(2):693-702.

Treves S, Anderson AA, Ducreux S, Divet A, Bleunven C, Grasso C, Paesante S, Zorzato F. 2005. Ryanodine receptor 1 mutations, dysregulation of calcium homeostasis and neuromuscular. Neuromuscul Disord 15(9-10):577-587.

Wagenknecht T, Grassucci R, Frank J, Saito A, Inui M, Fleischer S. 1989. Three-dimensional architecture of the calcium channel/foot structure of sarcoplasmic reticulum. Nature 338(6211):167-70.

Waldron-Mease E, Klein LV, Rosenberg H, Leitch M. 1981. Malignant hyperthermia in a halothane-anesthetized horse. J Am Vet Med Assoc 179(9):896-8.

Wappler F, Fiege M, Antz M, Esch JSA. 2000. Hemodynamic and metabolic alterations in response to graded exercise in a patient susceptible to malignant hyperthermia. Anesthesiology 92(1):268-272.

Wehner M, Rueffert H, Koenig F, Meinecke CD, Olthoff D. 2003. The Ile2453Thr mutation in the ryanodine receptor gene 1 is associated with facilitated calcium release from sarcoplasmic reticulum by 4-chloro-m-cresol in human myotubes. Cell Calcium 34(2):163-8.

Wehner M, Rueffert H, Koenig F, Olthoff D. 2004. Functional characterization of malignant hyperthermia-associated RyR1 mutations in exon 44, using the human myotube model. Neuromuscul Disord 14(7):429-37.

Wei L, Gallant EM, Dulhunty AF, Beard NA. 2009. Junctin and triadin each activate skeletal ryanodine receptors but junctin alone mediates functional interactions with calsequestrin. Int J Biochem Cell Biol 41(11):2214-24.

Weiss RG, O'Connell KMS, Flucher BE, Allen PD, Grabner M, Dirksen RT. 2004. Functional analysis of the R1086H malignant hyperthermia mutation in the DHPR reveals an unexpected influence of the III-IV loop on skeletal muscle EC coupling. Am J Physiol Cell Physiol 287(4):C1094-C1102.

Yamaguchi N, Xin CL, Meissner G. 2001. Identification of apocalmodulin and Ca^{2+}-calmodulin regulatory domain in skeletal muscle Ca^{2+} release channel, ryanodine receptor. J Biol Chem 276(25):22579-22585.

Yang T, Riehl J, Esteve E, Matthaei KI, Goth S, Allen PD, Pessah IN, Lopez JR. 2006. Pharmacologic and functional characterization of malignant hyperthermia in the R163C *RyR1* knock-in mouse. Anesthesiology 105(6):1164-75.

Yang TZ, Ta TA, Pessah IN, Allen PD. 2003. Functional defects in six ryanodine receptor isoform-1 (*RyR1*) mutations associated with malignant hyperthermia and their impact on skeletal excitation-contraction coupling. J Biol Chem 278(28):25722-25730.

Zhang Y, Chen HS, Khanna VK, De Leon S, Phillips MS, Schappert K, Britt BA, Browell AK, MacLennan DH. 1993. A mutation in the human ryanodine receptor gene associated with central core disease. Nat Genet 5(1):46-50.

Zhou H, Brockington M, Jungbluth H, Monk D, Stanier P, Sewry CA, Moore GE, Muntoni F. 2006. Epigenetic allele silencing unveils recessive RYR1 mutations in core myopathies. Am J Hum Genet 79(5):859-68.

Zhou H, Jungbluth H, Sewry CA, Feng L, Bertini E, Bushby K, Straub V, Roper H, Rose MR, Brockington M and others. 2007. Molecular mechanisms and phenotypic variation in RYR1-related congenital myopathies. Brain 130(Pt 8):2024-36.

Zorzato F, Fujii J, Otsu K, Phillips M, Green NM, Lai FA, Meissner G, MacLennan DH. 1990. Molecular cloning of cDNA encoding human and rabbit forms of the Ca^{2+} release channel (ryanodine receptor) of skeletal muscle sarcoplasmic reticulum. J Biol Chem 265(4):2244-56.

Zvaritch E, Depreux F, Kraeva N, Loy RE, Goonasekera SA, Boncompagni S, Kraev A, Gramolini AO, Dirksen RT, Franzini-Armstrong C and others. 2007. An $Ryr1^{I4895T}$ mutation abolishes Ca^{2+} release channel function and delays development in homozygous offspring of a mutant mouse line. Proc Natl Acad Sci U S A 104(47):18537-42.

APPENDICES

Appendix 1 Primers used for PCR and mutagenesis of *RYR1* cDNA

Primer	F/R	Position (bp)	Sequence 5'-3'	Reaction	Mutation
-7	F	-15	TTCCGACCTCGACATCATGGGTGACG	P	
C130T	F	116	AGGGCTTCGGCAACTGCCTGTGCTT	M	R44C
163	F	457	TCCAAGCAGAGGTCTGAAGGAGAA	P	
C487T	F	475	GGAGAAAAGGTCTGCGTTGGGGAT	M	R163C
G742A	F	730	GTCTACTATGAGAGGGGAGCTGTGT	M	G248R
248	R	773	GTGGCTCCAGCCTCCAGA	P, M	
952	F	952	TCCAAGGAGAAGCTGGATGT	P	
G1021A	F	1007	CTGAGATCAAGTACAGGGAGTCA	M	G341R
341	R	1066	TCTGGAGCGGCATAGGTGAG	P, M	
C1201T	F	1196	CCGCCTGCATGATCCACAGCACCAA	M	R401C
C1202A	F	1196	CCGCCCACATGATCCACAGCACCAA	M	R401H
522Fwt	F	1447	CTCTCCATGGTCCTGAATTGCATAGAC	P	
C1597T	R	1610	GCACAGTTGCTACAATTGCCACGGAT	M	R533C
G1598A	R	1610	GCACAGTTGCTATGATTGCCACGGAT	M	R533H
1755	R	1755	TGCTTGTCCAGGAGGGAAGATG	P, M	
1927	F	1926	CATCCGCCCCAACATCTTTGTG	P	
3016	F	3016	TACAGCGCAGTGCAGGACATC	P	
3065	R	3065	CTTCATCCAGCAGGCGGTAGG	P	
4262	F	4265	ACCCCGAGATCATCCTCAACA	P	
4296	R	4299	GCAAAGACCCTCACGGAGTAA	P	
4520	F	4523	TCAGCCACACGGACCTTGTCA	P	
4800	R	4803	GGCATGCGGCTCCAGGACACT	P	
5285	F	5288	CGGGAGTTGGAGTCACCACTT	P	
5555	R	5558	TCACATCCTCATCGCCAAAGA	P	
5880	F	5883	TGCGGAGCGCTATGTGGACAA	P	
6763	R	6766	GCCACTGTTCTCCAGCAGGTA	P	
6841	F	6841	ATTGACAACAATGAGCTGGC	P	
7039	R	7042	CACCACCACATTGGCGTTCTC	P	
2434	F	7215	CTTTGGTGAGGAACCGCCTGAAG	P	
7393	R	7396	GAGGCTGATGATGCCCACAAG	P	
7642	F	7645	GCCGTGAACCGCTACCTGTG	P	
8025	R	8028	AAAGATGCCCCAGAAGAGTTTC	P	
8525	F	8528	CACAAAGTGCCCAGACCTATG	P	
8789	R	8792	TAACCGCGTAGCCATTCATCT	P	

9442	F	9445	CAGCACCAGTTCGGAGATGA	P	
9769	R	9772	TGTGTAGCGGGCACCTGACTC	P	
10052	F	10055	AGCTCCTGCAGTCCCACTTCA	P	
10109	R	10112	CTCCTCCTCGGACACCACCT	P	
10809	F	10827	CGAGCACCCTTACAAGTCTAA	P	
11213	R	11231	AGACCTCAACCTCCTCTTCAG	P	
11787	R	11805	ATGACATCCTTGCCCGAGTAG	P	
13903	F	13921	GAACCCGCCCTGCGGTGTCTG	M	
C14477T	R	14465	GAGGACAGGATGATGCGCAGCGTCT	M	T4826I
C14497T	R	14483	TTCCCATTGTAGGTGACAGAGGACA	M	H4833Y
G14582A	R	14564	CTTGTGGAAGAAGTTGAAGGCCA	M	R4861H
T14693C	R	14682	ATCTCGTCCCCAGTGCCTCCGCCA	M	I4898T
G14695A	R	14682	ATCTCGTCCCTAATGCCTCCGCCA	M	G4899R

Primers are listed according to the position on human *RYR1* sequence MIM# 180901 (from 5' terminus). F and R indicate forward and reverse primers, respectively and P and M indicate PCR and mutagenesis, respectively. Mutations introduced by mutagenesis using mutant primers in this project are listed.

Appendix 2 *RYR1* cDNA sequence in pcDNA3.1

Putative transcription start

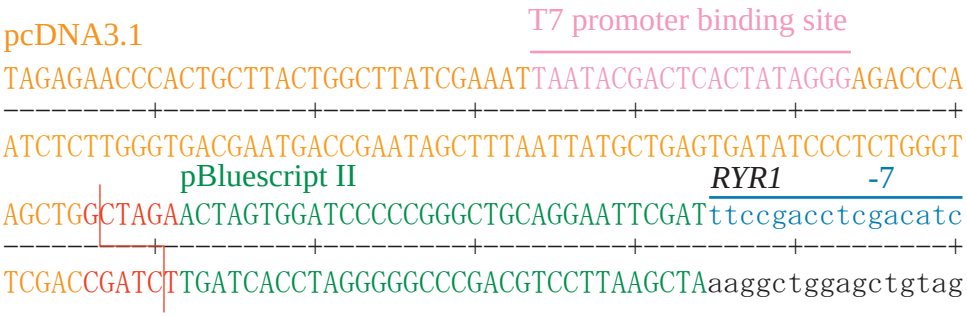

Translation start


Arg163Cys
C487T
SalI
Gly248Arg
G742A
248
exon 10
952
ApaI
G1021A
Gly341Arg
341R
Ala359

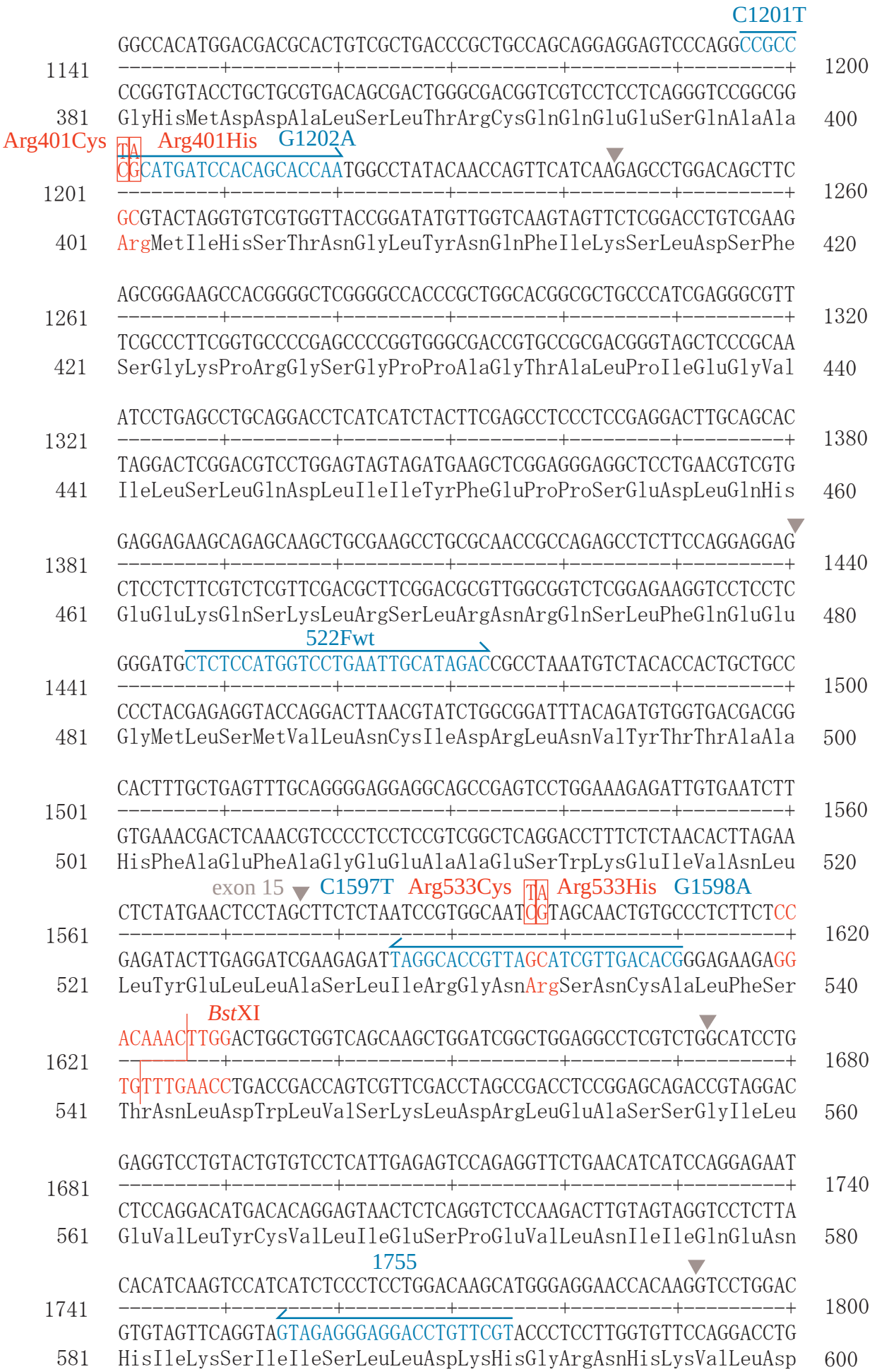
C1201T
Arg401Cys
Arg401His
G1202A
522Fwt
exon 15
C1597T
Arg533Cys
Arg533His
G1598A
BstXI
1755

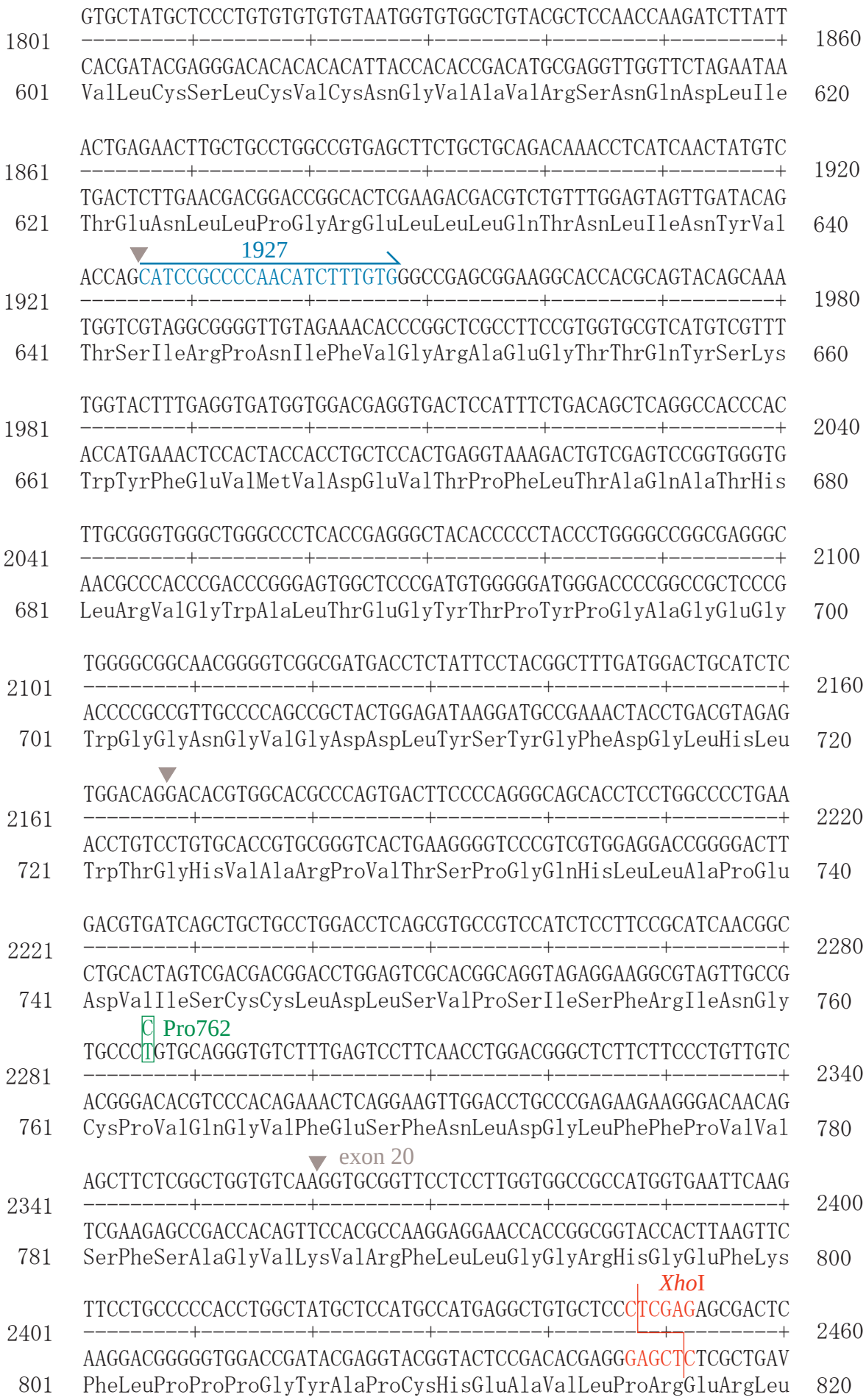
1927
Pro762
exon 20
XhoI


SfiI
SacI
G Thr981
T Asn993
3016
BssHII
3065


GCCGTGCGCACCCTCCTGGGCTACGGCTACAACATCGAGCCTCCTGACCAGGAGCCCAGT
3121
3180
CGGCACGCGTGGGAGGACCCGATGCCGATGTTGTAGCTCGGAGGACTGGTCCTCGGGTCA
1041
AlaValArgThrLeuLeuGlyTyrGlyTyrAsnIleGluProProAspGlnGluProSer
1060
exon 25
CAGGTGGAGAACCAGTCTCGTTGTGACCGGGTGCGCATCTTCCGGGCAGAGAAATCCTAT
3181
3240
GTCCACCTCTTGGTCAGAGCAACACTGGCCCACGCGTAGAAGGCCCGTCTCTTTAGGATA
1061
GlnValGluAsnGlnSerArgCysAspArgValArgIlePheArgAlaGluLysSerTyr
1080
NotI
ACAGTGCAGAGCGGCCGCTGGTACTTCGAGTTTGAAGCAGTCACCACAGGCGAGATGCGC
3241
3300
TGTCACGTCTCGCCGGCGACCATGAAGCTCAAACTTCGTCAGTGGTGTCCGCTCTACGCG
1081
ThrValGlnSerGlyArgTrpTyrPheGluPheGluAlaValThrThrGlyGluMetArg
1100
GTGGGCTGGGCGAGGCCCGAGCTGAGGCCTGATGTAGAGCTGGGAGCTGACGAGCTGGCC
3301
3360
CACCCGACCCGCTCCGGGCTCGACTCCGGACTACATCTCGACCCTCGACTGCTCGACCGG
1101
ValGlyTrpAlaArgProGluLeuArgProAspValGluLeuGlyAlaAspGluLeuAla
1120
TATGTCTTCAATGGGCACCGCGGCCAGCGCTGGCACTTGGGCAGTGAACCATTTGGGCGC
3361
3420
ATACAGAAGTTACCCGTGGCGCCGGTCGCGACCGTGAACCCGTCACTTGGTAAACCCGCG
1121
TyrValPheAsnGlyHisArgGlyGlnArgTrpHisLeuGlySerGluProPheGlyArg
1140
CCCTGGCAGCCGGGCGATGTCGTTGGCTGTATGATCGACCTCACAGAGAACACCATTATC
3421
3480
GGGACCGTCGGCCCGCTACAGCAACCGACATACTAGCTGGAGTGTCTCTTGTGGTAATAG
1141
ProTrpGlnProGlyAspValValGlyCysMetIleAspLeuThrGluAsnThrIleIle
1160
TTCACCCTCAATGGCGAGGTCCTCATGTCTGACTCAGGCTCCGAAACAGCCTTCCGGGAG
3481
3540
AAGTGGGAGTTACCGCTCCAGGAGTACAGACTGAGTCCGAGGCTTTGTCGGAAGGCCCTC
1161
PheThrLeuAsnGlyGluValLeuMetSerAspSerGlySerGluThrAlaPheArgGlu
1180
ATTGAGATTGGGGACGGCTTCCTGCCCGTCTGCAGCTTGGGACCTGGCCAGGTGGGTCAT
3540
3600
TAACTCTAACCCCTGCCGAAGGACGGGCAGACGTCGAACCCTGGACCGGTCCACCCAGTA
1181
IleGluIleGlyAspGlyPheLeuProValCysSerLeuGlyProGlyGlnValGlyHis
1200
CTGAACCTGGGCCAGGACGTGAGCTCTCTGAGGTTCTTTGCCATCTGTGGCCTCCAGGAA
3061
3660
GACTTGGACCCGGTCCTGCACTCGAGAGACTCCAAGAAACGGTAGACACCGGAGGTCCTT
1201
LeuAsnLeuGlyGlnAspValSerSerLeuArgPhePheAlaIleCysGlyLeuGlnGlu
1220
GGCTTCGAGCCATTTGCCATCAACATGCAGCGCCCAGTCACCACCTGGTTCAGCAAAGGC
3660
3720
CCGAAGCTCGGTAAACGGTAGTTGTACGTCGCGGGTCAGTGGTGGACCAAGTCGTTTCCG
1221
GlyPheGluProPheAlaIleAsnMetGlnArgProValThrThrTrpPheSerLysGly
1240
CTGCCCCAGTTTGAGCCAGTGCCCCTTGAACACCCTCACTATGAGGTATCCCGAGTGGAC
3721
3780
GACGGGGTCAAACTCGGTCACGGGGAACTTGTGGGAGTGATACTCCATAGGGCTCACCTG
1241
LeuProGlnPheGluProValProLeuGluHisProHisTyrGluValSerArgValAsp
1260

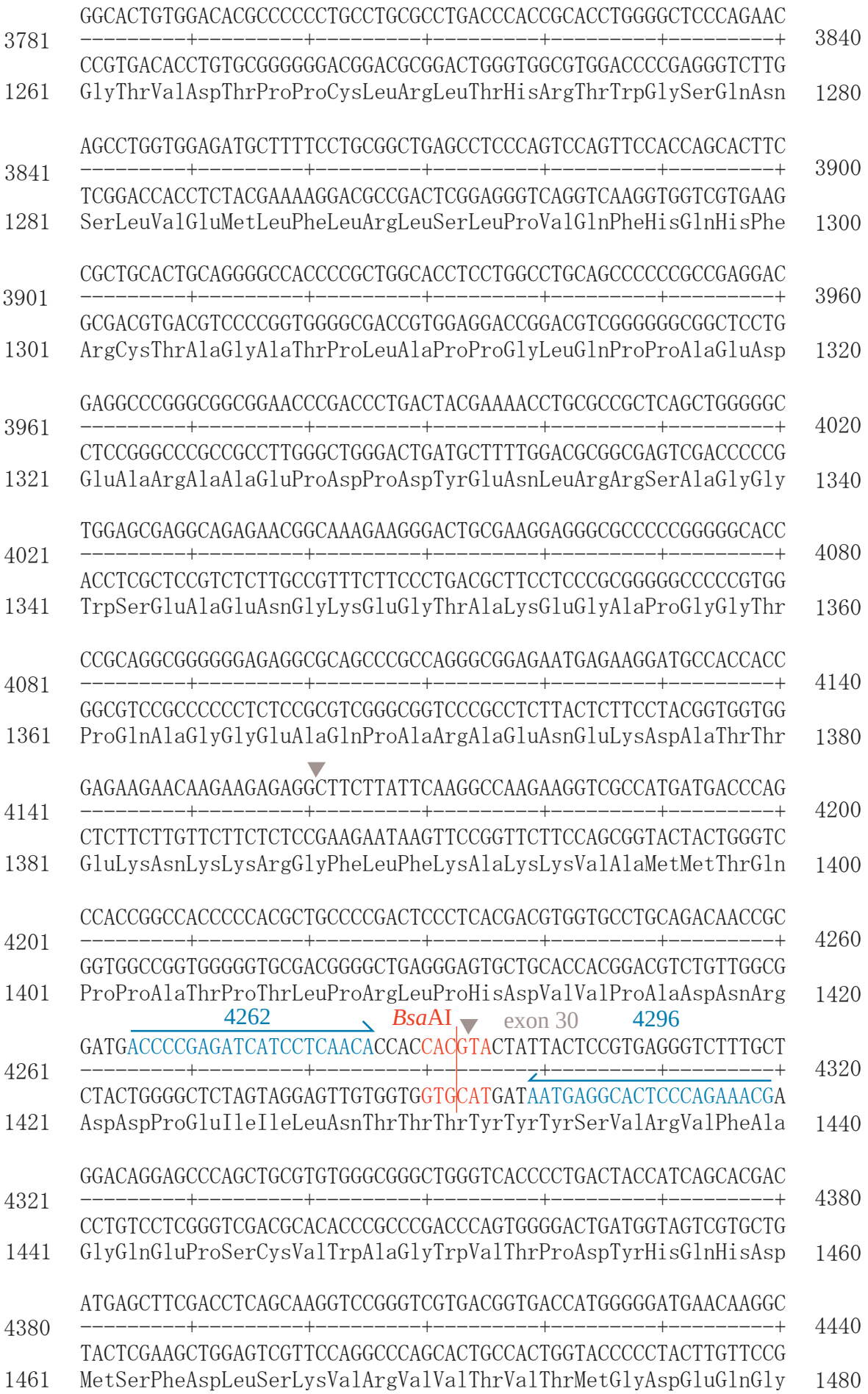
GGCACTGTGGACACGCCCCCCTGCCTGCGCCTGACCCACCGCACCTGGGGCTCCCAGAAC
3781
3840
CCGTGACACCTGTGCGGGGGGACGGACGCGGACTGGGTGGCGTGGACCCCGAGGGTCTTG
1261
GlyThrValAspThrProProCysLeuArgLeuThrHisArgThrTrpGlySerGlnAsn
1280
AGCCTGGTGGAGATGCTTTTCCTGCGGCTGAGCCTCCCAGTCCAGTTCCACCAGCACTTC
3841
3900
TCGGACCACCTCTACGAAAAGGACGCCGACTCGGAGGGTCAGGTCAAGGTGGTCGTGAAG
1281
SerLeuValGluMetLeuPheLeuArgLeuSerLeuProValGlnPheHisGlnHisPhe
1300
CGCTGCACTGCAGGGGCCACCCCGCTGGCACCTCCTGGCCTGCAGCCCCCCGCCGAGGAC
3901
3960
GCGACGTGACGTCCCCGGTGGGGCGACCGTGGAGGACCGGACGTCGGGGGGCGGCTCCTG
1301
ArgCysThrAlaGlyAlaThrProLeuAlaProProGlyLeuGlnProProAlaGluAsp
1320
GAGGCCCGGGCGGCGGAACCCGACCCTGACTACGAAAACCTGCGCCGCTCAGCTGGGGGC
3961
4020
CTCCGGGCCCGCCGCCTTGGGCTGGGACTGATGCTTTTGGACGCGGCGAGTCGACCCCCG
1321
GluAlaArgAlaAlaGluProAspProAspTyrGluAsnLeuArgArgSerAlaGlyGly
1340
TGGAGCGAGGCAGAGAACGGCAAAGAAGGGACTGCGAAGGAGGGCGCCCCCGGGGGCACC
4021
4080
ACCTCGCTCCGTCTCTTGCCGTTTCTTCCCTGACGCTTCCTCCCGCGGGGGCCCCCGTGG
1341
TrpSerGluAlaGluAsnGlyLysGluGlyThrAlaLysGluGlyAlaProGlyGlyThr
1360
CCGCAGGCGGGGGGAGAGGCGCAGCCCGCCAGGGCGGAGAATGAGAAGGATGCCACCACC
4081
4140
GGCGTCCGCCCCCCTCTCCGCGTCGGGCGGTCCCGCCTCTTACTCTTCCTACGGTGGTGG
1361
ProGlnAlaGlyGlyGluAlaGlnProAlaArgAlaGluAsnGluLysAspAlaThrThr
1380
GAGAAGAACAAGAAGAGAGGCTTCTTATTCAAGGCCAAGAAGGTCGCCATGATGACCCAG
4141
4200
CTCTTCTTGTTCTTCTCTCCGAAGAATAAGTTCCGGTTCTTCCAGCGGTACTACTGGGTC
1381
GluLysAsnLysLysArgGlyPheLeuPheLysAlaLysLysValAlaMetMetThrGln
1400
CCACCGGCCACCCCCACGCTGCCCCGACTCCCTCACGACGTGGTGCCTGCAGACAACCGC
4201
4260
GGTGGCCGGTGGGGGTGCGACGGGGCTGAGGGAGTGCTGCACCACGGACGTCTGTTGGCG
1401
ProProAlaThrProThrLeuProArgLeuProHisAspValValProAlaAspAsnArg
1420
4262
BsaAI
exon 30
4296
GATGACCCCGAGATCATCCTCAACACCACCACGTACTATTACTCCGTGAGGGTCTTTGCT
4261
4320
CTACTGGGGCTCTAGTAGGAGTTGTGGTGGTGCATGATAATGAGGCACTCCCAGAAACGA
1421
AspAspProGluIleIleLeuAsnThrThrTyrTyrTyrSerValArgValPheAla
1440
GGACAGGAGCCCAGCTGCGTGTGGGCGGGCTGGGTCACCCCTGACTACCATCAGCACGAC
4321
4380
CCTGTCCTCGGGTCGACGCACACCCGCCCGACCCAGTGGGGACTGATGGTAGTCGTGCTG
1441
GlyGlnGluProSerCysValTrpAlaGlyTrpValThrProAspTyrHisGlnHisAsp
1460
ATGAGCTTCGACCTCAGCAAGGTCCGGGTCGTGACGGTGACCATGGGGGATGAACAAGGC
4380
4440
TACTCGAAGCTGGAGTCGTTCCAGGCCCAGCACTGCCACTGGTACCCCCTACTTGTTCCG
1461
MetSerPheAspLeuSerLysValArgValValThrValThrMetGlyAspGluGlnGly
1480

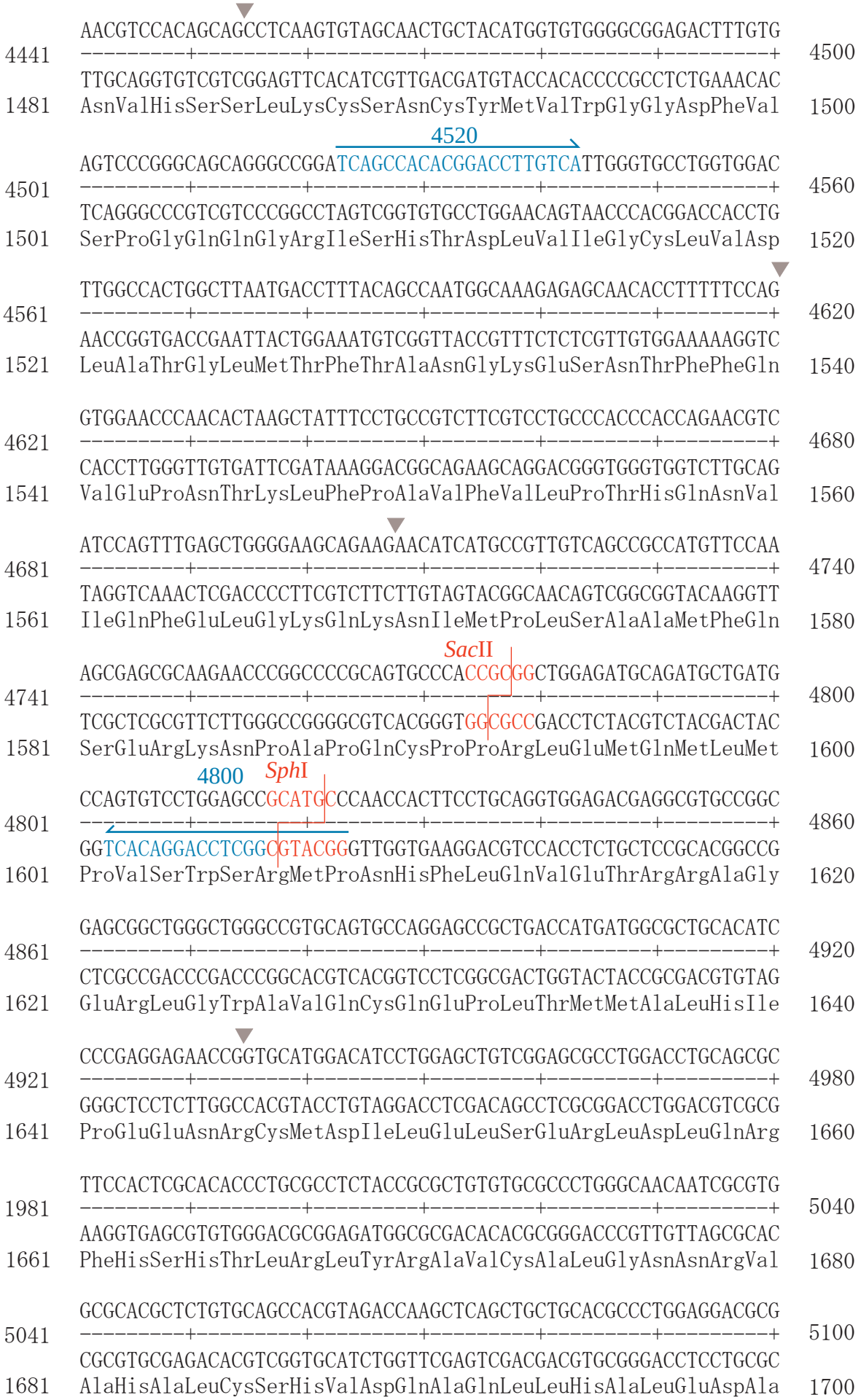
4520
SacII
4800
SphI

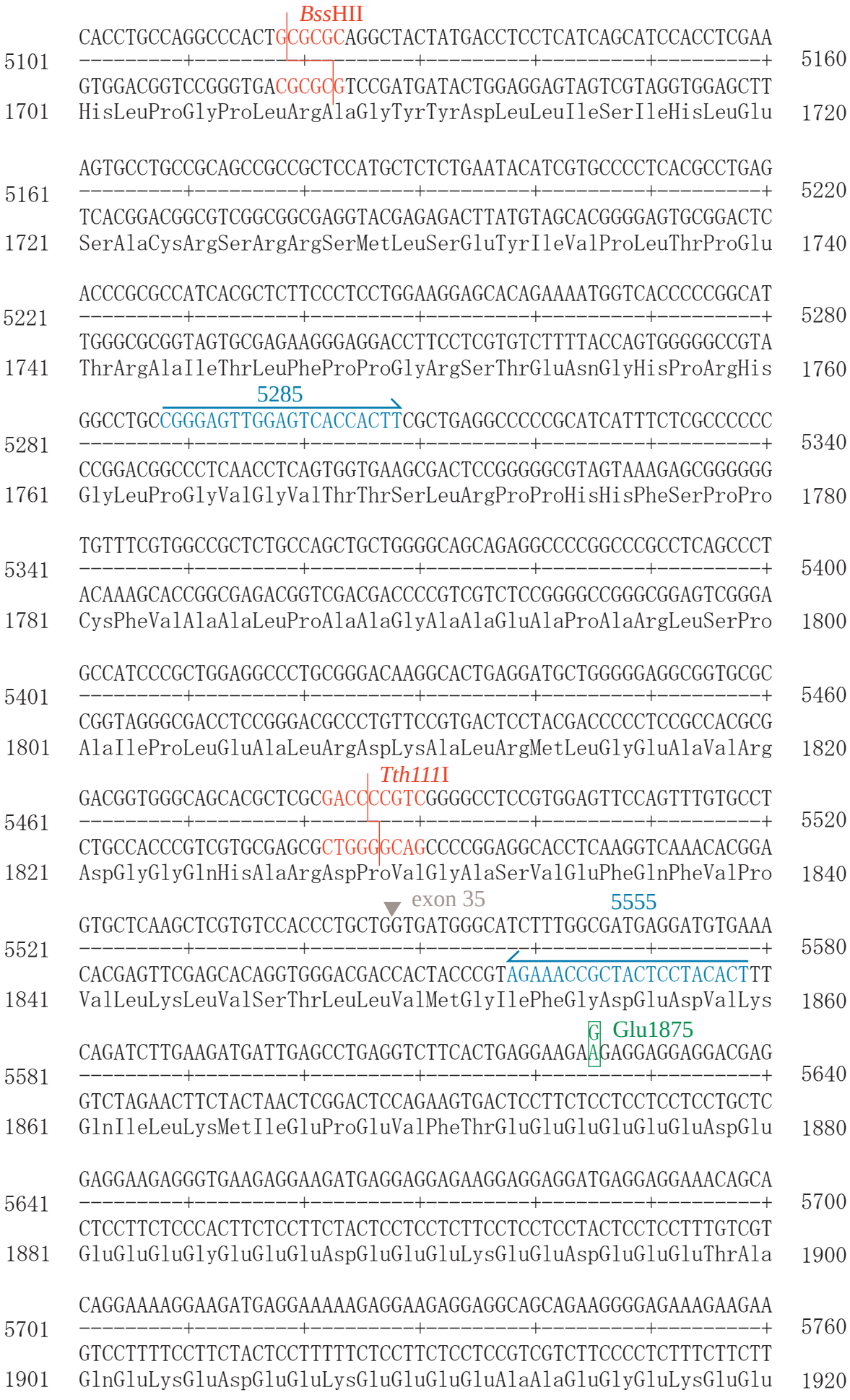
BssHII
5285
Tth111I
exon 35
5555
Glu1875


GGCTTGGAGGAAGGGCTGCTCCAGATGAAGTTGCCAGAGTCTGTGAAGTTACAGATGTGC
5761 5820
CCGAACCTCCTTCCCGACGAGGTCTACTTCAACGGTCTCAGACACTTCAATGTCTACACG
1921 GlyLeuGluGluGlyLeuLeuGlnMetLysLeuProGluSerValLysLeuGlnMetCys 1940
CACCTGCTGGAGTATTTCTGTGACCAAGAGCTGCAGCACCGTGTGGAGTCCCTGGCAGCC
5821 5880
GTGGACGACCTCATAAAGACACTGGTTCTCGACGTCGTGGCACACCTCAGGGACCGTCGG
1941 HisLeuLeuGluTyrPheCysAspGlnGluLeuGlnHisArgValGluSerLeuAlaAla 1960
5880
TTTGCGGAGCGCTATGTGGACAAGCTCCAGGCCAACCAGCGGAGCCGCTATGGCCTCCTC
5881 5940
AAACGCCTCGCGATACACCTGTTCGAGGTCCGGTTGGTCGCCTCGGCGATACCGGAGGAG
1961 PheAlaGluArgTyrValAspLysLeuGlnAlaAsnGlnArgSerArgTyrGlyLeuLeu 1980
ATAAAAGCCTTCAGCATGACCGCAGCAGAGACTGCAAGACGTACCCGTGAGTTCCGCTCC
5941 6000
TATTTTCGGAAGTCGTACTGGCGTCGTCTCTGACGTTCTGCATGGGCACTCAAGGCGAGG
1981 IleLysAlaPheSerMetThrAlaAlaGluThrAlaArgArgThrArgGluPheArgSer 2000
CCACCCCAGGAACAGATCAATATGCTATTGCAATTCAAAGATGGTACAGATGAGGAAGAC
6001 6060
GGTGGGGTCCTTGTCTAGTTATACGATAACGTTAAGTTTCTACCATGTCTACTCCTTCTG
2001 ProProGlnGluGlnIleAsnMetLeuLeuGlnPheLysAspGlyThrAspGluGluAsp 2020
TGTCCTCTCCCTGAAGAGATTCGACAGGATTTGCTTGACTTTCATCAAGACCTGCTGGCA
6061 6120
ACAGGAGAGGGACTTCTCTAAGCTGTCCTAAACGAACTGAAAGTAGTTCTGGACGACCGT
2021 CysProLeuProGluGluIleArgGlnAspLeuLeuAspPheHisGlnAspLeuLeuAla 2040
CACTGTGGAATTCAGCTAGATGGAGAGGAGGAGGAACCAGAGGAAGAGACCACCCTGGGC
6121 6180
GTGACACCTTAAGTCGATCTACCTCTCCTCCTCCTTGGTCTCCTTCTCTGGTGGGACCCG
2041 HisCysGlyIleGlnLeuAspGlyGluGluGluGluProGluGluGluThrThrLeuGly 2060
AGCCGCCTCATGAGCCTGTTGGAGAAAGTGCGGCTGGTGAAGAAGAAGGAAGAGAAACCT
6181 6240
TCGGCGGAGTACTCGGACAACCTCTTTCACGCCGACCACTTCTTCTTCCTTCTCTTTGGA
2061 SerArgLeuMetSerLeuLeuGluLysValArgLeuValLysLysLysGluGluLysPro 2080
GAGGAGGAGCGGTCAGCAGAGGAGAGCAAACCCCGGTCCCTGCAGGAGCTGGTGTCCCAC
6241 6300
CTCCTCCTCGCCAGTCGTCTCCTCTCGTTTGGGGCCAGGGACGTCCTCGACCACAGGGTG
2081 GluGluGluArgSerAlaGluGluSerLysProArgSerLeuGlnGluLeuValSerHis 2100
ATGGTGGTGCGCTGGGCCCAAGAGGACTTCGTGCAGAGCCCCGAGCTGGTGCGGGCCATG
6301 6360
TACCACCACGCGACCCGGGTTCTCCTGAAGCACGTCTCGGGGCTCGACCACGCCCGGTAC
2101 MetValValArgTrpAlaGlnGluAspPheValGlnSerProGluLeuValArgAlaMet 2120
TTCAGCCTCCTGCACCGGCAGTACGACGGGCTGGGTGAGCTGCTGCGTGCCCTGCCGCGG
6361 6420
AAGTCGGAGGACGTGGCCGTCATGCTGCCCGACCCACTCGACGACGCACGGGACGGCGCC
2121 PheSerLeuLeuHisArgGlnTyrAspGlyLeuGlyGluLeuLeuArgAlaLeuProArg 2140


XhoI
exon 40
6763
6841
7039
KpnI

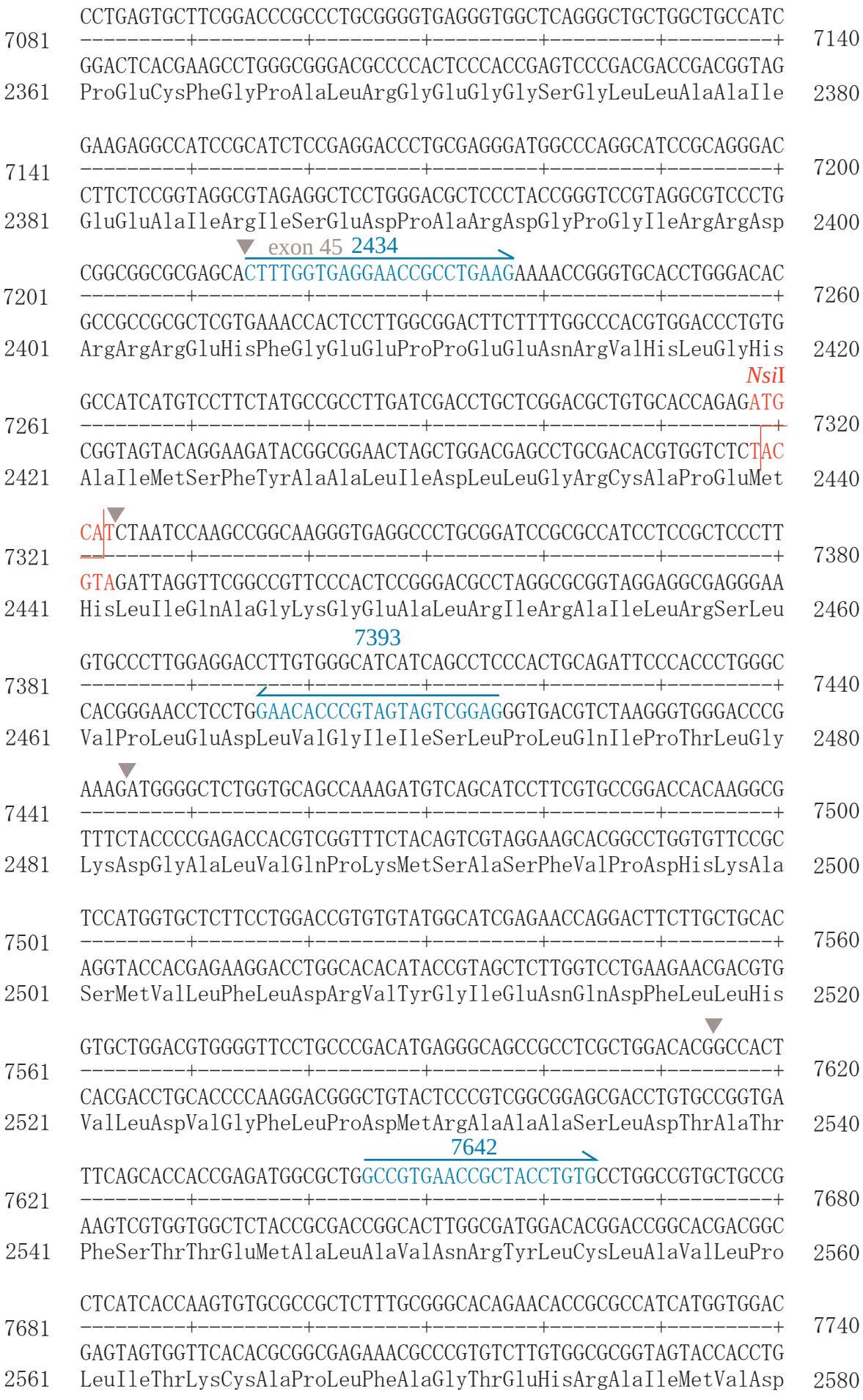
CCTGAGTGCTTCGGACCCGCCCTGCGGGGTGAGGGTGGCTCAGGGCTGCTGGCTGCCATC
7081
7140
GGACTCACGAAGCCTGGGCGGGACGCCCCACTCCCACCGAGTCCCGACGACCGACGGTAG
2361 ProGluCysPheGlyProAlaLeuArgGlyGluGlyGlySerGlyLeuLeuAlaAlaIle 2380
GAAGAGGCCATCCGCATCTCCGAGGACCCTGCGAGGGATGGCCCAGGCATCCGCAGGGAC
7141
7200
CTTCTCCGGTAGGCGTAGAGGCTCCTGGGACGCTCCCTACCGGGTCCGTAGGCGTCCCTG
2381 GluGluAlaIleArgIleSerGluAspProAlaArgAspGlyProGlyIleArgArgAsp 2400
exon 45
2434
CGGCGGCGCGAGCACTTTGGTGAGGAACCGCCTGAAGAAAACCGGGTGCACCTGGGACAC
7201
7260
GCCGCCGCGCTCGTGAAACCACTCCTTGGCGGACTTCTTTTGGCCCACGTGGACCCTGTG
2401 ArgArgArgGluHisPheGlyGluGluProProGluGluAsnArgValHisLeuGlyHis 2420
NsiI
GCCATCATGTCCTTCTATGCCGCCTTGATCGACCTGCTCGGACGCTGTGCACCAGAGATG
7261
7320
CGGTAGTACAGGAAGATACGGCGGAACTAGCTGGACGAGCCTGCGACACGTGGTCTCTAC
2421 AlaIleMetSerPheTyrAlaAlaLeuIleAspLeuLeuGlyArgCysAlaProGluMet 2440
CATCTAATCCAAGCCGGCAAGGGTGAGGCCCTGCGGATCCGCGCCATCCTCCGCTCCCTT
7321
7380
GTAGATTAGGTTCGGCCGTTCCCACTCCGGGACGCCTAGGCGCGGTAGGAGGCGAGGGAA
2441 HisLeuIleGlnAlaGlyLysGlyGluAlaLeuArgIleArgAlaIleLeuArgSerLeu 2460
7393
GTGCCCTTGGAGGACCTTGTGGGCATCATCAGCCTCCCACTGCAGATTCCCACCCTGGGC
7381
7440
CACGGGAACCTCCTGGAACACCCGTAGTAGTCGGAGGGTGACGTCTAAGGGTGGGACCCG
2461 ValProLeuGluAspLeuValGlyIleIleSerLeuProLeuGlnIleProThrLeuGly 2480
AAAGATGGGGCTCTGGTGCAGCCAAAGATGTCAGCATCCTTCGTGCCGGACCACAAGGCG
7441
7500
TTTCTACCCCGAGACCACGTCGGTTTCTACAGTCGTAGGAAGCACGGCCTGGTGTTCCGC
2481 LysAspGlyAlaLeuValGlnProLysMetSerAlaSerPheValProAspHisLysAla 2500
TCCATGGTGCTCTTCCTGGACCGTGTGTATGGCATCGAGAACCAGGACTTCTTGCTGCAC
7501
7560
AGGTACCACGAGAAGGACCTGGCACACATACCGTAGCTCTTGGTCCTGAAGAACGACGTG
2501 SerMetValLeuPheLeuAspArgValTyrGlyIleGluAsnGlnAspPheLeuLeuHis 2520
GTGCTGGACGTGGGGTTCCTGCCCGACATGAGGGCAGCCGCCTCGCTGGACACGGCCACT
7561
7620
CACGACCTGCACCCCAAGGACGGGCTGTACTCCCGTCGGCGGAGCGACCTGTGCCGGTGA
2521 ValLeuAspValGlyPheLeuProAspMetArgAlaAlaAlaSerLeuAspThrAlaThr 2540
7642
TTCAGCACCACCGAGATGGCGCTGGCCGTGAACCGCTACCTGTGCCTGGCCGTGCTGCCG
7621
7680
AAGTCGTGGTGGCTCTACCGCGACCGGCACTTGGCGATGGACACGGACCGGCACGACGGC
2541 PheSerThrThrGluMetAlaLeuAlaValAsnArgTyrLeuCysLeuAlaValLeuPro 2560
CTCATCACCAAGTGTGCGCCGCTCTTTGCGGGCACAGAACACCGCGCCATCATGGTGGAC
7681
7740
GAGTAGTGGTTCACACGCGGCGAGAAACGCCCGTGTCTTGTGGCGCGGTAGTACCACCTG
2561 LeuIleThrLysCysAlaProLeuPheAlaGlyThrGluHisArgAlaIleMetValAsp 2580


TCTATGCTGCATACCGTGTACCGCCTGTCTCGGGGTCGTTCGCTCACCAAGGCGCAGCGT
7741
7800
AGATACGACGTATGGCACATGGCGGACAGAGCCCCAGCAAGCGAGTGGTTCCGCGTCGCA
2581 SerMetLeuHisThrValTyrArgLeuSerArgGlyArgSerLeuThrLysAlaGlnArg 2600
AatII
GACGTCATCGAGGACTGCCTCATGTCGCTCTGCAGGTACATCCGCCCGTCGATGCTGCAG
7801
7860
CTGCAGTAGCTCCTGACGGAGTACAGCGAGACGTCCATGTAGGCGGGCAGCTACGACGTC
2601 AspValIleGluAspCysLeuMetSerLeuCysArgTyrIleArgProSerMetLeuGln 2620
T His2621
CACCTGTTGCGCCGCCTGGTGTTCGACGTGCCCATCCTCAACGAGTTCGCCAAGATGCCA
7861
7920
GTGGACAACGCGGCGGACCACAAGCTGCACGGGTAGGAGTTGCTCAAGCGGTTCTACGGT
2621 HisLeuLeuArgArgLeuValPheAspValProIleLeuAsnGluPheAlaLysMetPro 2640
exon 50
A Thr2659
CTCAAGCTCCTCACCAACCACTATGAGCGCTGTTGGAAGTACTACTGCCTACCCACGGGC
7921
7980
GAGTTCGAGGAGTGGTTGGTGATACTCGCGACAACCTTCATGATGACGGATGGGTGCCCG
2641 LeuLysLeuLeuThrAsnHisTyrGluArgCysTrpLysTyrTyrCysLeuProThrGly 2660
8025
TGGGCCAACTTCGGGGTCACCTCAGAGGAGGAGCTGCACCTCACACGGAAACTCTTCTGG
7981
8040
ACCCGGTTGAAGCCCCAGTGGAGTCTCCTCCTCGACGTGGAGTGTGCCTTTGAGAAGACC
2661 TrpAlaAsnPheGlyValThrSerGluGluGluLeuHisLeuThrArgLysLeuPheTrp 2680
GGCATCTTTGACTCTCTGGCCCATAAGAAATACGACCCGGAGCTGTACCGCATGGCCATG
8041
8100
CCGTAGAAACTGAGAGACCGGGTATTCTTTATGCTGGGCCTCGACATGGCGTACCGGTAC
2681 GlyIlePheAspSerLeuAlaHisLysLysTyrAspProGluLeuTyrArgMetAlaMet 2700
C Ile2706
CCTTGTCTGTGCGCCATTGCCGGGGCTCTGCCCCCCGACTATGTGGATGCCTCATACTCA
8101
8160
GGAACAGACACGCGGTAACGGCCCCGAGACGGGGGGCTGATACACCTACGGAGTATGAGT
2701 ProCysLeuCysAlaIleAlaGlyAlaLeuProProAspTyrValAspAlaSerTyrSer 2720
C Asp2730
TCTAAGGCAGAGAAAAAGGCCACAGTGGATGCTGAAGGCAACTTTGATCCCCGGCCTGTG
8161
8220
AGATTCCGTCTCTTTTTCCGGTGTCACCTACGACTTCCGTTGAAACTAGGGGCCGGACAC
2721 SerLysAlaGluLysLysAlaThrValAspAlaGluGlyAsnPheAspProArgProVal 2740
GAGACCCTCAATGTGATCATCCCGGAGAAGCTGGACTCCTTCATTAACAAGTTTGCGGAG
8221
8280
CTCTGGGAGTTACACTAGTAGGGCCTCTTCGACCTGAGGAAGTAATTGTTCAAACGCCTC
2741 GluThrLeuAsnValIleIleProGluLysLeuAspSerPheIleAsnLysPheAlaGlu 2760
A Glu2779
TACACACACGAGAAGTGGGCCTTCGACAAGATCCAGAACAACTGGTCCTATGGAGAGAAC
8281
8340
ATGTGTGTGCTCTTCACCCGGAAGCTGTTCTAGGTCTTGTTGACCAGGATACCTCTCTTG
2761 TyrThrHisGluLysTrpAlaPheAspLysIleGlnAsnAsnTrpSerTyrGlyGluAsn 2780
ATAGACGAGGAGCTGAAGACCCACCCCATGCTGAGGCCCTACAAGACCTTTTCAGAGAAG
8341
8400
TATCTGCTCCTCGACTTCTGGGTGGGGTACGACTCCGGGATGTTCTGGAAAAGTCTCTTC
2781 IleAspGluGluLeuLysThrHisProMetLeuArgProTyrLysThrPheSerGluLys 2800


8525
XhoI
exon 55
8789
exon 60


CCGGCTAAAGTGCTGGGCAGCGGTGGCCACGCCTCTAACAAGGAGAAGGAAATGATCACC
9061
9120
GGCCGATTTCACGACCCGTCGCCACCGGTGCGGAGATTGTTCCTCTTCCTTTACTAGTGG
3021
ProAlaLysValLeuGlySerGlyGlyHisAlaSerAsnLysGluLysGluMetIleThr
3040
AGCCTCTTCTGCAAACTTGCTGCTCTCGTCCGCCACCGAGTCTCTCTCTTTGGGACAGAC
9121
9180
TCGGAGAAGACGTTTGAACGACGAGAGCAGGCGGTGGCTCAGAGAGAGAAACCCTGTCTG
3041
SerLeuPheCysLysLeuAlaAlaLeuValArgHisArgValSerLeuPheGlyThrAsp
3060
G
Pro3062
GCCCCAGCTGTGGTCAACTGTCTTCACATCCTGGCCCGCTCCCTGGATGCCAGGACAGTG
9181
9240
CGGGGTCGACACCAGTTGACAGAAGTGTAGGACCGGGCGAGGGACCTACGGTCCTGTCAC
3061
AlaProAlaValValAsnCysLeuHisIleLeuAlaArgSerLeuAspAlaArgThrVal
3080
ATGAAGTCAGGCCCTGAGATCGTGAAGGCTGGCCTCCGCTCCTTCTTCGAGAGTGCCTCG
9241
9300
TACTTCAGTCCGGGACTCTAGCACTTCCGACCGGAGGCGAGGAAGAAGCTCTCACGGAGC
3081
MetLysSerGlyProGluIleValLysAlaGlyLeuArgSerPhePheGluSerAlaSer
3100
GAGGACATCGAGAAGATGGTGGAGAACCTGCGGCTGGGCAAGGTGTCGCAGGCGCGCACC
9301
9360
CTCCTGTAGCTCTTCTACCACCTCTTGGACGCCGACCCGTTCCACAGCGTCCGCGCGTGG
3101
GluAspIleGluLysMetValGluAsnLeuArgLeuGlyLysValSerGlnAlaArgThr
3120
CAGGTGAAAGGCGTGGGCCAGAACCTCACCTACACCACTGTGGCACTGCTGCCGGTCCTC
9361
9420
GTCCACTTTCCGCACCCGGTCTTGGAGTGGATGTGGTGACACCGTGACGACGGCCAGGAG
3121
GlnValLysGlyValGlyGlnAsnLeuThrTyrThrThrValAlaLeuLeuProValLeu
3140
9442
ACCACCCTCTTCCAGCACATCGCCCAGCACCAGTTCGGAGATGACGTCATCCTGGACGAC
9421
9480
TGGTGGGAGAAGGTCGTGTAGCGGGTCGTGGTCAAGCCTCTACTGCAGTAGGACCTGCTG
3141
ThrThrLeuPheGlnHisIleAlaGlnHisGlnPheGlyAspAspValIleLeuAspAsp
3160
GTCCAGGTCTCTTGCTACCGAACGCTGTGCAGTATCTACTCCCTGGGAACCACCAAGAAC
9481
9540
CAGGTCCAGAGAACGATGGCTTGCGACACGTCATAGATGAGGGACCCTTGGTGGTTCTTG
3161
ValGlnValSerCysTyrArgThrLeuCysSerIleTyrSerLeuGlyThrThrLysAsn
3180
exon 65
ACTTATGTGGAAAAGCTTCGGCCAGCCCTCGGGGAGTGCCTGGCCCGTCTGGCAGCAGCC
9541
9600
TGAATACACCTTTTCGAAGCCGGTCGGGAGCCCCTCACGGACCGGGCAGACCGTCGTCGG
3181
ThrTyrValGluLysLeuArgProAlaLeuGlyGluCysLeuAlaArgLeuAlaAlaAla
3200
ATGCCGGTGGCGTTCCTGGAGCCGCAGCTGAACGAGTACAACGCCTGCTCCGTGTACACC
9601
9660
TACGGCCACCGCAAGGACCTCGGCGTCGACTTGCTCATGTTGCGGACGAGGCACATGTGG
3201
MetProValAlaPheLeuGluProGlnLeuAsnGluTyrAsnAlaCysSerValTyrThr
3220
SacII
ACCAAGTCTCCGCGGGAGCGGGCCATCCTGGGGCTCCCCAACAGTGTGGAGGAGATGTGT
9661
9720
TGGTTCAGAGGCGCCCTCGCCCGGTAGGACCCCGAGGGGTTGTCACACCTCCTCTACACA
3221
ThrLysSerProArgGluArgAlaIleLeuGlyLeuProAsnSerValGluGluMetCys
3240


CCCGACATCCCGGTGCTGGAGCGGCTCATGGCAGACATTGGGGGGCTGGCCGAGTCAGGT
9721
9780
GGGCTGTAGGGCCACGACCTCGCCGAGTACCGTCTGTAACCCCCCGACCGGCTCAGTCCA
3241
ProAspIleProValLeuGluArgLeuMetAlaAspIleGlyGlyLeuAlaGluSerGly
3260
9769
GCCCGCTACACAGAGATGCCGCATGTCATCGAGATCACGCTGCCCATGCTATGCAGCTAC
9781
9840
CGGGCGATGTGTCTCTACGGCGTACAGTAGCTCTAGTGCGACGGGTACGATACGTCGATG
3261
AlaArgTyrThrGluMetProHisValIleGluIleThrLeuProMetLeuCysSerTyr
3280
CTGCCCCGATGGTGGGAGCGCGGGCCCGAGGCACCCCCTTCCGCCCTGCCCGCCGGCGCC
9841
9900
GACGGGGCTACCACCCTCGCGCCCGGGCTCCGTGGGGGAAGGCGGGACGGGCGGCCGCGG
3281
LeuProArgTrpTrpGluArgGlyProGluAlaProProSerAlaLeuProAlaGlyAla
3300
CCCCCACCCTGCACAGCTGTCACCTCTGACCACCTCAACTCCCTGCTGGGGAATATCCTG
9901
9960
GGGGGTGGGACGTGTCGACAGTGGAGACTGGTGGAGTTGAGGGACGACCCCTTATAGGAC
3301
ProProProCysThrAlaValThrSerAspHisLeuAsnSerLeuLeuGlyAsnIleLeu
3320
AGAATCATCGTCAACAACCTGGGCATTGACGAGGCCTCCTGGATGAAGCGGCTGGCTGTG
9961
10020
TCTTAGTAGCAGTTGTTGGACCCGTAACTGCTCCGGAGGACCTACTTCGCCGACCGACAC
3321
ArgIleIleValAsnAsnLeuGlyIleAspGluAlaSerTrpMetLysArgLeuAlaVal
3340
PstI
10052
TTCGCACAGCCCATTGTGAGCCGTGCACGGCCGGAGCTCCTGCAGTCCCACTTCATCCCA
10021
10080
AAGCGTGTCGGGTAACACTCGGCACGTGCCGGCCTCGAGGACGTCAGGGTGAAGTAGGGT
3341
PheAlaGlnProIleValSerArgAlaArgProGluLeuLeuGlnSerHisPheIlePro
3360
10109
ACTATCGGGCGGCTGCGCAAGAGGGCAGGGAAGGTGGTGTCCGAGGAGGAGCAGCTGCGC
10081
10140
TGATAGCCCGCCGACGCGTTCTCCCGTCCCTTCCACCACAGGCTCCTCCTCGTCGACGCG
3361
ThrIleGlyArgLeuArgLysArgAlaGlyLysValValSerGluGluGluGlnLeuArg
3380
T
Asp3396
CTGGAGGCCAAGGCGGAGGCCCAGGAGGGCGAGCTGCTGGTGCGGGACCGAGTTCTCTGTG
10141
10200
GACCTCCGGTTCCGCCTCCGGGTCCTCCCGCTCGACGACCACGCCCTGCTCAAGAGACAC
3381
LeuGluAlaLysAlaGluAlaGlnGluGlyGluLeuLeuValArgAspGluPheSerVal
3400
CTCTGCCGGGACCTCTACGCCCTGTATCCGCTGCTCATCCGCTACGTGGACAACAACAGG
10201
10260
GAGACGGCCCTGGAGATGCGGGACATAGGCGACGAGTAGGCGATGCACCTGTTGTTGTCC
3401
LeuCysArgAspLeuTyrAlaLeuTyrProLeuLeuIleArgTyrValAspAsnAsnArg
3420
GCGCAGTGGCTGACGGAGCCGAATCCCAGCGCGGAGGAGCTGTTCAGGATGGTGGGCGAG
10261
10320
CGCGTCACCGACTGCCTCGGCTTAGGGTCGCGCCTCCTCGACAAGTCCTACCACCCGCTC
3421
AlaGlnTrpLeuThrGluProAsnProSerAlaGluGluLeuPheArgMetValGlyGlu
3440
ATCTTCATCTACTGGTCCAAGTCCCACAACTTCAAGCGCGAGGAGCAGAACTTTGTGGTC
10321
10380
TAGAAGTAGATGACCAGGTTCAGGGTGTTGAAGTTCGCGCTCCTCGTCTTGAAACACCAG
3441
IlePheIleTyrTrpSerLysSerHisAsnPheLysArgGluGluGlnAsnPheValVal
3460


10809
exon 70
exon 75
HindIII


11041
11100
3681
3700
11101
11160
3701
3720
EcoRV
11161
11220
3721
3740
11213
11221
11280
3741
3760
11281
11340
3761
3780
exon 80
11341
11400
3781
3800
11401
11460
3801
3820
11461
11520
3821
3840
11521
11580
3841
3860
pSVK3.5
EcoRI
11581
11640
3861
3880
A
Gly3893
exon 85
11641
11700
3881
3900

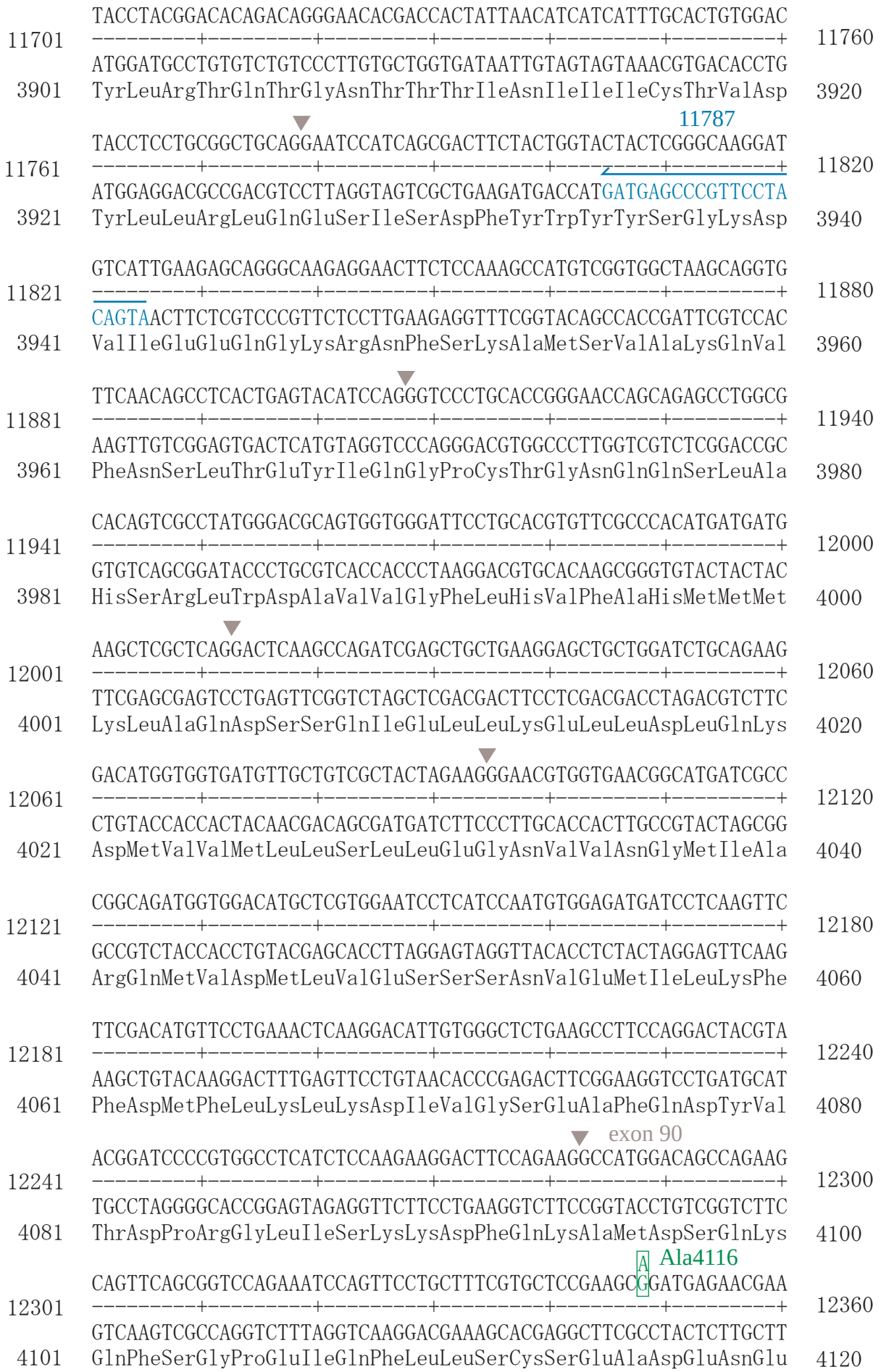
11787
exon 90
Ala4116

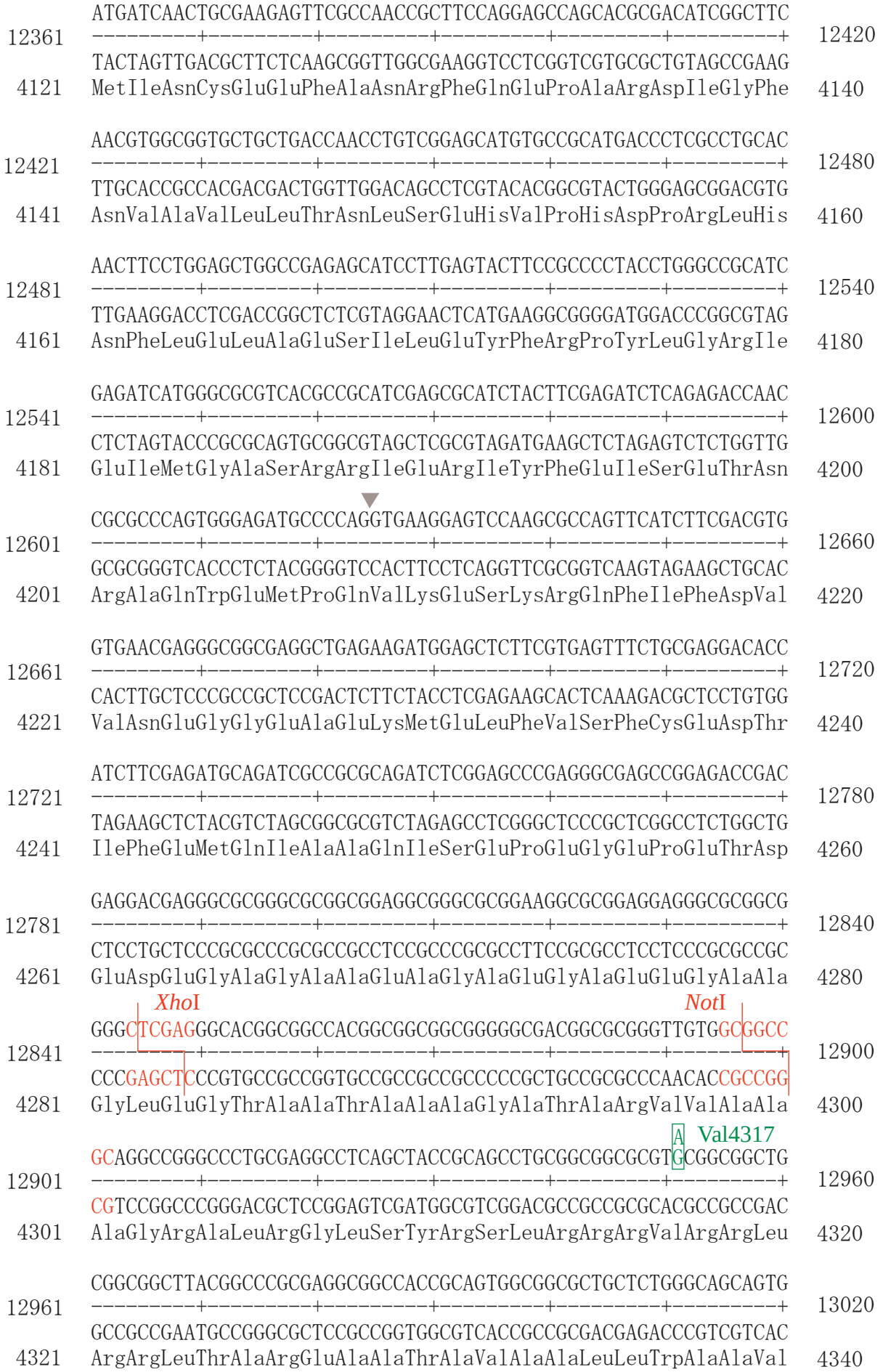
ATGATCAACTGCGAAGAGTTCGCCAACCGCTTCCAGGAGCCAGCACGCGACATCGGCTTC
12361
12420
TACTAGTTGACGCTTCTCAAGCGGTTGGCGAAGGTCCTCGGTCGTGCGCTGTAGCCGAAG
4121
MetIleAsnCysGluGluPheAlaAsnArgPheGlnGluProAlaArgAspIleGlyPhe
4140
AACGTGGCGGTGCTGCTGACCAACCTGTCGGAGCATGTGCCGCATGACCCTCGCCTGCAC
12421
12480
TTGCACCGCCACGACGACTGGTTGGACAGCCTCGTACACGGCGTACTGGGAGCGGACGTG
4141
AsnValAlaValLeuLeuThrAsnLeuSerGluHisValProHisAspProArgLeuHis
4160
AACTTCCTGGAGCTGGCCGAGAGCATCCTTGAGTACTTCCGCCCCTACCTGGGCCGCATC
12481
12540
TTGAAGGACCTCGACCGGCTCTCGTAGGAACTCATGAAGGCGGGGATGGACCCGGCGTAG
4161
AsnPheLeuGluLeuAlaGluSerIleLeuGluTyrPheArgProTyrLeuGlyArgIle
4180
GAGATCATGGGCGCGTCACGCCGCATCGAGCGCATCTACTTCGAGATCTCAGAGACCAAC
12541
12600
CTCTAGTACCCGCGCAGTGCGGCGTAGCTCGCGTAGATGAAGCTCTAGAGTCTCTGGTTG
4181
GluIleMetGlyAlaSerArgArgIleGluArgIleTyrPheGluIleSerGluThrAsn
4200
CGCGCCCAGTGGGAGATGCCCCAGGTGAAGGAGTCCAAGCGCCAGTTCATCTTCGACGTG
12601
12660
GCGCGGGTCACCCTCTACGGGGTCCACTTCCTCAGGTTCGCGGTCAAGTAGAAGCTGCAC
4201
ArgAlaGlnTrpGluMetProGlnValLysGluSerLysArgGlnPheIlePheAspVal
4220
GTGAACGAGGGCGGCGAGGCTGAGAAGATGGAGCTCTTCGTGAGTTTCTGCGAGGACACC
12661
12720
CACTTGCTCCCGCCGCTCCGACTCTTCTACCTCGAGAAGCACTCAAAGACGCTCCTGTGG
4221
ValAsnGluGlyGlyGluAlaGluLysMetGluLeuPheValSerPheCysGluAspThr
4240
ATCTTCGAGATGCAGATCGCCGCGCAGATCTCGGAGCCCGAGGGCGAGCCGGAGACCGAC
12721
12780
TAGAAGCTCTACGTCTAGCGGCGCGTCTAGAGCCTCGGGCTCCCGCTCGGCCTCTGGCTG
4241
IlePheGluMetGlnIleAlaAlaGlnIleSerGluProGluGlyGluProGluThrAsp
4260
GAGGACGAGGGCGCGGGCGCGGCGGAGGCGGGCGCGGAAGGCGCGGAGGAGGGCGCGGCG
12781
12840
CTCCTGCTCCCGCGCCCGCGCCGCCTCCGCCCGCGCCTTCCGCGCCTCCTCCCGCGCCGC
4261
GluAspGluGlyAlaGlyAlaAlaGluAlaGlyAlaGluGlyAlaGluGluGlyAlaAla
4280
XhoI
NotI
GGGCTCGAGGGCACGGCGGCCACGGCGGCGGCGGGGGCGACGGCGCGGGTTGTGGCGGCC
12841
12900
CCCGAGCTCCCGTGCCGCCGGTGCCGCCGCCGCCCCCGCTGCCGCGCCCAACACCGCCGG
4281
GlyLeuGluGlyThrAlaAlaThrAlaAlaAlaGlyAlaThrAlaArgValValAlaAla
4300
A
Val4317
GCAGGCCGGGCCCTGCGAGGCCTCAGCTACCGCAGCCTGCGGCGGCGCGTGCGGCGGCTG
12901
12960
CGTCCGGCCCGGGACGCTCCGGAGTCGATGGCGTCGGACGCCGCCGCGCACGCCGCCGAC
4301
AlaGlyArgAlaLeuArgGlyLeuSerTyrArgSerLeuArgArgArgValArgArgLeu
4320
CGGCGGCTTACGGCCCGCGAGGCGGCCACCGCAGTGGCGGCGCTGCTCTGGGCAGCAGTG
12961
13020
GCCGCCGAATGCCGGGCGCTCCGCCGGTGGCGTCACCGCCGCGACGAGACCCGTCGTCAC
4321
ArgArgLeuThrAlaArgGluAlaAlaThrAlaValAlaAlaLeuLeuTrpAlaAlaVal
4340

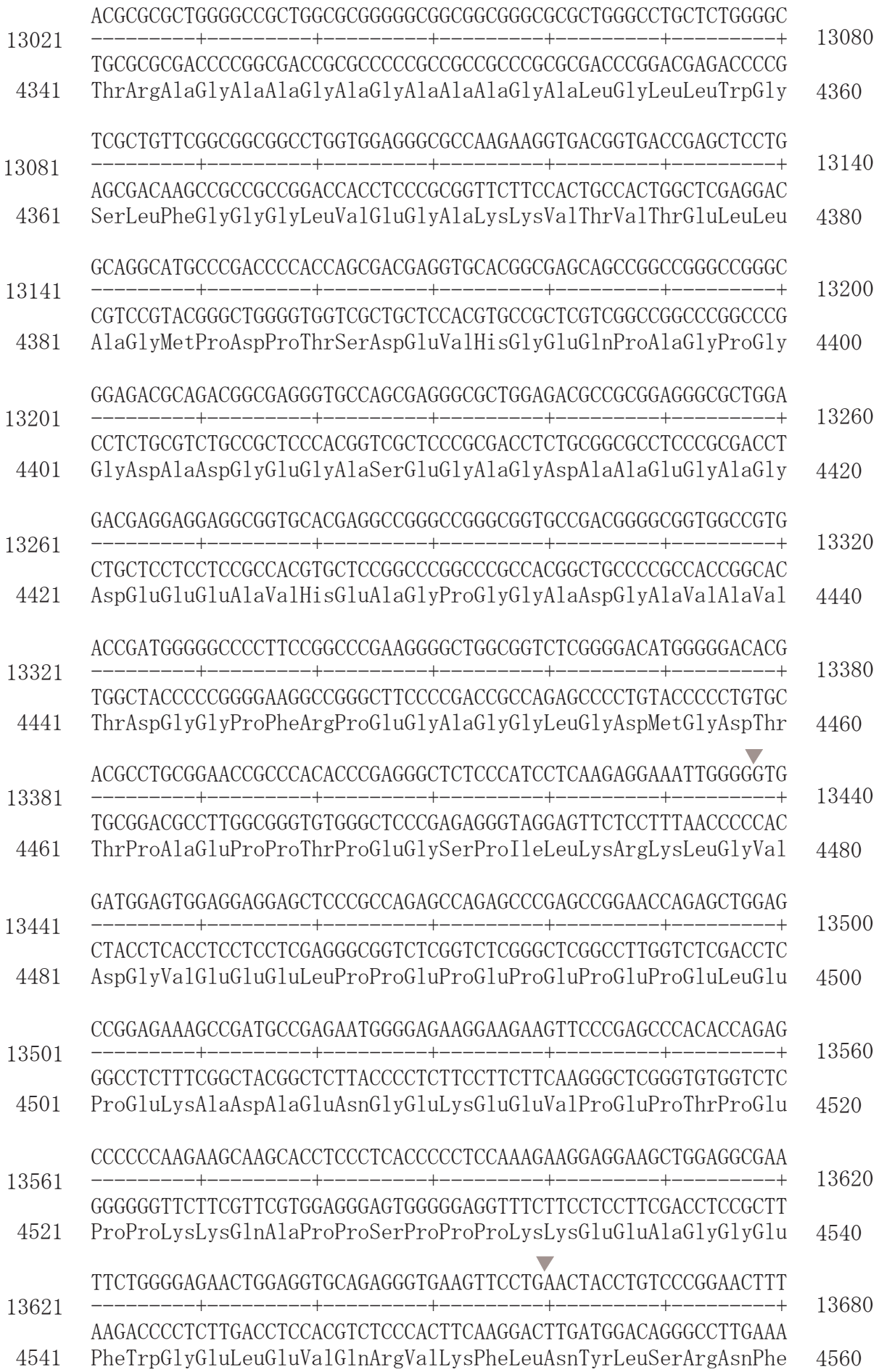
ACGCGCGCTGGGGCCGCTGGCGCGGGGGCGGCGGCGGGCGCGCTGGGCCTGCTCTGGGGC
13021 13080
TGCGCGCGACCCCGGCGACCGCGCCCCCGCCGCCGCCCGCGCGACCCGGACGAGACCCCG
4341 ThrArgAlaGlyAlaAlaGlyAlaGlyAlaAlaAlaGlyAlaLeuGlyLeuLeuTrpGly 4360
TCGCTGTTCGGCGGCGGCCTGGTGGAGGGCGCCAAGAAGGTGACGGTGACCGAGCTCCTG
13081 13140
AGCGACAAGCCGCCGCCGGACCACCTCCCGCGGTTCTTCCACTGCCACTGGCTCGAGGAC
4361 SerLeuPheGlyGlyGlyLeuValGluGlyAlaLysLysValThrValThrGluLeuLeu 4380
GCAGGCATGCCCGACCCCACCAGCGACGAGGTGCACGGCGAGCAGCCGGCCGGGCCGGGC
13141 13200
CGTCCGTACGGGCTGGGGTGGTCGCTGCTCCACGTGCCGCTCGTCGGCCGGCCCGGCCCG
4381 AlaGlyMetProAspProThrSerAspGluValHisGlyGluGlnProAlaGlyProGly 4400
GGAGACGCAGACGGCGAGGGTGCCAGCGAGGGCGCTGGAGACGCCGCGGAGGGCGCTGGA
13201 13260
CCTCTGCGTCTGCCGCTCCCACGGTCGCTCCCGCGACCTCTGCGGCGCCTCCCGCGACCT
4401 GlyAspAlaAspGlyGluGlyAlaSerGluGlyAlaGlyAspAlaAlaGluGlyAlaGly 4420
GACGAGGAGGAGGCGGTGCACGAGGCCGGGCCGGGCGGTGCCGACGGGGCGGTGGCCGTG
13261 13320
CTGCTCCTCCTCCGCCACGTGCTCCGGCCCGGCCCGCCACGGCTGCCCCGCCACCGGCAC
4421 AspGluGluGluAlaValHisGluAlaGlyProGlyGlyAlaAspGlyAlaValAlaVal 4440
ACCGATGGGGGCCCCTTCCGGCCCGAAGGGGCTGGCGGTCTCGGGGACATGGGGGACACG
13321 13380
TGGCTACCCCCGGGGAAGGCCGGGCTTCCCCGACCGCCAGAGCCCCTGTACCCCCTGTGC
4441 ThrAspGlyGlyProPheArgProGluGlyAlaGlyGlyLeuGlyAspMetGlyAspThr 4460
ACGCCTGCGGAACCGCCCACACCCGAGGGCTCTCCCATCCTCAAGAGGAAATTGGGGGTG
13381 13440
TGCGGACGCCTTGGCGGGTGTGGGCTCCCGAGAGGGTAGGAGTTCTCCTTTAACCCCCAC
4461 ThrProAlaGluProProThrProGluGlySerProIleLeuLysArgLysLeuGlyVal 4480
GATGGAGTGGAGGAGGAGCTCCCGCCAGAGCCAGAGCCCGAGCCGGAACCAGAGCTGGAG
13441 13500
CTACCTCACCTCCTCCTCGAGGGCGGTCTCGGTCTCGGGCTCGGCCTTGGTCTCGACCTC
4481 AspGlyValGluGluGluLeuProProGluProGluProGluProGluProGluLeuGlu 4500
CCGGAGAAAGCCGATGCCGAGAATGGGGAGAAGGAAGAAGTTCCCGAGCCCACACCAGAG
13501 13560
GGCCTCTTTCGGCTACGGCTCTTACCCCTCTTCCTTCTTCAAGGGCTCGGGTGTGGTCTC
4501 ProGluLysAlaAspAlaGluAsnGlyGluLysGluGluValProGluProThrProGlu 4520
CCCCCCAAGAAGCAAGCACCTCCCTCACCCCCTCCAAAGAAGGAGGAAGCTGGAGGCGAA
13561 13620
GGGGGGTTCTTCGTTCGTGGAGGGAGTGGGGGAGGTTTCTTCCTCCTTCGACCTCCGCTT
4521 ProProLysLysGlnAlaProProSerProProProLysLysGluGluAlaGlyGlyGlu 4540
TTCTGGGGAGAACTGGAGGTGCAGAGGGTGAAGTTCCTGAACTACCTGTCCCGGAACTTT
13621 13680
AAGACCCCTCTTGACCTCCACGTCTCCCACTTCAAGGACTTGATGGACAGGGCCTTGAAA
4541 PheTrpGlyGluLeuGluValGlnArgValLysPheLeuAsnTyrLeuSerArgAsnPhe 4560

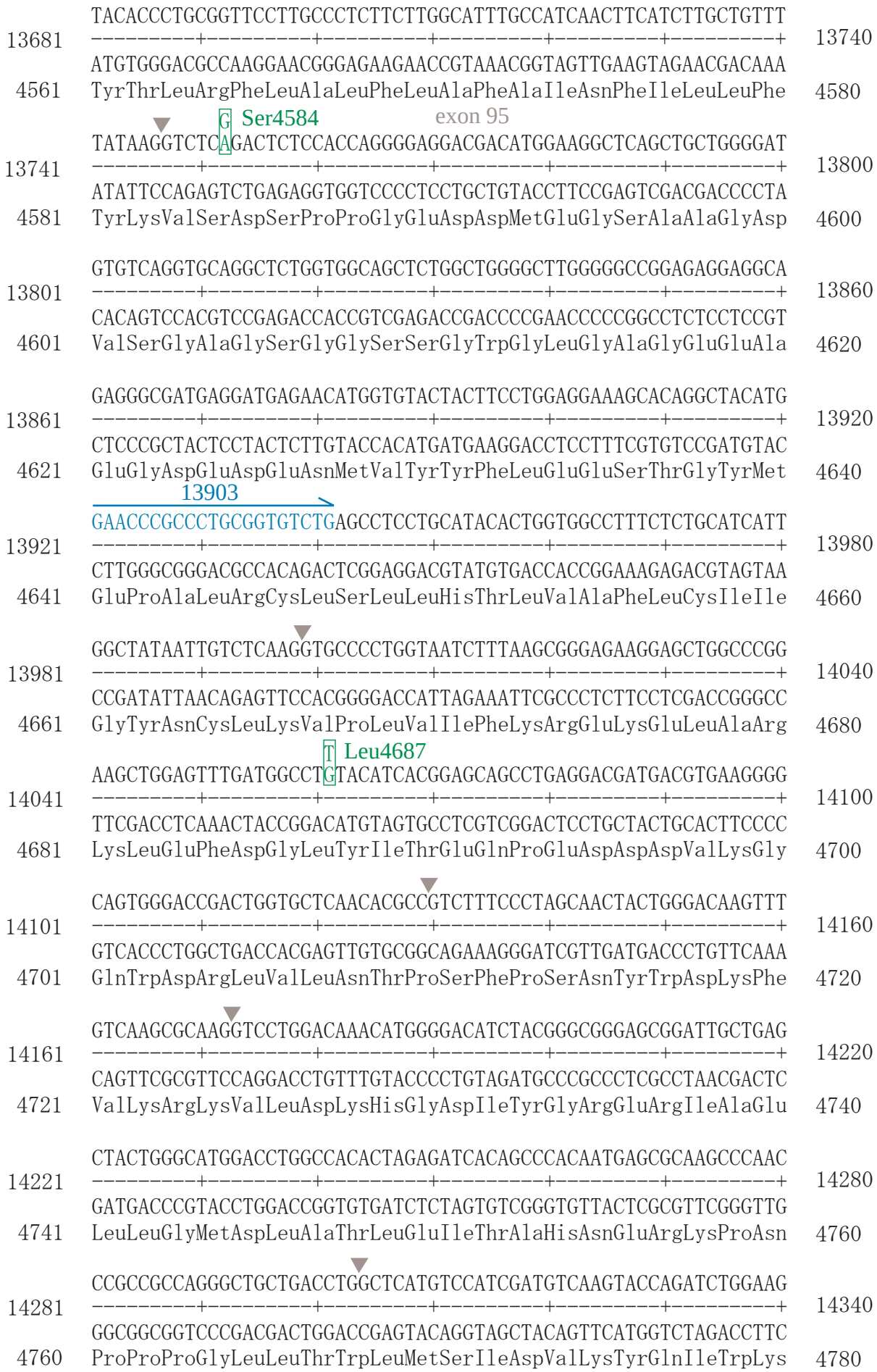
TACACCCTGCGGTTCCTTGCCCTCTTCTTGGCATTTGCCATCAACTTCATCTTGCTGTTT
13681 13740
ATGTGGGACGCCAAGGAACGGGAGAAGAACCGTAAACGGTAGTTGAAGTAGAACGACAAA
4561 TyrThrLeuArgPheLeuAlaLeuPheLeuAlaPheAlaIleAsnPheIleLeuLeuPhe 4580
G Ser4584
exon 95
TATAAGGTCTCAGACTCTCCACCAGGGGAGGACGACATGGAAGGCTCAGCTGCTGGGGAT
13741 13800
ATATTCCAGAGTCTGAGAGGTGGTCCCCTCCTGCTGTACCTTCCGAGTCGACGACCCCTA
4581 TyrLysValSerAspSerProProGlyGluAspAspMetGluGlySerAlaAlaGlyAsp 4600
GTGTCAGGTGCAGGCTCTGGTGGCAGCTCTGGCTGGGGCTTGGGGGCCGGAGAGGAGGCA
13801 13860
CACAGTCCACGTCCGAGACCACCGTCGAGACCGACCCCGAACCCCCGGCCTCTCCTCCGT
4601 ValSerGlyAlaGlySerGlyGlySerSerGlyTrpGlyLeuGlyAlaGlyGluGluAla 4620
GAGGGCGATGAGGATGAGAACATGGTGTACTACTTCCTGGAGGAAAGCACAGGCTACATG
13861 13920
CTCCCGCTACTCCTACTCTTGTACCACATGATGAAGGACCTCCTTTCGTGTCCGATGTAC
4621 GluGlyAspGluAspGluAsnMetValTyrTyrPheLeuGluGluSerThrGlyTyrMet 4640
13903
GAACCCGCCCTGCGGTGTCTGAGCCTCCTGCATACACTGGTGGCCTTTCTCTGCATCATT
13921 13980
CTTGGGCGGGACGCCACAGACTCGGAGGACGTATGTGACCACCGGAAAGAGACGTAGTAA
4641 GluProAlaLeuArgCysLeuSerLeuLeuHisThrLeuValAlaPheLeuCysIleIle 4660
GGCTATAATTGTCTCAAGGTGCCCCTGGTAATCTTTAAGCGGGAGAAGGAGCTGGCCCGG
13981 14040
CCGATATTAACAGAGTTCCACGGGGACCATTAGAAATTCGCCCTCTTCCTCGACCGGGCC
4661 GlyTyrAsnCysLeuLysValProLeuValIlePheLysArgGluLysGluLeuAlaArg 4680
T Leu4687
AAGCTGGAGTTTGATGGCCTGTACATCACGGAGCAGCCTGAGGACGATGACGTGAAGGGG
14041 14100
TTCGACCTCAAACTACCGGACATGTAGTGCCTCGTCGGACTCCTGCTACTGCACTTCCCC
4681 LysLeuGluPheAspGlyLeuTyrIleThrGluGlnProGluAspAspValLysGly 4700
CAGTGGGACCGACTGGTGCTCAACACGCCGTCTTTCCCTAGCAACTACTGGGACAAGTTT
14101 14160
GTCACCCTGGCTGACCACGAGTTGTGCGGCAGAAAGGGATCGTTGATGACCCTGTTCAAA
4701 GlnTrpAspArgLeuValLeuAsnThrProSerPheProSerAsnTyrTrpAspLysPhe 4720
GTCAAGCGCAAGGTCCTGGACAAACATGGGGACATCTACGGGCGGGAGCGGATTGCTGAG
14161 14220
CAGTTCGCGTTCCAGGACCTGTTTGTACCCCTGTAGATGCCCGCCCTCGCCTAACGACTC
4721 ValLysArgLysValLeuAspLysHisGlyAspIleTyrGlyArgGluArgIleAlaGlu 4740
CTACTGGGCATGGACCTGGCCACACTAGAGATCACAGCCCACAATGAGCGCAAGCCCAAC
14221 14280
GATGACCCGTACCTGGACCGGTGTGATCTCTAGTGTCGGGTGTTACTCGCGTTCGGGTTG
4741 LeuLeuGlyMetAspLeuAlaThrLeuGluIleThrAlaHisAsnGluArgLysProAsn 4760
CCGCCGCCAGGGCTGCTGACCTGGCTCATGTCCATCGATGTCAAGTACCAGATCTGGAAG
14281 14340
GGCGGCGGTCCCGACGACTGGACCGAGTACAGGTAGCTACAGTTCATGGTCTAGACCTTC
4760 ProProProGlyLeuLeuThrTrpLeuMetSerIleAspValLysTyrGlnIleTrpLys 4780


exon 100
C14477T T Thr4826Ile C14497T T His4833Tyr
G14582A
A Arg4861His
T14693C Ile4898Thr C A Gly4899Arg
G14695A
exon 105

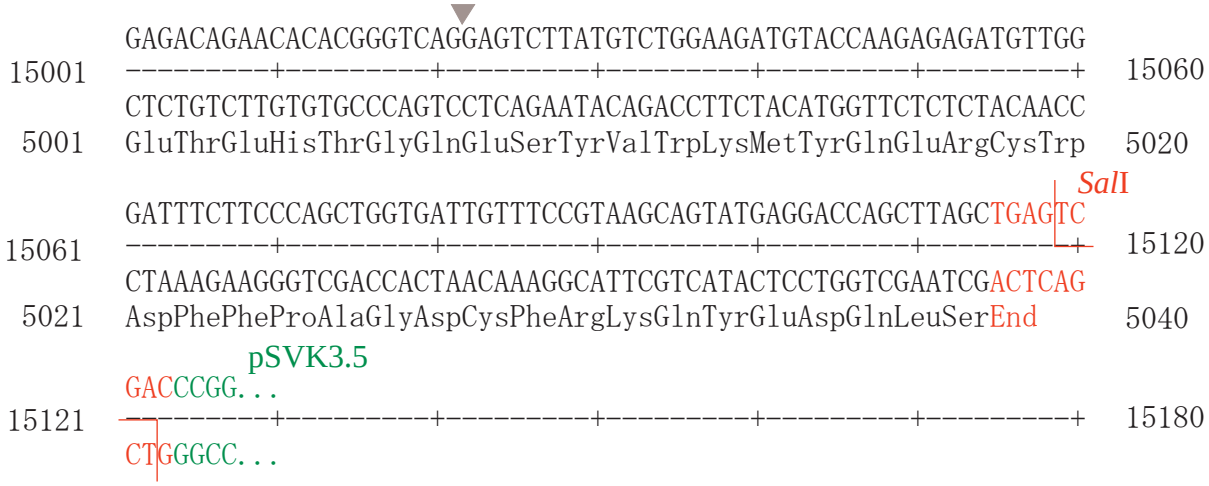

Primers used in this project are described in blue arrows. *RYR1* mutations and restriction endonuclease sites are shown in red. Polymorphisms are shown in green. Exon boundaries are shown in gray arrows.

Appendix 3 Polymorphisms identified within pcRYR1

Ala359	Pro762
Thr981	Asn993
Glu1875	His2621
Thr2659	Ile2706
Asp2730	Glu2779
Pro3062	Asp3396
Gly3893	Ala4116
Val4317	Ser4584
Leu4687	

Seventeen polymorphisms were identified by direct sequencing of the complete *RYR1* cDNA coding regions in the complete vector pcRYR1. These polymorphisms were silent and did not introduce on amino acid change.